Technical Report Documentation Page

1. Report No.	2. Government Accession No.	3. Recipient's Catalog No.
FHWA/TX-92+1169-5F		

4. Title and Subtitle	5. Report Date
IMPROVED DESIGN AND CONSTRUCTION PROCEDURES FOR CONCRETE PAVEMENTS BASED ON MECHANISTIC MODELING TECHNIQUES	June 1992
	6. Performing Organization Code

7. Author(s)	8. Performing Organization Report No.
Mehmet M. Kunt and B. Frank McCullough	Research Report 1169-5F

9. Performing Organization Name and Address	10. Work Unit No. (TRAIS)
Center for Transportation Research The University of Texas at Austin Austin, Texas 78712-1075	11. Contract or Grant No. Research Study 3-8-88/1-1169
	13. Type of Report and Period Covered
12. Sponsoring Agency Name and Address Texas Department of Transportation Transportation Planning Division P. O. Box 5051 Austin, Texas 78763-5051	Final
	14. Sponsoring Agency Code

15. Supplementary Notes
Study conducted in cooperation with the U.S. Department of Transportation, Federal Highway Administration
Research Study Title: "Concrete Pavement Design Update (AASHTO)"

16. Abstract

This report describes an improved set of concrete pavement design and construction procedures. In developing these improvements, we used a systems approach to incorporate material characterization subsystems and mechanistic techniques into the JRCP-5 computer program. The data obtained from such an approach were then used to develop, analyze, evaluate, and implement the best procedure for designing concrete pavement reinforcement and for determining pavement sawing time and depth.

Whereas the original models used to characterize concrete properties could not distinguish the effect of coarse aggregate types (CAT), the improved model now has this capability. Because several aggregate sources are used in Texas, incorporation of the effect of CAT substantially improved the prediction models.

Additionally, we updated the transverse reinforcement formula according to the findings of CTR Project 459. We also developed a probabilistic sawing depth and time prediction model, with all improvements and updates subsequently input into the JRCP-5 computer program. In concluding this report, we make recommendations for improving the prediction accuracy of the models.

17. Key Words	18. Distribution Statement
jointed reinforced concrete pavement design, JRCP-5 program, prediction models, probabilistic sawing depth, sawing time, coarse aggregates, design crack spacing, subbase friction	No restrictions. This document is available to the public through the National Technical Information Service, Springfield, Virginia 22161.

19. Security Classif. (of this report)	20. Security Classif. (of this page)	21. No. of Pages	22. Price
Unclassified	Unclassified	94	

IMPROVED DESIGN AND CONSTRUCTION PROCEDURES FOR CONCRETE PAVEMENTS BASED ON MECHANISTIC MODELING TECHNIQUES

by

Mehmet M. Kunt
B. Frank McCullough

Research Report 1169-5F

Concrete Pavement Design Update (AASHTO)
Research Project 3-8-88/1-1169

conducted for the

Texas Department of Transportation

in cooperation with the

U.S. Department of Transportation
Federal Highway Administration

by the

CENTER FOR TRANSPORTATION RESEARCH
Bureau of Engineering Research
THE UNIVERSITY OF TEXAS AT AUSTIN

June 1992

NOT INTENDED FOR CONSTRUCTION,
PERMIT, OR BIDDING PURPOSES

B. Frank McCullough, P.E. (Texas No. 19914)
Research Supervisor

The contents of this report reflect the views of the authors, who are responsible for the facts and the accuracy of the data presented herein. The contents do not necessarily reflect the official views or policies of the Federal Highway Administration or the Texas Department of Transportation. This report does not constitute a standard, specification, or regulation.

There was no invention or discovery conceived or first actually reduced to practice in the course of or under this contract, including any art, method, process, machine, manufacture, design or composition of matter, or any new and useful improvement thereof, or any variety of plant which is or may be patentable under the patent laws of the United States of America or any foreign country.

PREFACE

This is the fifth and final report for Research Project 1169, "Concrete Pavement Design Update." This research project was conducted by the Center for Transportation Research (CTR), The University of Texas at Austin, as part of the Cooperative Highway Research Program sponsored by the Texas Department of Transportation.

This report describes the development of an improved design method for reinforced concrete pavements. Such topics as reinforcement design, sawing time, and sawing depth are particularly discussed.

The authors would like to express their gratitude to all those who contributed their time and effort toward the completion of this report. In particular, we thank Mr. James Brown and Mr. Andrew J. Wimsatt of the Texas Department of Transportation for their instructive counsel. In addition, we would like to extend thanks to Dr. W. R. Hudson, to Mr. Terrence E. Dossey, and to all the rest of the staff at the Center for Transportation Research for their support and guidance.

Mehmet M. Kunt
B. Frank McCullough

LIST OF REPORTS

Research Report 1169-1, "A Study of Drainage Coefficients for Concrete Pavements in Texas," by Venkatakrisna Shyam, Humberto Castedo, W. R. Hudson, and B. Frank McCullough, discusses efforts to determine coefficients of drainage for concrete pavements with three subbase types and within a range of rainfall conditions. May 1989.

Research Report 1169-2, "Mechanistic Analysis of Continuously Reinforced Concrete Pavements Considering Material Characteristics, Variability, and Fatigue," by Mooncheol Won, Kenneth Hankins, and B. Frank McCullough, presents a mechanistic model for estimating continuously reinforced concrete (CRC) pavement life in terms of frequency of punchouts. This model, incorporated into the CRCP-5 computer program, uses the stochastic nature of the materials' properties and the fatigue behavior of pavement concrete to predict the extent and time of occurrence of punchouts in CRC pavements. April 1990.

Research Report 1169-3, "Development of Load Transfer Coefficients for Use with the AASHTO Guide for Design of Rigid Pavements Based on Field Measurements," by Chao Wei, B. Frank McCullough, W. R. Hudson, and Kenneth Hankins, presents a rational procedure for estimating load transfer coefficients for use with the AASHTO Pavement Design Guide. This procedure, developed from information available in the rigid pavement database at the Center for Transportation Research at The University of Texas at Austin, relates to the design of rigid pavements based on field deflection measurements and on the derived load transfer coefficients. It can be used for the design of continuously reinforced concrete pavements (CRCP) in Texas. May 1991.

Research Report 1169-4, "Terminal Movement in Continuously Reinforced Concrete Pavements," by Wan-Yi Wu and B. Frank McCullough, analyzes the terminal movement characteristics of CRCP using a mechanistic model, PSCP2, developed at the Center for Transportation Research. January 1992.

Research Report 1169-5F, "Improved Design and Construction Procedures for Concrete Pavements Based on Mechanistic Modeling Techniques," by Mehmet M. Kunt and B. Frank McCullough, describes the development of improved design and construction procedures for reinforced concrete pavements. June 1992.

ABSTRACT

This report describes an improved set of concrete pavement design and construction procedures. In developing these improvements, we used a systems approach to incorporate material characterization subsystems and mechanistic techniques into the JRCP-5 computer program. The data obtained from such an approach were then used to develop, analyze, evaluate, and implement the best procedure for designing concrete pavement reinforcement and for determining pavement sawing time and depth.

Whereas the original models used to characterize concrete properties could not distinguish the effect of coarse aggregate types (CAT), the improved model now has this capability. Because several aggregate sources are used in Texas, incorporation of the effect of CAT substantially improved the prediction models.

Additionally, we updated the transverse reinforcement formula according to the findings of CTR Project 459. We also developed a probabilistic sawing depth and time prediction model, with all improvements and updates subsequently input into the JRCP-5 computer program. In concluding this report, we make recommendations for improving the prediction accuracy of the models.

KEY WORDS: Jointed reinforced concrete pavement design, JRCP-5 program, prediction models, probabilistic sawing depth, sawing time, coarse aggregates, design crack spacing, subbase friction, steel reinforcement design, concrete properties, shrinkage, concrete tensile strength, concrete modulus of elasticity, joint sealant design, subgrade drag theory.

SUMMARY

In the past, concrete pavement design methods very often were deterministic; that is, they were fixed with respect to time and space. But concrete pavement material properties vary with time, and certain design parameters vary from place to place within the pavement structure. Moreover, because time and available funds for the study of material properties are limited, such material variability is often excluded from pavement analysis. Thus, this study undertook to improve the reinforced concrete pavement design method by considering more rational prediction models for the cement concrete properties that comprise the pavement.

IMPLEMENTATION STATEMENT

This study has provided several benefits. Most importantly, the prediction models relating to concrete properties have been substantially improved, with all such improvements incorporated in the JRCP-5 computer program. In addition, the transverse reinforcement formula has been updated according to the new findings of CTR Project 459. A probabilistic sawing depth and time prediction model has also been developed. Finally, recommendations are made for future enhancement of the prediction accuracy of the models.

TABLE OF CONTENTS

METRIC (SI*) CONVERSION FACTORS

APPROXIMATE CONVERSIONS TO SI UNITS

Symbol	When You Know	Multiply by	To Find	Symbol
		LENGTH		
in	inches	2.54	centimeters	cm
ft	feet	0.3048	meters	m
yd	yards	0.914	meters	m
mi	miles	1.61	kilometers	km
		AREA		
in^2	square inches	645.2	millimeters squared	mm^2
ft^2	square feet	0.0929	meters squared	m^2
yd^2	square yards	0.836	meters squared	m^2
mi^2	square miles	2.59	kilometers squared	km^2
ac	acres	0.395	hectares	ha
		MASS (weight)		
oz	ounces	28.35	grams	g
lb	pounds	0.454	kilograms	kg
T	short tons (2,000 lb)	0.907	megagrams	Mg
		VOLUME		
fl oz	fluid ounces	29.57	milliliters	mL
gal	gallons	3.785	liters	L
ft^3	cubic feet	0.0328	meters cubed	m^3
yd^3	cubic yards	0.0765	meters cubed	m^3

NOTE: Volumes greater than 1,000 L shall be shown in m^3.

		TEMPERATURE (exact)		
°F	Fahrenheit temperature	5/9 (after subtracting 32)	Celsius temperature	°C

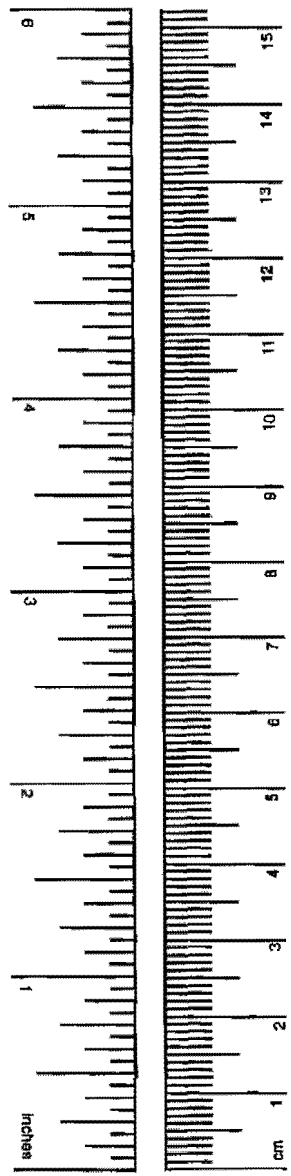

APPROXIMATE CONVERSIONS FROM SI UNITS

Symbol	When You Know	Multiply by	To Find	Symbol
		LENGTH		
mm	millimeters	0.039	inches	in
m	meters	3.28	feet	ft
m	meters	1.09	yards	yd
km	kilometers	0.621	miles	mi
		AREA		
mm^2	millimeters squared	0.0016	square inches	in^2
m^2	meters squared	10.764	square feet	ft^2
m^2	meters squared	1.20	square yards	yd^2
km^2	kilometers squared	0.39	square miles	mi^2
ha	hectares (10,000 m^2)	2.53	acres	ac
		MASS (weight)		
g	grams	0.0353	ounces	oz
kg	kilograms	2.205	pounds	lb
Mg	megagrams (1,000 kg)	1.103	short tons	T
		VOLUME		
mL	milliliters	0.034	fluid ounces	fl oz
L	liters	0.264	gallons	gal
m^3	meters cubed	35.315	cubic feet	ft^3
m^3	meters cubed	1.308	cubic yards	yd^3
		TEMPERATURE (exact)		
°C	Celsius temperature	9/5 (then add 32)	Fahrenheit temperature	°F

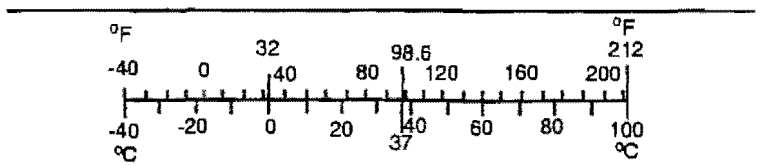

These factors conform to the requirement of FHWA Order 5190.1A.

* SI is the symbol for the International System of Measurements

CHAPTER 1. INTRODUCTION

BACKGROUND

Despite significant improvements in pavement performance design methods—the 1985 version of the *AASHTO Design Guide* is one such example—actual pavement performance very often fails to equal that specified in the original design. These performance inconsistencies result primarily from miscalculations of structural damage that occurs during the pavement's early and older age. Usually, damage resulting from traffic and/or the environment can be predicted. But if the early-age damage is not assessed, its impact on long-term damage will not be known. One of the major consequences of this can be over-prediction of pavement life. This potential problem is a central focus of this study, which identifies improved concrete pavement design and construction procedures that may be used to assess and reduce early-age damage.

Specifically, this study attempts to eliminate as far as possible these demonstrated design and actual performance inconsistencies by (1) improving prediction models relating to concrete properties, (2) developing a probabilistic sawing depth model, and (3) modifying the percent-reinforcement formula. In addressing these issues, we developed three subsystems to handle each task using the systems engineering techniques shown in Figure 1.1. The first subsystem generates alternative models to predict concrete pavement properties. In selecting these alternatives, we sought to determine the compatibility of each model's characteristics to the actual concrete property characteristics. The best alternative was then used to modify the jointed reinforced concrete pavement (JRCP) computer program, a program developed in the mid-1970s to simulate the effect of the environment on the early-age behavior of both jointed plain concrete (JPC) and jointed reinforced concrete (JRC) pavements.

For the second subsystem, we developed a probabilistic sawing model for predicting both the required sawing depth and the most suitable sawing time. These two construction variables cannot be determined by experience alone. The effectiveness of this subsystem, which can also enhance our understanding of the factors causing pavement cracking, relies on the implementation of the first subsystem.

The third subsystem is used to select a more comprehensive procedure for steel design in concrete pavements. The procedure will be useful for the transverse reinforcement design of all concrete pavements and for the longitudinal reinforcement design of jointed reinforced concrete pavements. Usually, subgrade drag theory (see Ref 15) is used for reinforcement design. Yet because there are several factors that affect the required reinforcement, two alternatives will be evaluated. The first alternative is a modified subgrade drag formula; the second uses the improved JRCP computer program.

Using these subsystems, this study proposes improvements to the different prediction tasks. Important implementations include: (1) percent-steel design for transverse reinforcement, and (2) sawing time and depth prediction for longitudinal joints of continuously reinforced concrete pavements (CRCP). The report also discusses the impact on other construction procedures, including joint spacing.

Of the four PCC pavement types—jointed plain, jointed reinforced, continuously reinforced, and prestressed—only jointed reinforced concrete pavements are considered here. While this common pavement type offers several advantages, it also has various problems that can perhaps be best addressed by improved design methodology.

Finally, it should be noted that concrete pavement design procedures require revision based on assessment and feedback. Accordingly, since the algorithm of the JRCP computer program is based on prediction models, the improvement to these models through continuing assessment should, in turn, improve the program's overall prediction.

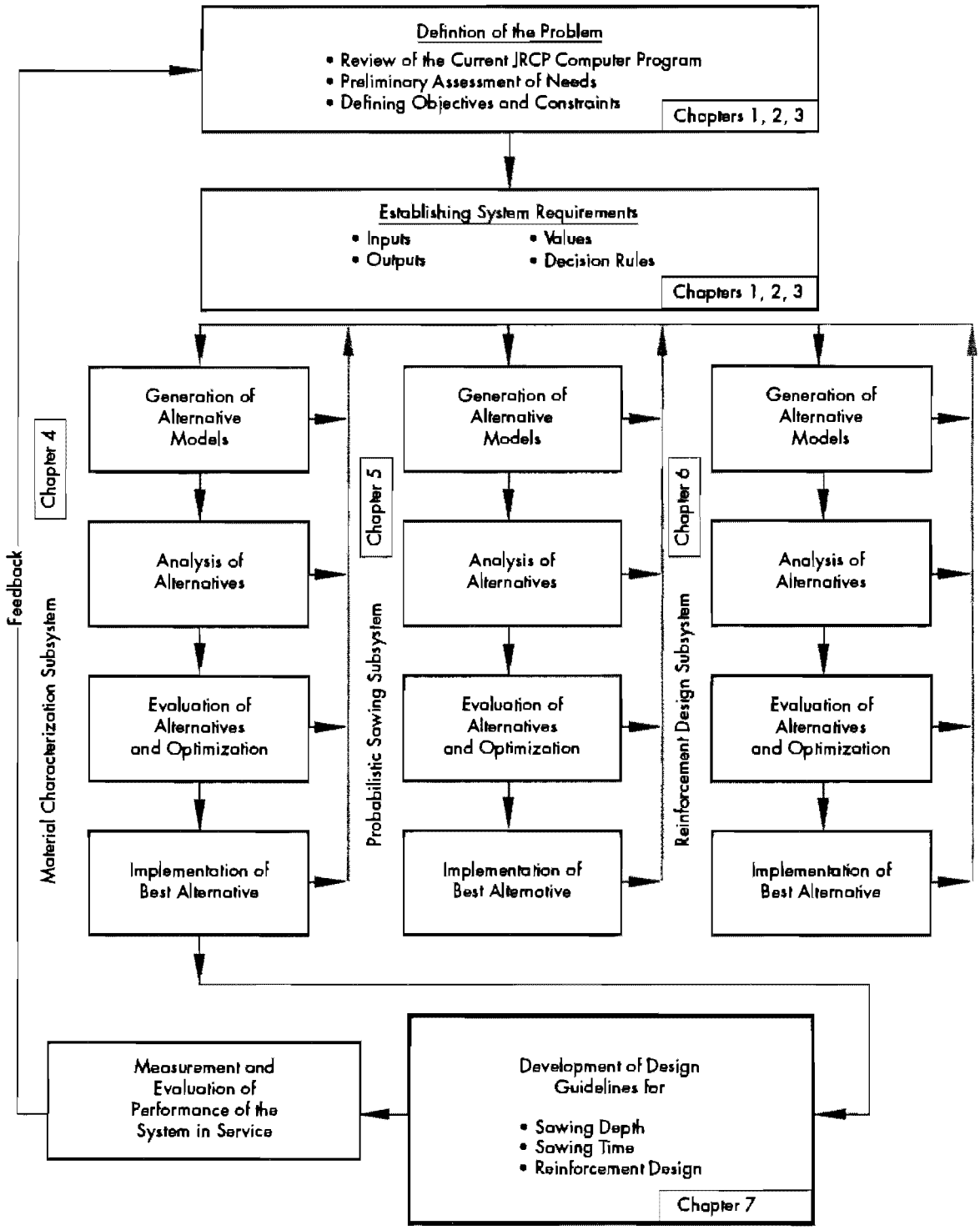

Figure 1.1 Study summary

PREVIOUS STUDIES

Rivero-Vallejo and McCullough (Ref 1) created the first version of the JRCP computer program in 1975. That program was developed to simulate only the effect of the environment on the early-age behavior of JPC and JRC pavements. Since then, the program has been modified with results obtained from field observations. (The main features of each version of the program are described in Appendix A.) This study was initiated to modify some of those prediction models.

OBJECTIVES OF THE STUDY

The primary objective of this study was to improve the predicted response of jointed plain and jointed reinforced concrete pavements exposed to environmental changes. Within this specific objective, the following tasks were identified:

(1) to upgrade the prediction models for concrete properties;
(2) to implement the improved prediction models in the JRCP computer program;
(3) to use the JRCP computer program to evaluate the theoretical formula used for percent reinforcement prediction;
(4) to develop a probabilistic sawing depth model to predict the required sawing depth for the given concrete properties; and
(5) to use the improved JRCP computer program in the reinforcement design and concrete stress prediction for probabilistic sawing depth and time model.

SCOPE OF STUDY

To accomplish these objectives, a systems methodology was used in which:

(1) concrete properties were characterized by considering only the coarse aggregate type, age, and concrete pavement geometry;
(2) the improved characterization prediction models were compared with laboratory test results;
(3) a probabilistic sawing method was developed based on field measurements and observations; and
(4) evaluation of the JRCP-5 computer program was based on steel stress, crack width, and joint opening.

SCOPE OF THE REPORT

Whereas this chapter has provided background and objectives, Chapter 2 identifies the limitations of the current JRCP computer program. Chapter 3 summarizes concrete property responses to different environmental conditions and briefly explains the major factors contributing to pavement cracking. Chapter 4 discusses the prediction model modifications, along with the evaluation of the previous models used in the computer program and describes the implementation of the prediction models into the JRCP computer program.

Chapter 5 documents the development of a probabilistic sawing depth model to predict the required saw depth for given concrete properties. The chapter also discusses the JRCP computer program relating to the implementation of sawing. Chapter 6 evaluates the theoretical-percent-reinforcement formula and includes the implementation of the new JRCP computer program in the reinforcement design and concrete stress prediction for probabilistic sawing depth and time model. Futhermore, this chapter compares the subgrade drag formula for percent-reinforcement estimation with the computer program capabilities.

Chapter 7 discusses the development of design guidelines for reinforcement design and for sawing depth and time. Finally, Chapter 8 evaluates the research findings and concludes that the improvement in the prediction models of concrete properties reduces the discrepancies between the predicted and the actual properties.

CHAPTER 2. JOINTED REINFORCED CONCRETE PAVEMENT BEHAVIOR

INTRODUCTION

This chapter describes, first, concrete pavement behavior in general and, second, the failure of the current JRCP computer program to predict such behavior accurately. Treating these subjects in tandem was considered necessary, since the adequacy of the JRCP computer program cannot be determined without some knowledge of concrete pavement behavior.

CONCRETE PAVEMENT BEHAVIOR

Concrete pavements exhibit some characteristics that are common to all concrete structures and some that are specific to their functioning as pavements. Because literature on the common characteristics of concrete structures (e.g., gaining strength with age) is readily available, this chapter discusses only those characteristics specific to concrete pavements, particularly newly constructed concrete pavements. These discussions are then used as a basis for the modifications to the JRCP computer program described in Chapter 4.

Factors Affecting JRCP Behavior

Pavement behavior is influenced variously by several factors. These factors include (1) indirect environmental factors, (2) direct environmental factors, and (3) external load. Obviously, the more factors considered, the more time required to develop the design inputs. For reasons of practicality, only direct environmental factors were investigated. It was anticipated that such an approach, because it related to early-age pavements, would lead to more precise explanations of concrete pavement behavior. The other two factors (external load and indirect environmental factors) did not directly pertain to the study, since they relate primarily to older pavements.

The direct environmental factors affecting concrete pavement include those that induce tensile or compressive stresses in the slab as a result of temperature and moisture variation. In the previous versions of the JRCP computer program (JRCP Versions 1-4), curing temperature, used as the reference temperature, was defined as the ambient temperature at the time of placement. Actually, concrete starts to gain strength (cure) some time after placement, when concrete temperature is higher than ambient temperature (a result of the heat of hydration and the prevailing weather conditions in the field). Accordingly, concrete temperature corresponding to the onset of strength gain should be considered the curing temperature.

The available field information shows that during sunny days the ambient and slab temperatures more or less follow a sinusoidal curve, as illustrated in Figure 2.1. Also capable of being represented by a sinusoidal curve is daily slab temperature variation, as confirmed by Richardson and Armaghani (Ref 4). The consequent assumption of these findings—that the surface temperature of the slab is basically the ambient temperature lagged for several hours—greatly simplifies the slab temperature calculation at any given time.

There are other direct environmental factors affecting concrete pavement. For example, concrete drying shrinkage, which is dependent on the temperature and moisture variation, causes compressive stress in steel and tensile stress in concrete (a consequence of the thermal coefficients of concrete and steel being approximately of the same magnitude). The moisture variation within concrete, typically assumed to be constant, causes differential drying shrinkage. (A detailed explanation of this phenomenon is included in the cracking process section of this chapter.)

JCP and JRCP Behavior

JCP and JRCP generally exhibit similar behavior. Behavioral differences derive from the use of steel reinforcement in the latter, though such usage does not always increase the strength of the concrete. When a concrete pavement cracks, the steel becomes active and transfers the load across the crack. Differential soil movement underneath the pavement can lead to slab cracking and thus

to load transfer through the reinforcing steel. For this reason, frictional resistance at the slab-subbase interface is also an important factor in the analysis of JRCP.

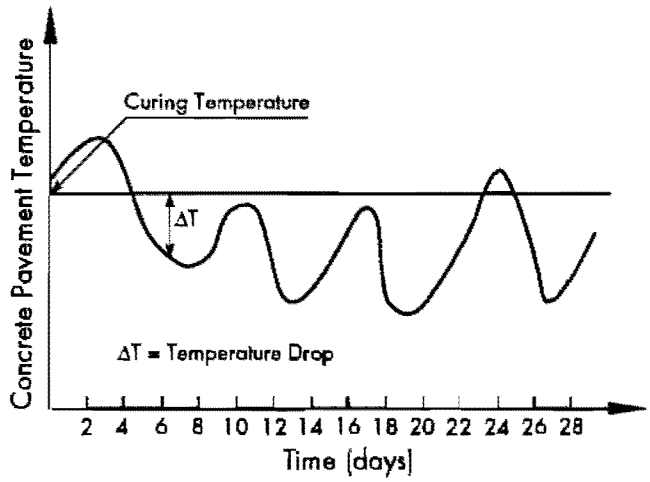

Figure 2.1 Variation of daily temperature with time

The purpose of using reinforcing steel in jointed concrete is to limit crack size and spacing. Such usage yields cracks that (1) are tight enough to prevent water percolation, (2) provide high load-transfer efficiency, and (3) minimize spalling. This is also true for joint opening. Thus, in the analysis of JRCP, the following can be used as design criteria to control the problems mentioned above:

(1) joint opening,
(2) crack width, and
(3) steel stress (JRCP).

CRACKING PROCESS

The following discussion, based on a literature review, focuses on the major causes of cracking. Also discussed is the progression of concrete properties toward their maximum values under the influence of variable environmental conditions.

Factors Causing Cracking in Concrete

Concrete generally cracks when its combined stresses exceed its tensile strength. Cracking is more likely to occur during the early age of the pavement, when concrete strength is low and concrete property variations increase the probability of distress manifestations.

Cracking in concrete structures can be the result of the following stresses or conditions:

(1) environment;
(2) modulus of elasticity and tensile strength of the pavement;
(3) related properties of concrete (e.g., drying shrinkage, thermal coefficient);
(4) slab-subbase interface frictional resistance; and
(5) wheel load stress.

Only the first four factors, because they are influential during the pavement's early ages, are covered in this study. Wheel load stress is influential only after the pavement is opened to traffic.

Although cracking cannot be prevented, it can be controlled. An effective pavement design can address a combination of the above factors in a way that yields cracks of minimum width and, hence, pavements that require less maintenance. But what is a good combination? Or the best combination? Because such questions cannot be answered intuitively, the study team used a computer program to identify the optimum combination yielding the most favorable concrete pavement response. The types and causes of concrete cracking, both before and after hardening, are shown in Figures 2.2 and 2.3, respectively.

Drying Shrinkage

Although certain assumptions are made when modeling the drying shrinkage of concrete, the actual factors affecting this condition—listed in Table 2.1—should be well understood.

First, drying shrinkage is either reversible or irreversible. Neville (Ref 7) showed that for given conditions, reversible drying shrinkage occurred only at 100 percent relative humidity. Although the rate of shrinkage was reduced considerably with time, it never reversed at less than 100 percent relative humidity. It is therefore reasonable to assume that the drying shrinkage of concrete pavements is irreversible.

Another important relationship exists between shrinkage and volume/surface area ratio, as illustrated in Figure 2.4 (Ref 7). The relationship between drying shrinkage and volume/surface area ratio is shown for two different aggregate types, Elgin gravel and sandstone, represented respectively by the symbols (■) and (●). Figure 2.4 clearly shows that the higher the volume/surface area ratio, the lower the ultimate shrinkage. Additionally, the less surface exposed to the environment, the lower the ultimate shrinkage.

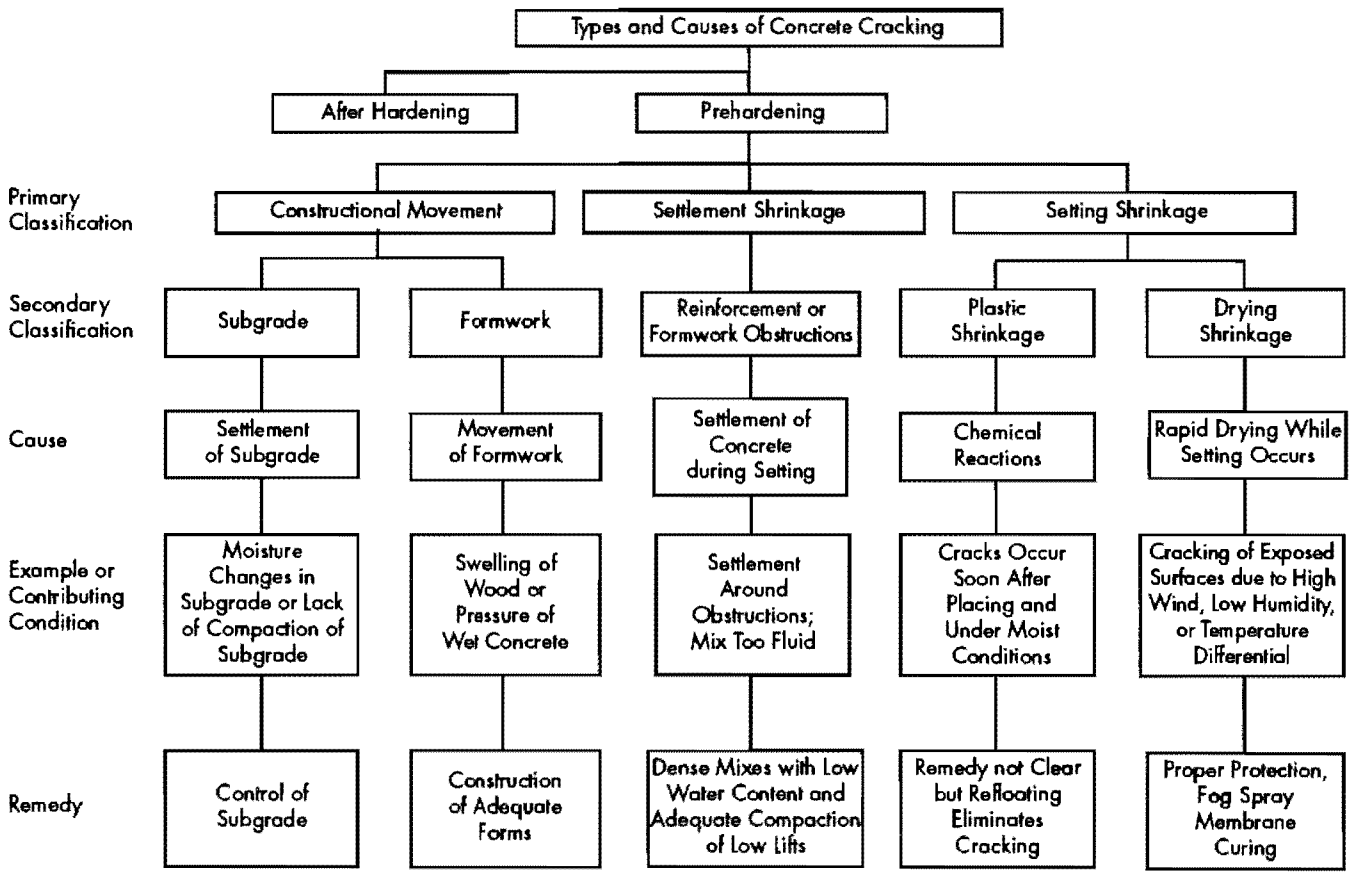

Figure 2.2 Types and causes of concrete cracking, prehardening [5]

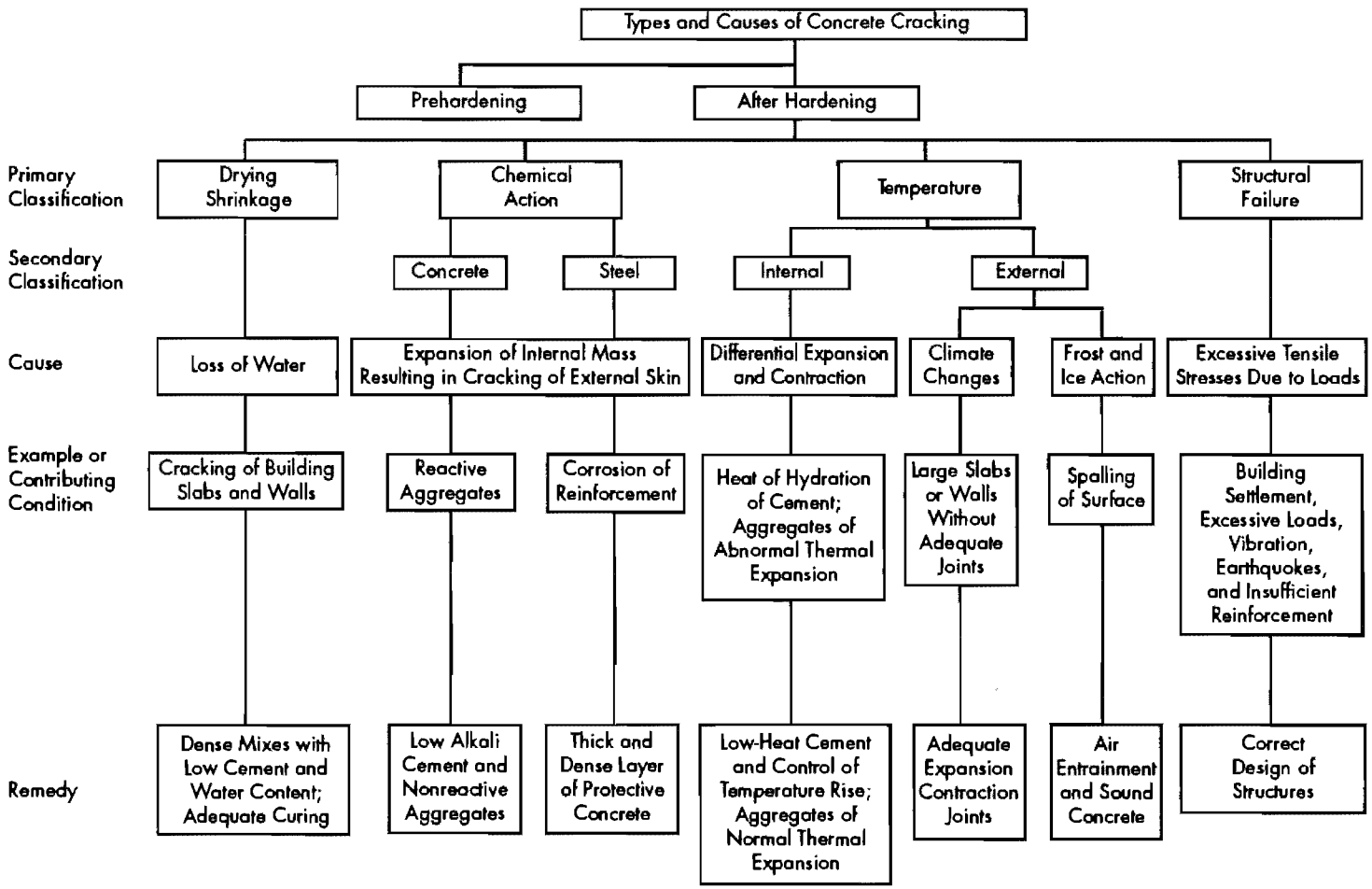

Figure 2.3 Types and causes of concrete cracking, after hardening [5]

Table 2.1 Parameters affecting drying shrinkage and creep

Paste parameters
- Porosity, Age of paste } w/c ratio and degree of hydration
- Curing temperature
- Cement composition
- Moisture content
- Admixtures

Concrete parameters
- Aggregate stiffness
- Aggregate content (cement content)
- Volume/surface ratio
- Thickness

Environmental parameters
- Applied stress, Duration of load } affect only creep
- Relative humidity
- Rate of drying
- Time of drying

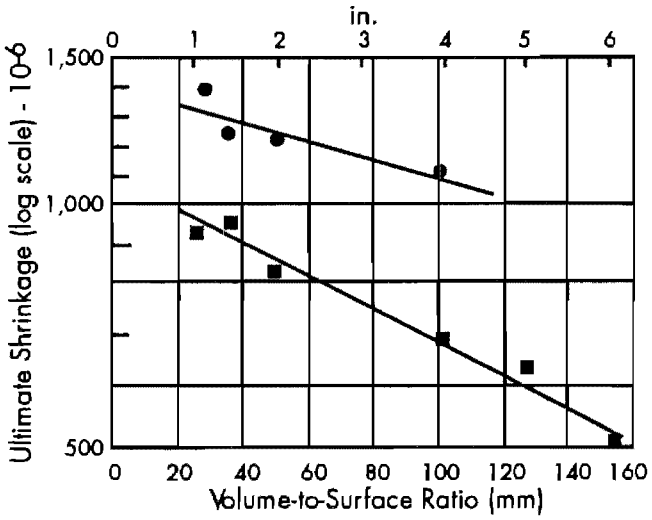

Figure 2.4 Effect of volume/surface area ratio on drying shrinkage for two aggregate types (Ref 7) (■ = Elgin gravel and ● = sandstone)

Data analysis indicates high correlation between concrete strength and the concrete modulus of elasticity. One inconsistency in this relationship is the moisture dependency of concrete properties: During the curing period, the strength of dry concrete is greater than the strength of saturated concrete; however, the opposite holds for modulus of elasticity. Therefore, the degree of correlation depends on curing condition.

During a concrete's early age, both drying shrinkage and temperature variation have equally strong effects on concrete stress. As the pavement ages, drying shrinkage ultimately reaches its maximum percentage, leaving temperature variation as the single dominant (environmental) effect. The stresses induced by temperature variation depend on the magnitude of the thermal coefficient of concrete.

The variation of concrete drying shrinkage among the different coarse aggregate types is shown in Figure 2.5. As indicated, there is significant variation in the drying shrinkage of different aggregates (similar to the influence of aggregate type on other concrete properties). But because these results were obtained through controlled experiments, they do not necessarily represent the precise shrinkage of a structure built in a variable environment.

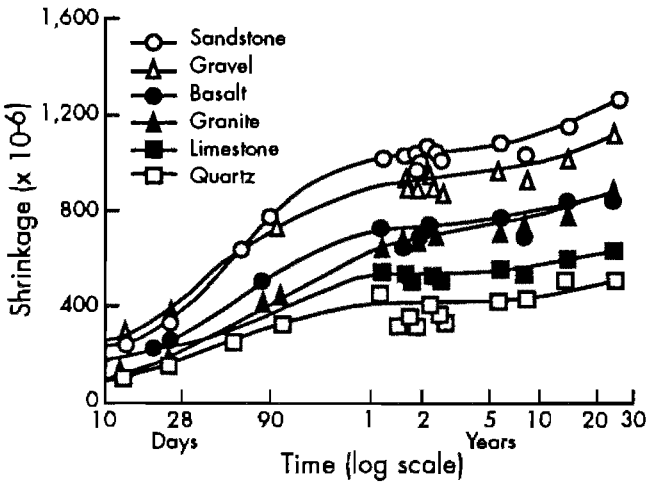

Figure 2.5 Aggregate effect on concrete shrinkage: air temperature at 21°C (70°F) and relative humidity at 50 percent (Ref 7)

A high percentage of drying shrinkage occurs during the early age of the concrete, as shown in Figure 2.6. The following percentages (lower and upper limits) were observed:

(1) 14 to 34 percent of the 20-year shrinkage occurs within 2 weeks,
(2) 40 to 80 percent of the 20-year shrinkage occurs within 3 months, and
(3) 66 to 85 percent of the 20-year shrinkage occurs within 1 year.

Relative humidity is another important parameter that should be considered in the model. Figure 2.7 shows the trend in shrinkage of concrete specimens with time for three different relative humidities: 50, 70, and 100 percent. It is clear that shrinkage occurs at a diminishing rate over time for 50 and 70 percent relative humidity. On

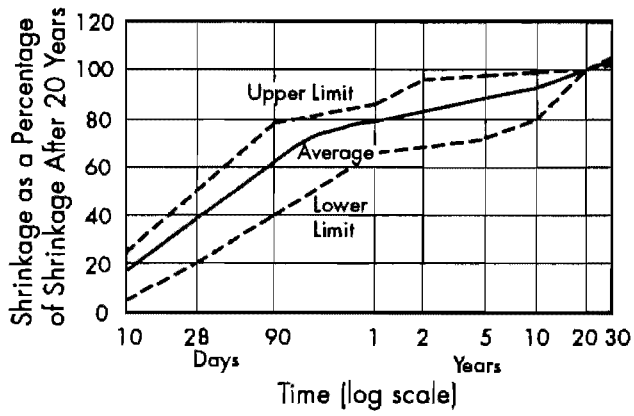

Figure 2.6 Range of drying shrinkage of concrete (Ref 7)

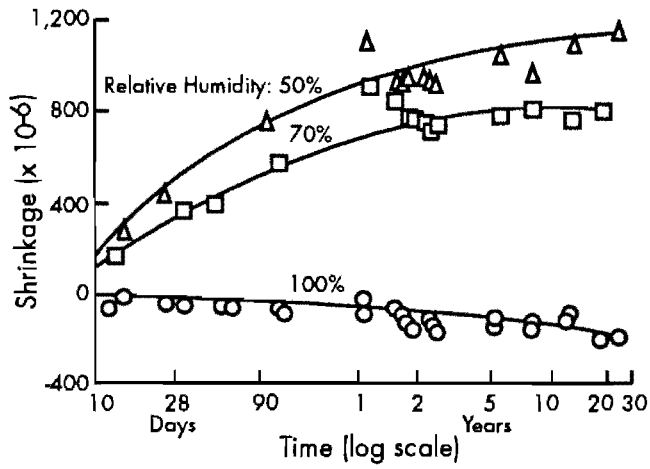

Figure 2.7 Relationship between drying shrinkage and relative humidity of concrete (Ref 7)

the other hand, it recovers after a certain age at 100 percent relative humidity, suggesting that a certain portion of the shrinkage is recoverable when environmental conditions are favorable.

Several researchers (Refs 7, 8) used the volume/surface area ratio as a parameter to establish a relationship between shrinkage and volume/surface area ratio. For concrete pavement, we can assume that moisture moves only from the surface; thus, the volume/surface area ratio equals the thickness of the pavement. Although the volume/surface ratio affects the rate of drying shrinkage, the ultimate drying shrinkage remains unchanged.

The shrinkage will differ with different slab thicknesses, with the measured difference dependent on the sensitivity of the shrinkage prediction model to the thickness of the pavement. In support of the above approach, Figure 2.4 illustrates the linear relationship between volume/surface area ratio and the logarithm of the ultimate shrinkage. As shown in that figure, the ultimate shrinkage decreases as the thickness increases.

Drying shrinkage alone may cause cracks under certain conditions—for example, when the shrinkage strain is higher than the tensile strength (f_t)/modulus of elasticity (E_c) ratio. The ratio of tensile strength to modulus of elasticity is defined as the tensile strain capacity of concrete.

Under field conditions, concrete stress is caused not only by shrinkage, but also by the interaction of concrete, reinforcement, and the frictional resistance at the slab and subbase interface. The effect of temperature drop results in slab movement, which is restrained by the subbase friction (the magnitude of friction is proportional to the movement). Since the thermal coefficients of both concrete and steel are approximately the same, each restrains the other equally. Therefore, concrete shrinkage is a primary contributor to the tensile stress in the concrete and to the compressive stress in the steel.

SUMMARY

In addition to describing the effect of environment on pavement behavior, this chapter has identified the current model's weakness in estimating environmental effects. The revision of the model, which is discussed in Chapter 4, covers the procedures identified in this chapter.

The cracking process, literature, and influence of the environment on each property of concrete were also discussed. As outlined, moisture has an adverse effect on the compressive strength and modulus of elasticity of concrete. This was one of the primary reasons that the Center for Transportation Research of The University of Texas at Austin (Ref 11) developed separate prediction models for each property of concrete. These prediction models are included in Chapter 4 of this report.

CHAPTER 3. EXISTING DESIGN PROCEDURE AND NEEDED RESEARCH

INTRODUCTION

JRCP-4, the jointed reinforced concrete pavement analysis program used for pavement design, is limited in its ability to predict actual pavement response. This chapter summarizes the capabilities and limitations of this analysis program.

CURRENT DESIGN PROCEDURE

In JRCP-1, the computer program developed to predict the behavior of JPC and JRC pavements, prediction models were mathematical formulations of the relationship between independent variables and the dependent variable represented by the concrete property. Because correct implementation of these mathematical models required certain assumptions, the program was updated several times, culminating in the current JRCP-4 version. Now, revision of the prediction models in the JRCP-4 computer program is necessary to implement recent findings. (Details of these models are included in Chapter 4.)

In looking at current JRCP design procedures, we note that they are based on a model that includes the following:

(1) Transverse joints should have cost-effective, optimum spacing to minimize joint roughness.
(2) Steel is used to control crack spacing and width.
(3) Sufficient reinforcement should be used to keep the crack widths tight enough to minimize water percolation and to ensure acceptable steel stresses.
(4) Load transfer devices (dowels) are used across the transverse joint.

Using these guidelines and principles, the following section evaluates the JRCP model used in the JRCP-4 computer program.

EVALUATING THE JRCP-4 PROGRAM

The JRCP-4 computer program algorithm consists of several mathematical models, each of which affects the results of the program. The major shortcoming of the JRCP-4 algorithm is the limitation of its models in predicting the behavior of actual concrete properties. For this reason, the prediction models should be revised to include factors believed to be relevant. While some of these problems can be corrected with very little effort, the rest require enormous revision (e.g., rewriting the program). Thus, only the former group of problems is considered here, with modifications addressing only the model's (1) use of daily temperature exclusively, (2) lack of hourly temperature input, and (3) limited ability to predict concrete properties (and thus its requirement for revision to incorporate results from recent studies).

NEEDED RESEARCH

Engineers often develop mathematical models to simulate observed behavior. Although such models invariably contain certain limitations and assumptions, they should obey some boundary conditions, be valid for certain assumptions, and be practical enough to provide for quick, reliable, and logical simulations of reality. In attempting to fulfill these requirements, the study team included in the updated model two parameters not considered in earlier versions of the JRCP program. These parameters are (1) frictional resistance of the subbase layer, and (2) variability of concrete properties.

Frictional Resistance of the Subbase Layer

Current research results (Refs 2 and 3) are included in the updated model in order to eliminate

further misrepresentation of any subbase type. The formula for the design of transverse reinforcement of continuously reinforced concrete pavements was thus revised and is included in Chapter 5.

Variability of Concrete Properties

Because the accuracy of the probabilistic model depends on the accuracy of the deterministic model on which it is based, the study team sought first to improve the deterministic model. Furthermore, in improving the deterministic model, study personnel used average values of actual field conditions and laboratory data. Only important concrete properties relating to the sawing depth procedure were assumed to vary, primarily because of the excessive time required for a probabilistic approach and because of the relative effects of each property.

NEW PROGRAM

Following an evaluation of JRCP-4, we developed a new version of the computer program, designated JRCP-5, which now features a modified algorithm that substantially improves the prediction models. The principles guiding the development of this program are briefly discussed below.

Systems Approach to the Development of the New Program

The systems methodology for this project consists of the following:

(1) generation of alternative methods;
(2) analysis of alternatives;
(3) evaluation of alternatives and optimization; and
(4) implementation of best alternative.

Generation of Alternative Methods

Following the evaluation of the current method, a set of alternatives was selected either to replace or modify the current method. The purpose of generating alternative strategies or methods is to implement fully the contents of the objectives while satisfying the limiting criteria.

Analysis of Alternatives

The capabilities and the accuracy of each alternative should be analyzed before any evaluation of the alternatives. Therefore, every alternative was analyzed to reveal all positive and negative findings associated with that specific alternative.

Evaluation of Alternatives and Optimization

Evaluation of the alternatives involves comparing their accuracy and ability to address the demands set by the objectives. The findings of the above analysis were used to evaluate every alternative and to optimize the benefits of the best alternative.

Implementation of Best Alternative

Upon the selection of the best alternative, appropriate implementation completes the cycle of the systems methodology. The implementation step, which allows the user to observe the difference between the best alternative and the actual problem, is one of the key elements in this approach. Following this step within the systems methodology, feedback is used to begin the cycle again. For this study, only one cycle of the systems methodology was implemented.

CHAPTER 4. MATERIAL CHARACTERIZATION SUBSYSTEM

BACKGROUND

This chapter describes the modification of the JRCP-5 computer program prediction models. Following the description of the prediction programs, the sufficiency of each model is evaluated and the significance of the modifications is explained. The concrete properties measurements performed at The University of Texas at Austin served as the main feedback source for modifying the prediction models. Particularly useful were the findings of Center for Transportation Research (CTR) Project 422, "Evaluation of Pavement Concrete Using Texas Coarse Aggregates," which described the relationship between concrete properties and time (see Ref 11).

Finally, because the verification of models used for concrete properties characterization relies on both laboratory and field measurements, the research team investigated the adequacy of the models in predicting the response of concrete pavements under field and laboratory conditions.

DESIGN CONSTRAINTS

To accomplish the objectives stated in Chapter 1, the study team developed the prediction models described in this chapter according to the following:

(1) Prediction models should incorporate only the time dependency and effect of coarse aggregate type.
(2) The prediction model for drying shrinkage should incorporate the effect of concrete pavement thickness.
(3) The prediction models of concrete properties are valid only for the coarse aggregate types/ sources used within Texas.

GENERATION AND EVALUATION OF THE PREDICTION MODELS

The generation of alternatives is one of the steps of material characterization, as discussed in Chapter 1. In this section, drying shrinkage, tensile strength, and modulus of elasticity prediction models are generated and evaluated.

Drying Shrinkage Model

The current prediction model for drying shrinkage does not take into account the coarse aggregate type used. The formula developed by Hansen and Mattock (Ref 8) to predict the total drying shrinkage at any time (see Equation 4.1) served as a basis for the modified model. Because Hansen and Mattock relied on an aggregate type uncommon in Texas, their prediction model is not directly applicable to Texas conditions. What *is* applicable, however, is the formulation of the model. A summary of the drying-shrinkage-model evaluation study is illustrated in Figure 4.1.

$$\frac{Z_t}{Z_f} = \frac{t}{M + t} \tag{4.1}$$

where:

$M = 26e^{0.36[\frac{v}{s}]}$;
e = base of Naperian log;
t = time after concrete setting, days;
v = volume of the member, inch^3;
s = exposed surface area, inch^2;
Z_t = drying shrinkage at time t, and

$$= \left[\frac{t}{26e^{0.36D} + t}\right] Z_f;$$

Z_f = final drying shrinkage;

$\frac{v}{s}$ = D; and

D = slab thickness, in.

Equation 4.1 was developed from CTR Study 422 test results. During the experiment, the specimens were cured at 75°F and at 40 percent relative humidity. The new equation has the following form:

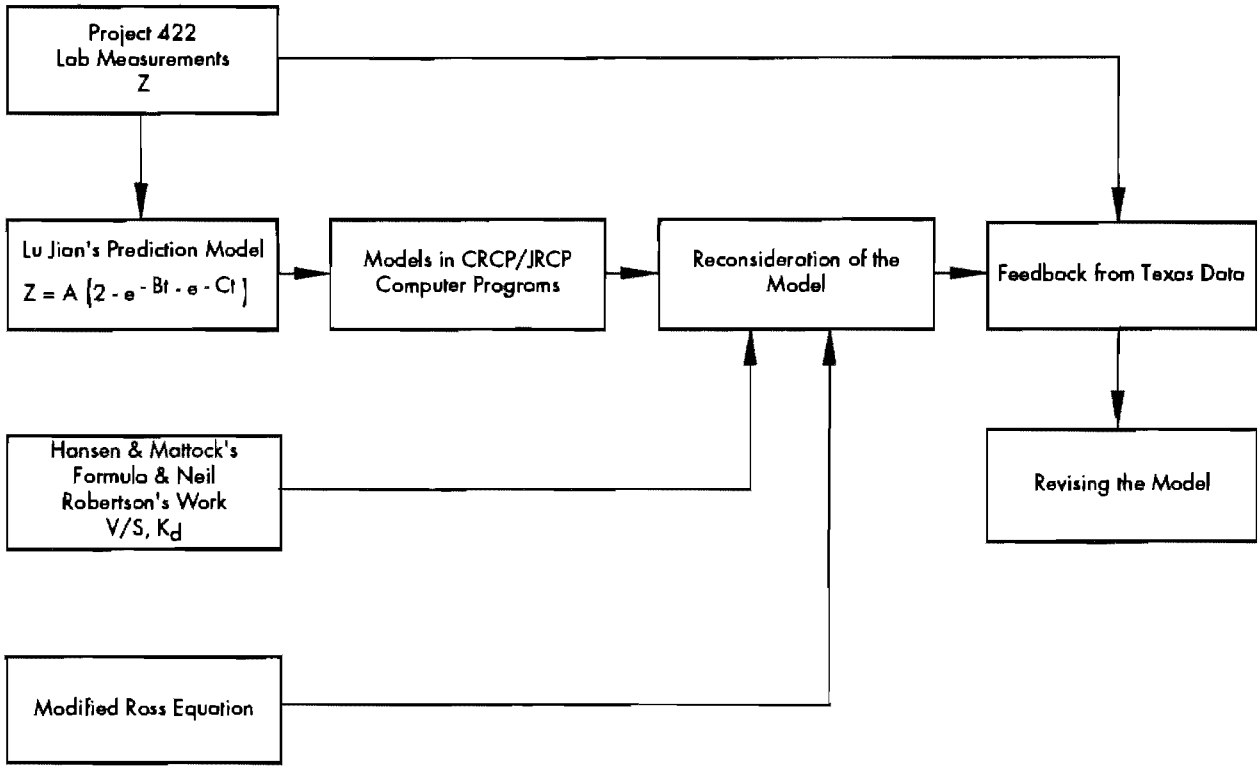

Figure 4.1 Summary of evaluation of available drying shrinkage models (Refs 8, 10, 11)

$$\frac{\varepsilon_{sh}}{\varepsilon_{ult}} = \frac{t}{BN_s + At} \qquad (4.2)$$

where:

ε_{sh} = the calculated drying shrinkage at age "t", in./in.;
ε_{ult} = the ultimate drying shrinkage, in./in.;
A, B = coefficients for the coarse aggregate type;
N_s = $26e^{0.36D}$; and
D = slab thickness, in.

The coefficients A and B are given in Table 4.1, and the predicted drying shrinkage values for different concrete pavement thicknesses are shown in Figure 4.2. A comparison of predicted and observed values with the new formula are given in Figures 4.3 and 4.4 for limestone and siliceous river gravel, respectively.

Another alternative prediction model (Ref 9) was considered as a candidate for the final drying shrinkage prediction model. Again, this model was developed from CTR Study 422 test results. The form of the equation is

$$\frac{Z_{(t)}}{Z_{28}} = A\left(2 - e^{-B*t} - e^{C*t}\right)$$

Table 4.1 The coefficients used in the modified Hansen and Mattock Equation

CAT	Coefficient A	Coefficient B
Granite	0.96791	0.28324
Dolomite	0.87947	0.69540
Vega	0.85818	0.80719
BridgeTT	0.87036	0.72199
West-Tacosta	0.86383	0.76564
Ferris	0.96674	0.34472
Limestone	0.85424	0.91540
SRG	0.95164	0.65761

This model has several limitations. First, the effect of thickness is not included in the formula. Second, drying shrinkage remains the same after 28 days. Because these two observations contradict the field observations, this model was dropped from the alternative list.

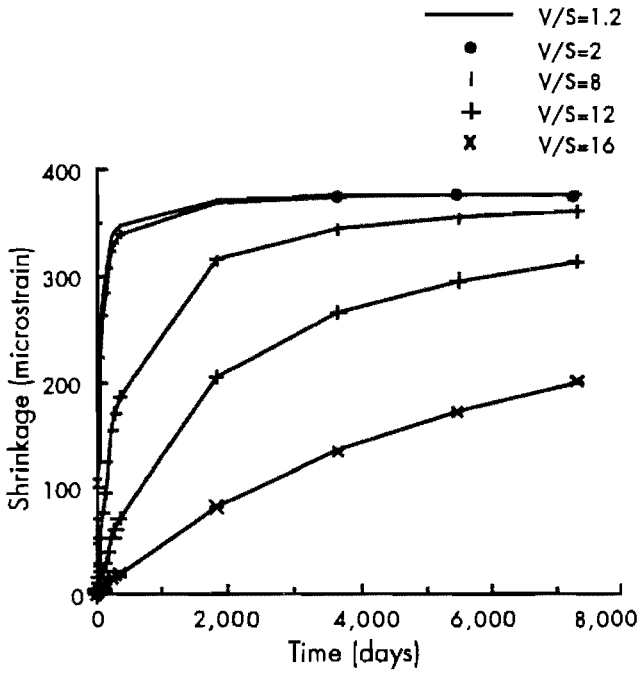

Figure 4.2 Revised Hansen and Mattock equation, CAT = dolomite (from Equation 4.2)

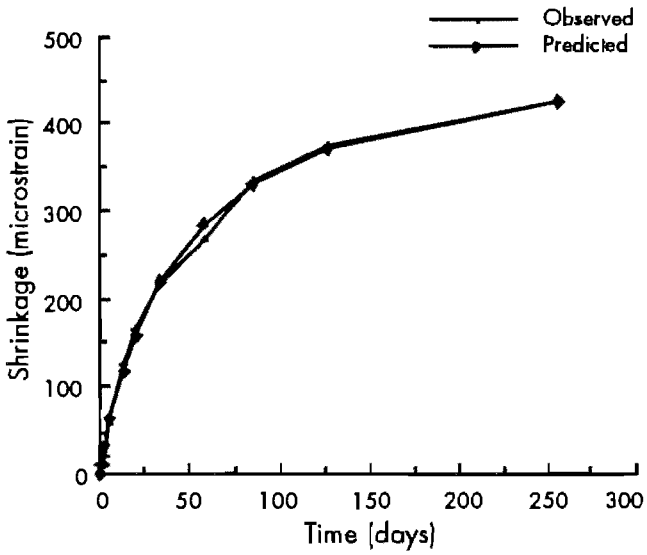

Figure 4.3 Comparison of predicted shrinkage values with calculated values, CAT = limestone. (Each point of observed values represents the average of three specimens.)

Tensile Strength Model

In the previous version of the JRCP computer program, the user input the tensile strength at certain ages (from 1 day to 28 days). CTR Project 422 (Ref 11) developed a tensile strength formula that enables the JRCP-5 program to predict tensile strength at any age and for any aggregate type. The formula is given in Equation 4.3:

$$\frac{ft_{(t)}}{ft_{28}} = A\left(2 - e^{-B*t} - e^{C*t}\right) \qquad (4.3)$$

where:

$ft_{(t)}$ = splitting tensile strength of concrete at any age (t), psi;
ft_{28} = splitting tensile strength of concrete at age of 28 days; and
A, B, C = coefficients for the coarse aggregate type.

The coefficients A, B, and C are listed in Table 4.2.

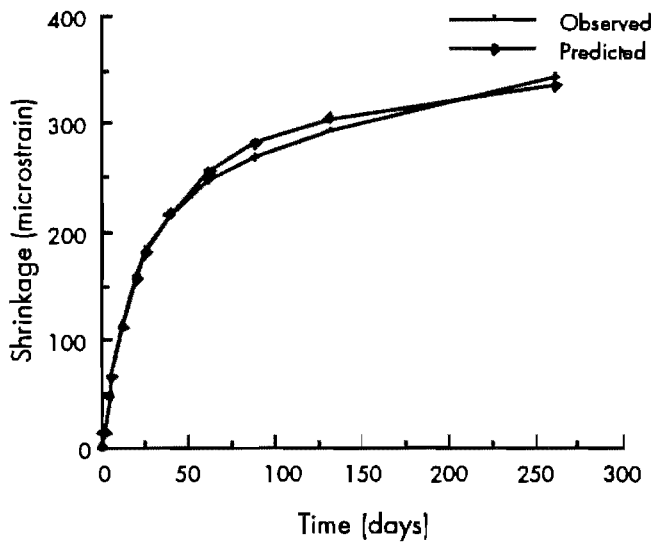

Figure 4.4 Comparison of predicted drying shrinkage values with calculated values, CAT = siliceous river gravel. (Each point of observed values represents the average of three specimens.)

In searching for the most suitable prediction model, we also considered an alternative that identified the relationship between concrete tensile strength and compressive strength—a formulation used by the American Concrete Institute. This relationship assumes that compressive strength alone is sufficient for estimating tensile strength.

Ultimately, this alternative also proved to be flawed. In Texas, pavement engineers use different aggregates, including siliceous river gravel, limestone, or a blend of both. (Information on each aggregate type is given in Table 4.3.) Because the performance of each aggregate differs, the relationship used to derive tensile strength from compressive strength is not valid for this case. Consequently, this alternative was dropped from the evaluation. The best alternative is the prediction model shown in Equation 4.3.

Table 4.2 Tensile strength normalized to 28 days

Coarse Aggregate Type

Coefficient	Granite	Dolomite	Vega	BridgeTT	W-T	Ferris	LS	SRG
A	.504	.500	.500	.500	.501	.505	.502	.500
B	.15	.261	.302	.332	.198	.137	.177	.267
C	1.05	1.094	.3014	.723	2.505	2.479	1.068	.468

Table 4.3 The information on coarse aggregate sources used in Texas for construction of concrete pavement

CAT	Source	Producer	Origin
Granite	Granite	TxTx Aggregates	Scotland
Dolomite	Dolomitic limestone	El Paso Sand Products	McKelligan Canyon
Vega	Siliceous river gravel	Vega Sand and Gravel	Tom Green Pit
BridgeTT	SRG and limestone	Texas Industries	Tin Top Plant
West-Tacosta	SRG and limestone	Western Sand and Gravel	Tacosta Plant
Ferris	SRG and limestone	Texas Industries	Ferris Plant
Limestone	Limestone	Texas Crushed Stone	Georgetown
SRG	SRG	Fordyce Gravel	Chipley Pit

Modulus of Elasticity Model

The modulus of elasticity model used in the previous versions of the JRCP computer program was a function of unit weight and compressive strength. The coarse aggregate type effect was not considered in the formula given in Equation 4.4 below. Like the alternative given in the previous section for tensile strength prediction, this formula is also short of the required capability. First, there is only one relationship existing for any aggregate source. CTR Project 422 found that the relationship between compressive strength and modulus of elasticity varies from one ag-gregate type/source to another. Therefore, this relationship (Equation 4.4) does not completely characterize the aggregate types used in Texas.

$$E_c = \gamma^{1.5} 33 \sqrt{f'_c} \qquad (4.4)$$

where:

E_c = modulus of elasticity of concrete at 28 days, psi;
γ = unit weight of concrete, lb/ft^3; and
f'_c = compressive strength of concrete at 28 days, psi.

The new prediction formula for modulus of elasticity is given in Equation 4.5:

$$\frac{E_{(t)}}{E_{28}} = A\left(2 - e^{-B*t} - e^{C*t}\right) \qquad (4.5)$$

where:

E_t = modulus of elasticity of any age (t) measured by unconfined compression test, psi * 10^6;
E_{28} = modulus of elasticity at 28 days, psi * 10^6; and
A, B, C = coefficients for the coarse aggregate type.

The coefficients A, B, and C are shown in Table 4.4.

SUMMARY

In this chapter, a systems methodology has been implemented to generate, analyze, and evaluate alternative prediction models for concrete properties. The prediction models of the previous computer program were replaced with models capable of characterizing the concrete aggregate properties. Most of the prediction models were based on the correlation of concrete properties, with each having the advantage of predicting each property individually. As explained, the new models are preferable to earlier ones, though they are still not completely error free.

A new version of the JRCP computer program was developed to obtain essential information on concrete pavement response to variations in environment and material properties during early life. The program may be used for revising the specifications on sawing time and depth.

Table 4.4 Modulus of elasticity normalized to 28 days

Coarse Aggregate Type

Coefficient	Granite	Dolomite	Vega	BridgeTT	W-T	Ferris	LS	SRG
A	.500	.500	.500	.500	.500	.500	.500	.500
B	.78	.485	.301	.688	.688	.738	.535	.574
C	1.65	3.537	1.574	2.00	2.00	2.668E12	110.46	61,755.07

CHAPTER 5. PROBABILISTIC SAWING DEPTH AND TIME PREDICTION

INTRODUCTION

For as long as concrete pavements have been constructed, engineers have been concerned about the early cracks forming in those pavements. To mitigate such cracking, they use pavement joints; and if sawing is used to form these joints, then both the sawing depth and time become critical considerations if cracks are to be confined within the joint. While engineers in the past could only defer to experience in attempting to resolve these problems of crack formation, more precise solutions can now be obtained through probabilistic mathematical models. In this chapter, two different alternatives based on probabilistic methods are considered in the selection of the most suitable sawing model. This chapter describes the analysis and evaluation of both models.

Joint sawing is not a new method for controlling random cracking of concrete pavements. The sawing time of a joint was previously determined by observing pavement response to internal load (the load that is developed as a function of the temperature and moisture variation). Then, an adequate margin of safety was established between the time of first crack occurrence and sawing. Sawing time using the above approach will cause (1) the coarse aggregates to rotate, (2) the bond to loosen, and (3) premature weakness to develop in that area. On the other hand, early sawing of the joint eliminates random cracking near the joint.

GENERATION OF MATHEMATICAL MODELS

A probabilistic method does not guarantee the prediction of the actual pavement response. Since it is developed as a mathematical model, such a method might have some drawbacks. It is for this reason that, once the probabilistic model is developed, feedback is necessary to calibrate the model. Using a probabilistic model increases the accuracy of predicting the optimum sawing depth under given conditions. Thus, the percentage of pavement having random cracks will be reduced, resulting in less pavement repair, less maintenance cost, and greater structural integrity.

Using JRCP-5 Computer Program

This section covers the development of a probabilistic sawing method that uses the JRCP-5 computer program to predict concrete stress. This method is applicable both to transverse sawing of JCP and JRCP and to longitudinal sawing for any concrete pavement type. To minimize random cracking, a probabilistic method is developed to estimate the appropriate sawing depth and time for a given reliability level. The following sections of this chapter present a detailed explanation of the problem and its solution.

Theoretical Sawing Depth Model

This alternative, based on a probabilistic model, was developed to model random cracking observed in the field (Ref 12). Its development made use of the Monte Carlo Simulation Method to calculate the reliability level for the given set of inputs.

CONCEPTUAL APPROACH

In developing the probabilistic sawing model, we assumed that the variation in concrete unit strength (f_t) and pavement thickness (D) was normally distributed. The cross-sectional strength of concrete is the product of unit strength and the thickness, assuming that a unit length is used in the calculation. Since thickness is independent of unit tensile strength, this product is also normally distributed. Before describing the model, it is necessary to explain the importance of sawing time and depth. Because sawing is time independent, additional techniques are developed to give guidelines for sawing time as well.

Procedure for Sawing Time

Analyzing what occurs during and after sawing will clarify the importance of this operation. At the cracked concrete section, all the force carried by the concrete will be transferred to steel. But if the concrete cracks after sawing, the applied load, again transferred to steel, remains the same. Therefore, the benefit of timely sawing may be twofold. First, the probability of experiencing a random crack away from the joint should be substantially reduced. Second, the horizontal tensile force will be kept low enough to prevent the yielding of steel; therefore, a relationship should be established among reinforcement percentage, concrete tensile stress, and tensile strength.

The purpose of sawing a joint is to control premature cracking of portland cement concrete pavement and to reduce the roughness and spalling caused by pre-forming of the joint. (Premature random cracking away from the sawed joint may also result in spalling.) The sawing time and depth should be such that, for the given material variability and weather conditions, they fulfill their intended purpose. For the prediction of sawing time, the only practical method is the probabilistic procedure that calculates the required saw depth for the given conditions. The alternative—to convert JRCP-5 into a probabilistic model or algorithm—is more time-consuming and may not be as practical. Accordingly, the first alternative was implemented, with steel stress used as a limiting criterion to control the sawing time. The following section describes this approach.

Procedure of Predicting Concrete and Steel Stress

Again, the JRCP-5 computer program was used. A factorial was developed to predict concrete and steel stress at the middle of the slab at ages ranging from 1 hour to 28 hours. To minimize the number of runs from 61,236 to 2,187, the JRCP-5 computer program provided calculations based on the following: any value that is entered is used as mean 28-day concrete property; the program then internally calculates the value of the property for any age desired. If the age is known, as in this case, the program can be made to predict the range of values by checking only one age. The required range of each concrete property was manually calculated, and the values were then used as the 28-day values in the factorial. Thus, the size of the factorial was reduced to 1/28 of the original size. The computer program JRCP-5 uses concrete properties for the given age and calculates the response of the pavement (the calculation is independent of both previous- and subsequent-age predictions). The implementation of this approach is described in Chapter 7.

Formulas for Concrete and Steel Stress

From the JRCP-5 computer program simulations, the following regression equations have been developed:

$$\sigma_c = \frac{0.08*\left(1+100000*\alpha_c\right)^{2.471}*\left(1+\frac{L}{100}\right)^{1.674}*\left(1+\frac{\Delta T}{10}\right)^{2.313}*\left(1+1000000*\varepsilon_s\right)^{0.232}*\left(1+\frac{\tau_R}{10}\right)^{1.363}}{\left(1+\frac{D}{10}\right)^{1.142}} - 1 \quad (5.1)$$

$R^2 = 0.97$

SEE = 0.120

F = 4289.30

$$\sigma_s = 2688 * \left(\frac{\left(2 + (\alpha_c - 0.000005) * 100000\right)^{1.649} * \left(1 + \frac{L}{100}\right)^{0.08} \left(1 + \frac{\tau_R}{10} 0.066\right)}{\left(1 + \frac{E_c}{29000000}\right)^{20.664} \left(1 + \frac{\Delta T}{10}\right)^{0.513}} - 2 \right) \quad (5.2)$$

$R^2 = 0.79$

SEE = 0.084

F = 439.80

where:

σ_c = concrete stress, psi;
α_c = thermal coefficient of concrete, in./in./°F;
L = Length of pavement, ft;
ΔT = temperature drop, °F;
ε_s = shrinkage strain, in./in.;
τ_R = Friction at the slab and subbase interface, psi;
D = pavement thickness, in.;
σ_s = steel stress, psi; and
E_c = modulus of elasticity of concrete, psi.

Sawing Depth

Saw-cut depth is as important as sawing time. Whereas inadequate sawing depth will cause random cracking around the sawed joint, excessive sawing depth will deteriorate the area around the joint (Ref 13).

To continue with the material variability concept: in a deterministic approach, it is correct to assume that concrete properties are independent of space at a given time. On the other hand, in actuality, any property of the slab varies with time and space. In other words, the slab exhibits variation from one location to another. This material variation can be predicted by an appropriate probabilistic model, in which mean and standard deviation are the only parameters necessary to represent the characteristics of material variation in the model (Ref 19).

The probabilistic sawing model presented here is an adaptation of the model developed by Saraf and McCullough (Ref 12). This section covers the model and its use with the prediction models developed as part of CTR Project 422. (The probabilistic model is presented here in its final form. The reader is advised to consult Ref 12 for further information on the derivation of the probabilistic model.) A plan view of a randomly developed longitudinal crack along a sawed joint is shown in Figure 5.1.

Because of concrete strength variation, the sawing depth may be inadequate. It is not feasible to confine all the random cracks within the joint. Therefore, reliability concepts are also included in the analysis. Reliability levels will be assigned according to the importance of the concrete pavement.

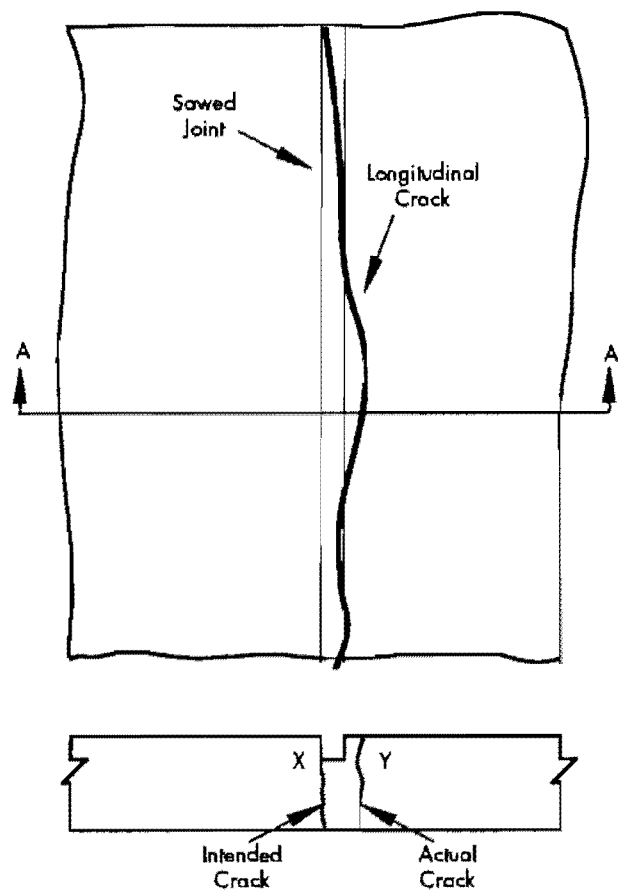

Figure 5.1 Concrete pavement with saw-cut joint and random longitudinal crack (Ref 1)

The tensile forces at the sawing location (section X-X) and at the section adjacent to it (section Y-Y) are approximately the same, that is:

$$F_{T-X} \approx F_{T-Y}. \quad (5.3)$$

The tensile strength can be calculated by

$$T_X = D_X * b * f_{tX} \quad (5.4)$$

$$T_Y = D_Y * b * f_{tY} \quad (5.5)$$

where:

T_X, T_Y = tensile strengths of pavement sections along X-X and Y-Y, respectively, lb;
D_X, D_Y = thickness of the pavement sections along X-X and Y-Y, in.;
b = assumed width of pavement sections, in.; and
f_{tX}, f_{tY} = tensile strength of concrete along sections X-X and Y-Y, psi.

Since the forces at the considered locations are approximately equal, cracking occurs at the location that has the lowest tensile strength, as expressed in the following equation:

$$T_X < F_{T-X} = F_{T-Y} > T_Y \quad (5.6)$$

Since the crack occurred at section Y-Y, tensile strength at section X-X is greater than the tensile strength at section Y-Y. Therefore, T_X/T_Y shows whether the crack is confined to the joint or not. For the example mentioned above, the strength ratio is greater than one. Assume that T_X/T_Y is equal to R. If R is less than one, the concrete will crack within the joint.

Thus, the reliability of the cracking occurring at the joint may be defined as follows:

$$P_\alpha = \text{Reliability} = (1-\alpha) \quad (5.7)$$

The normal density function for (ln R) shown in Figure 5.2 may be used to describe the meaning of these expressions. The probability of cracking outside the joint (α) is the area of the curve to the right of ln R = 0, and the reliability of the cracking at the joint is the area to the left. If a deeper saw cut is used, then the curve shifts to the left, thereby increasing the reliability.

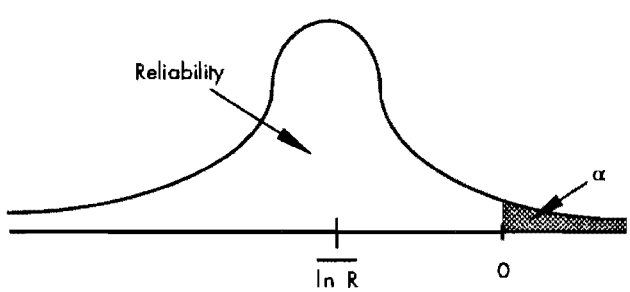

Figure 5.2 Normal density function curve of ln R

Saraf and McCullough (Ref 12) established a mathematical relationship between the tensile strengths at the two locations for use in a statistical model. In order to confine the cracks within the sawed joint, i.e., section X-X, an inequality relationship was defined. The equations are expressed as follows:

$$R = \frac{T_X}{T_Y} \quad (5.8)$$

For cracking at the joint:

$$R \le 1.0 \quad (5.9)$$

The probability of having cracks at the sawed joint is equal to the probability of the expression in Equation 5.9. Thus,

$$\text{Probability of cracking at joint} = P[R \le 1.0] = \alpha \quad (5.10)$$

Since R is the ratio of tensile forces, it can be transformed in terms of stress as follows:

$$R = \frac{T_X}{T_Y}$$

$$R = \frac{D_X * b * f_{tX}}{D_Y * b * f_{tY}}$$

and b, which is constant, can be dropped from the equation.

$$R = \frac{D_X * f_{tX}}{D_Y * f_{tY}} \quad (5.11)$$

Taking the natural log (ln) of each side results in the following equation:

$$\ln R = \ln D_X + \ln f_{tX} - \ln D_Y - \ln f_{tY} \quad (5.12)$$

If it is assumed that all parameters on the right-hand side of Equation 5.11 are normally distributed, then the logarithm of these values should also be normal.

Mean of ln R:

$$\overline{\ln R} = \overline{\ln D_X} + \overline{\ln f_{tX}} - \overline{\ln D_y} - \overline{\ln f_{ty}} \quad (5.13)$$

Assuming that all parameters are independent of each other, the standard deviation of ln R:

$$\sigma_{\ln R} = \left(\sigma^2_{\ln D_X} + \sigma^2_{\ln f_{tX}} + \sigma^2_{\ln D_y} + \sigma^2_{\ln f_{ty}}\right)^{1/2} \quad (5.14)$$

where:

$\overline{\ln D_X}, \overline{\ln f_{tX}}, \overline{\ln D_y}, \overline{\ln f_{ty}}$ = mean values of $\ln D_X$, $\ln f_{tX}$, $\ln D_y$, and $\ln f_{ty}$, respectively, and

$\sigma^2_{\ln D_X} + \sigma^2_{\ln f_{tX}} + \sigma^2_{\ln D_y} + \sigma^2_{\ln f_{ty}}$ = variance of $\ln D_X$, $\ln f_{tX}$, $\ln D_y$, and $\ln f_{ty}$.

Equations 5.13 and 5.14 completely describe the distribution parameters (i.e., μ, σ) of $\ln R$. Therefore, the probability of R (Equation 5.7) can be rewritten as

$$P[R \leq 1.0] = P[\ln R \leq 0.0] \quad (5.15)$$

The estimation of this probability can be made by utilizing the standard parameter Z_a for a normal distribution that has a mean of zero and a standard deviation of one. Z is defined as

$$Z_\alpha = \frac{\ln R_\alpha - \overline{\ln R}}{\sigma_{\ln R}}$$

if the probability of $\ln R \leq 0$ as estimated by the above formula takes the following form:

$$Z_\alpha = \frac{0 - \overline{\ln R}}{\sigma_{\ln R}} \quad (5.16)$$

ANALYSIS OF ALTERNATIVE SAWING METHODS

The first alternative calls for the use of JRCP-5 to develop a probabilistic sawing model. The JRCP-5 computer program, however, does not include the variability, and the effort needed to modify the program is not justified. Thus, the JRCP-5 program was used to generate some of the inputs for the selected probabilistic sawing procedure.

Since the emphasis is on the strength variability of concrete and not on stress variability, the JRCP-5 could be used to predict concrete stress for the average values. These values can be used in the PROSAW (developed in alternative two) to compare the strength and stress, and to observe if the randomly assigned strength value is less than the stress (i.e., the concrete cracks even before sawing). Even if the stress is less than the strength, the resultant stress force may be greater than what the concrete can carry. Therefore, a combination of both methods is needed to achieve the objective of this chapter.

EVALUATION AND OPTIMIZATION OF ALTERNATIVE SAWING METHODS

To complete the systems methodology approach, the alternatives should be evaluated to select the best method for implementation. Evaluation and optimization of the methods are described in this section, and the selection of the sawing depth method is described in the following section.

First Alternative

As mentioned earlier, the first alternative considered for the probabilistic sawing model called for the use of the JRCP-5 computer program. This alternative has a major disadvantage related to the implementation of the probabilistic pavement behavior simulation into JRCP-5. Since the original program is based on a deterministic approach, the effects of modifying this approach would not be immediately observed. Consequently, we decided against using an approach whose evaluation would require substantial time.

Second Alternative

The probabilistic approach, originally developed by Saraf and McCullough (Ref 12), is independent of the aggregate type, magnitude of the mean unit tensile strength, and concrete stress. Accordingly, this approach does not require the use of the JRCP-5 computer program to predict concrete stress for the given input parameters.

SELECTION OF A SAWING DEPTH METHOD

In the previous section, we evaluated alternative methods for sawing depth prediction. This section describes the development of the prediction procedure based on that evaluation.

Development of Sawing Method

In the derivation of the probabilistic model, a dimensionless variable, R, was assumed; and to confine the cracking within the sawed joint, the value of R was considered to be less than one. To satisfy this condition, the tensile strengths (force) at sections X-X and Y-Y were assumed to be independent of each other. We then developed a procedure using random numbers for a given

reliability level. The mean values of f_{t1}, f_{t2}, and D_2 were calculated by using the following equations:

$$f_{tX} = f_t(\text{predicted}) + RAN * s_o \quad (5.17)$$

$$f_{tY} = f_t(\text{predicted}) + RAN * s_o \quad (5.18)$$

$$D_Y = \overline{D_Y} - \emptyset + RAN * s_D \quad (5.19)$$

and

$$\ln R = \overline{\ln R} + RAN * \sigma_{\ln R} \quad (5.20)$$

The standard deviation is calculated from the following formula:

$$s_o, s_D = \mu(\text{predicted}) * CV \quad (5.21)$$

where:

μ(predicted) = mean tensile strength calculated from the prediction model, for the given aggregate type or mean pavement thickness;
RAN = randomly selected standard deviate of a normal distribution;
CV = coefficient of variance of tensile strength or thickness;
s_o = the standard deviation of tensile strength, psi; and
s_D = the standard deviation of the concrete pavement thickness, in.

Assumptions

The prediction of the required sawing depth uses several assumptions, one of which is based on the following excerpt of a technical memorandum by McCullough (Ref 14).

> One of the contributing factors relative to concrete strength was the fact that the strength along the centerline was greater than at any point away from the centerline. This may be attributed to the lack of a steel bar down the centerline and probably to better concrete vibration.

Thus, use of full strength at two different locations may be misleading. At various locations transversely across the pavement, the tensile strength (stress) may be lower and more variable owing to construction defects, and the effective thickness may be less owing to the reinforcing bar. The worst case is one in which these conditions occur at a location away from the saw-cut, as illustrated in Figure 5.3.

If the concrete beneath the rebar does not receive sufficient vibration (resulting in consolidation), a weak zone occurs. The impact of this weak zone on the sawing time and depth can be simulated by using reduced mean unit tensile strength (f_t) and standard deviation (s_t). Accordingly, this case is included in the model. If section Y-Y is assumed to be located at a rebar, the rebar will not carry any stress. Thus, the rebar reduces the actual thickness of the section Y-Y, and the effective thickness can be assumed to be the difference of actual thickness and the diameter of the rebar. For example, if the slab thickness is 12 inches and a #8 bar is used, the effective thickness would be 11 inches. With these two approaches, the effect may be considered independently or concurrently.

Procedure of the Probabilistic Sawing Depth Method

Concrete stress prediction is performed internally within the JRCP-5 computer program. Thus,

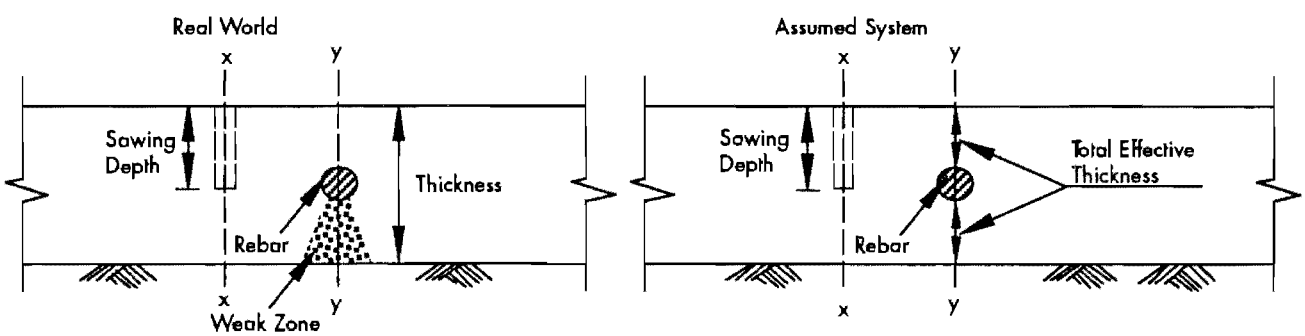

Figure 5.3 Conceptual comparison of real world and assumed system for the probabilistic sawing calculation

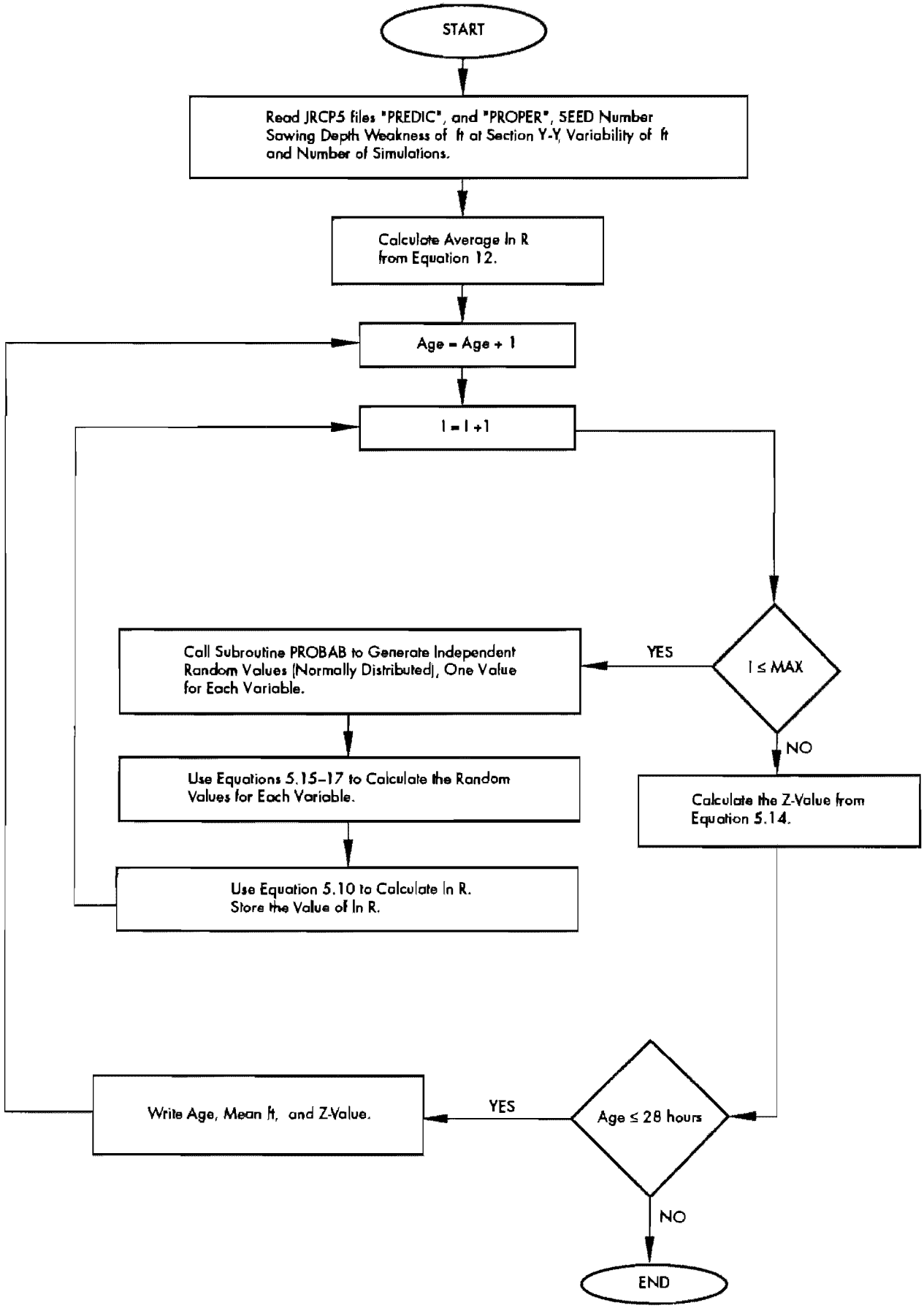

Figure 5.4 Flowchart of the PROSAW computer program

there is no need to develop a theoretical stress formula whose precision may not equal that of the computer program prediction. In JRCP-5, the predicted concrete stress for a given time is filed along with the predicted tensile strength and time.

These concrete stress predictions are used in another computer program, Probabilistic Sawing (PROSAW), the algorithm flowchart of which is shown in Figure 5.4. PROSAW randomly assigns unit tensile strength and thickness to locations X-X and Y-Y. The ln R value (refer to Equation 5.12) is calculated using the predicted concrete strength. This calculation is performed for every simulation, in this case 10,000 times. In the end, the $\overline{\ln R}$ and corresponding $\sigma_{\ln R}$ are calculated. Finally, Z_a value is calculated by using Equation 5.16. This value gives the reliability level for the simulated sawing case. Each sawing problem has concrete strength variation between sections X-X and Y-Y and desired saw depth as input. The calculated reliability levels were plotted against the variation in the concrete strength. (Further information on these plots is included in Chapter 7.)

SUMMARY

In this chapter, two different but interrelated tasks have been accomplished. The first was the development of a procedure for sawing time prediction; the second was the evaluation of the available methods for sawing depth prediction. Separate mathematical models were generated for sawing time and sawing depth. Following the development of the models, necessary tools (in this case computer programs) were used to obtain results. Based on the sawing time analysis, a set of regression equations was developed and will be used in Chapter 7 for implementation. Similarly, the results from the Monte Carlo Simulation for sawing depth were represented in chart form (included in Chapter 7).

CHAPTER 6. IMPROVEMENT IN REINFORCEMENT DESIGN

The reinforcement design formula for jointed concrete pavements, described in the *AASHTO Design Guide for Pavement Structures* (Ref 15), is based on a simple theoretical model that does not fully simulate field conditions. This chapter describes an improved alternative, the JRCP-5 computer program, which can be used to develop an empirical reinforcement formula. Following the description, the AASHTO theoretical formula, termed the "subgrade drag theory," is compared with the new formula to determine important relationships.

Three different reinforcement formulas are presented in this chapter. The first formula is recommended in the *AASHTO Design Guide for Pavement Structures* (Ref 15), as shown in Equation 6.1. The second formula, Equation 6.2 (Ref 16), is a revision of Equation 6.1. The final formula, Equation 6.3, was developed from the JRCP-5 computer program simulation. These formulas are briefly described and compared.

BACKGROUND ON REINFORCEMENT FORMULA

As explained previously, improvement in reinforcement design is one of the primary concerns of this study. The need to improve the formula recommended by AASHTO (Equation 6.1) was also underscored by Heinrichs in an independent study for FHWA (Ref 17). "The subgrade drag theory for JRCP design," concluded Heinrichs, "is very inadequate, and an improved procedure must be developed." The following is that formula recommended in the *AASHTO Design Guide for Pavement Structures* (Ref 15):

$$P_s = \frac{L\mu}{2f_s} * 100 \qquad (6.1)$$

where:

P_s = percent reinforcement;
L = length of the slab, ft;
μ = coefficient of friction; and
f_s = steel working stress, psi.

The reinforcement is a function not only of slab length, frictional resistance (or coefficient of friction), and steel yield strength as shown, but also of several important parameters not included. Thus, the effect of every parameter is represented by a simple formula. For this reason, the formula should be used only for preliminary analysis, insofar as it does not reflect actual values.

In analyzing the effect of reinforcement on pavement performance, some criteria have to be established. In this study, crack width, joint opening, and steel stress at the crack are used as the response parameters. The purpose of using the JRCP-5 computer program for developing a procedure is to obtain more complete information about the effect of design parameters on steel stress. This information can then be used for comparison with the theoretical formula.

Optimum Percent Reinforcement

Optimum reinforcement for jointed reinforced concrete pavements serves to maintain steel stress, joint opening, and crack widths within acceptable ranges. The reinforcement requirement for a given JRC pavement can be calculated by using a formula or a nomograph from the *AASHTO Guide for the Design of Pavement Structures* (Ref 15). A conceptual replica of the nomograph is illustrated in Figure 6.1. The current formula, Equation 6.1, includes a friction factor adopted from the classical friction concept (Ref 16).

GENERATION OF REINFORCEMENT FORMULA

The exclusion of some parameters from the reinforcement formula (Equation 6.1) reveals its limitation in accurately predicting the required reinforcement amount. Thus, in the selection of the new reinforcement formula, certain criteria have been included to offset this limitation. With these criteria, the new formulas should include

parameters that are more significant than those in Equation 6.1. Of course, for theoretical formulation the number of parameters will be limited.

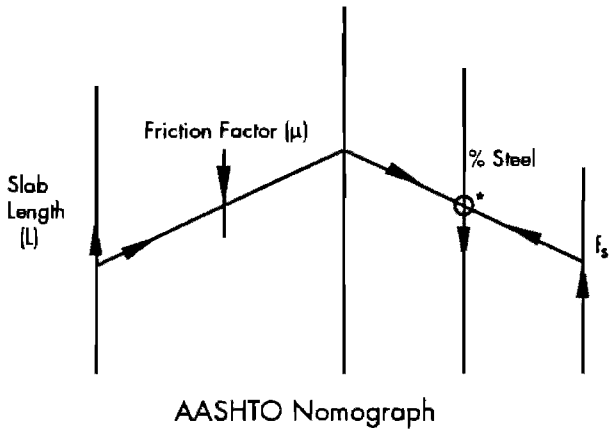

Figure 6.1 Nomograph used in the calculation of percent reinforcement (Ref 15)

Modifying Subgrade Drag Formula

Modification of the subgrade drag formula was the first alternative considered in this study, and the formula was changed according to recent findings on the frictional characteristics at the subbase–pavement interface. The friction factor, which is dimensionless, was replaced by frictional resistance (τ_R), or the total frictional force applied at the interface divided by the total contact area. Recent experiments by Wesevich (Ref 2) and Wimsatt (Ref 3) showed that there is no relationship between total frictional force and slab weight. Because the subgrade drag theory assumes that the total frictional force is proportional to the weight of the slab and the friction factor, this theory is not applicable for concrete pavements. The study team thus modified the formula to include thickness, believed to be one of the major parameters in reinforcement design.

Using JRCP-5 Computer Program for Reinforcement Design

As mentioned before, a theoretical formula, for practical reasons, is limited in the number of parameters that can be included in a closed form. However, using statistical tools to develop equations from computer simulations imposes virtually no limitation on the number of parameters that can be used. The only limitation is the exclusion of the statistically insignificant parameters from the equations. Using these tools, the research team created a factorial for reinforcement design.

ANALYSIS OF ALTERNATIVES

Proper evaluation of the alternatives requires that the characteristics (e.g., limitations and assumptions) of each alternative be identified. This can be accomplished through appropriate analysis of each alternative.

First Alternative: Modified Subgrade Drag Theory

The new formula, Equation 6.2, was derived using recent findings on the subbase friction concept (Refs 2, 3). The derived formula is expressed as

$$P_s = \frac{6 L \tau_R}{D f_s} * 100 \qquad (6.2)$$

where:

P_s, L, f_s = as defined before;
τ_R = frictional resistance, psi; and
D = thickness of the slab, in.

Figure 6.2 illustrates the greater utility of Equation 6.2. Instead of using only one line for a thickness range of 6 to 14 inches, Equation 6.2 uses one line for every thickness (since thickness is included in this formula).

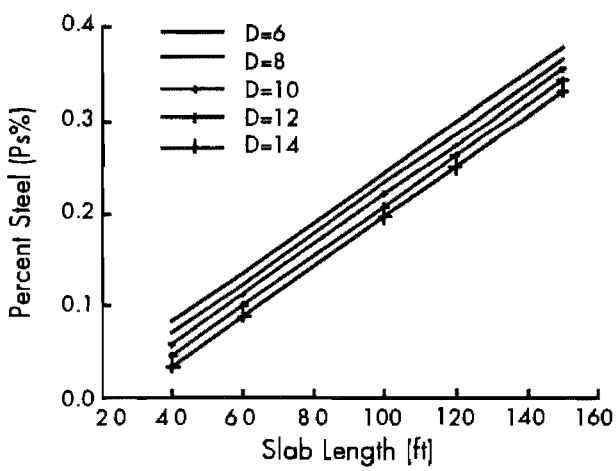

Figure 6.2 Calculated percent reinforcement from Equation 6.2 for different slab thicknesses as a function of slab length

Second Alternative: JRCP-5 Computer Program

To determine which parameters have a significant effect on reinforcement performance, the study team used the JRCP-5 computer program

with a factorial to perform a series of solutions. The criteria used for the analysis of the factorial run, as mentioned above, were steel stress, crack width, and joint opening. Both short-term effects (when drying shrinkage has a high progression rate) and long-term effects (necessary for joint sealant design) were considered in the analysis. Here, "short-term" represents the 28th day condition, whereas "long-term" identifies the point at which slab temperature drops to its minimum value.

Factorial Design

For practical purposes, the subbase drag formula (Equation 6.1) can be used to obtain a preliminary estimation of the required steel percentage. In the derivation of the formula, no limitation was used to keep the crack width and joint opening within the preferred range. Because there is no precise closed-form solution for percent steel estimation, the calculation of the desirable steel percentage in the final product is necessarily an iterative process, one that justifies the use of computer programs. Accordingly, the computer program JRCP-5 was employed with a factorial consisting of ten different variable-input parameters, each at three levels. These input parameters, together with the selected ranges, are presented in Table 6.1.

Results of the Reinforcement Factorial Run

A factorial was generated and used with the JRCP-5 computer program to simulate different conditions of JRCP longitudinal reinforcement and transverse reinforcement of concrete pavements. Based on the computer program computations, the significance of each input on both short-term and long-term behavior was tested. Then, the SAS® statistical package was used to develop a relationship for each design criterion, and the results are shown in Table 6.2.

Using the results of the analysis, the study gruop developed a set of regression equations—three for short-term and three for long-term. The next step was to compare the results of these empirical equations with those from the theoretical equations, as explained earlier in this chapter.

Three different criteria—steel stress, crack width, and joint opening—were used to find a relationship between percent steel reinforcement and input parameters. As expected, the various parameters differed in their influence on each given criterion for both short-term and long-term JRCP behavior. To keep the coefficient of correlation as high as possible, linear and nonlinear combinations were used. The coefficient of correlation for short-term crack width and for both short- and long-term joint opening ranged from 0.78 to 0.95, respectively. Because the number of parameters included in the joint opening prediction formula exceeded that used in other prediction formulas, the coefficient of correlation was higher.

There are other factors not covered in this study that are believed to affect both crack width and steel stress prediction. One of these factors is the bond development length at the interface of concrete and reinforcement. Bond development length is represented by bar diameter, slab thickness, and percent reinforcement. Therefore, the regression equations may under- or over-predict, depending on the particular circumstances. Nevertheless, the prediction capability of these regression equations proved to be more advanced than that obtained from either Equation 6.1 or 6.2.

where:

P_s = percent reinforcement;
$\emptyset$ = nominal bar diameter, in.;
D = slab thickness, in.;
L = slab length, or width, ft;
τ_R = subbase friction, psi;
Z = drying shrinkage, in./in.;
α_c = thermal coefficient of concrete, in./in./°F;
ΔT_{min} = minimum annual temperature drop of concrete, °F;
σ_S = steel stress at the crack, psi;
Δ_x = crack width, in.; and
Δ_{xj} = joint opening, in.

The regression equations Equations 6.3–6.8 are used to develop an interactive computer program capable of predicting both short- and long-term behavior with respect to steel stress, crack width, and joint opening. The program, Percent Reinforcement Optimization, or PRO1, is interactive, in which the algorithm of the PRO1 consists of Equations 6.3–6.8. The program automatically checks whether each input variable is within the range used in the factorial. Sample input and output files of the PRO1 program are included in Appendices F and G, respectively.

Table 6.1 Input variable for the factorial analysis

Variables	Low	Medium	High
Reinforcement (%)	0.01	0.10	0.30
Bar size	#3	#4	#5
Slab thickness (in.)	6	11	15
Length of the slab (ft)	20	60	150
Elastic modulus of concrete (*106 psi)	3.0	5.0	7.0
Subbase friction (psi)	1.0	2.0	15.0
Thermal coefficient of concrete (*10-6 in./in./°F)	4.0	6.0	8.0
Total drying shrinkage (*10-4 in./in.)	2.0	4.0	6.0
Minimum annual temperature (°F)	-20	-10	0
Curing temperature (°F)	50	75	100
Minimum daily temperature (°F)	36*, 23†, 15‡	67, 55, 48	93, 84, 82

*Day 1
†Days 2-6
‡Days 7-28. This layout is included in CTR Research Report 422-1.

Table 6.2 Significant input parameters on short- and long-term JRCP behavior

Variables	Steel Stress	Δ_x	Δ_{xj}
Reinforcement (%)	Y Y*	Y Y	Y Y
Bar size	Y Y	Y N	N N
Slab thickness (in.)	Y Y	Y Y	Y Y
Length of the slab (ft)	Y Y	Y Y	Y Y
Elastic modulus of concrete (*106 psi)	N N	N N	N N
Subbase friction (psi)	Y Y	Y Y	Y Y
Thermal coefficient of concrete (*10-6 in./in./°F)	N N	N Y	Y Y
Total drying shrinkage (*10-4 in./in.)	Y N	Y Y	Y Y
Immediate temperature drop (28-day value)	N N	N N	N N
Maximum drop in temperature (°F)	N Y	N N	N Y

* the first one is for short-term, and the second one for long-term
Y means that the input variable has a significant effect on the dependent variable
N means that the input variable does not have a significant effect on the dependent variable

Short-Term

$$\sigma_s = \frac{72277 * \left(1+\frac{L}{100}\right)^{1.894} * \left(1+\frac{\tau_R}{10}\right)^{0.983} * (1+1000*Z)^{0.567}}{(1+P_s)^{4.214} * (1+\emptyset)^{1.595} * (1+\frac{D}{10})^{0.463}} \quad R^2 = 0.82 \tag{6.3}$$

$$\Delta_x = \frac{0.0012 * \left(1+\frac{L}{100}\right)^{3.152} * \left(1+\frac{\tau_R}{10}\right)^{2.025} * (1+1000*Z)^{2.217} * (1+\emptyset)^{1.592}}{(1+P_s)^{9.922} * \left(1+\frac{D}{10}\right)^{0.984}} \quad R^2 = 0.81 \tag{6.4}$$

$$\Delta_{xj} = \frac{0.014 * \left(1+\frac{L}{100}\right)^{2.595} * (1+1000*Z)^{2.845} * (1+P_s)^{1.497} * \left(1+\frac{D}{10}\right)^{0.287} * (1+100000\,\alpha_c)^{0.934}}{\left(1+\frac{\tau_R}{10}\right)^{0.464}} \quad R^2 = 0.95 \tag{6.5}$$

$$\sigma_s = \frac{64565 * \left(1+\frac{L}{100}\right)^{1.8} * \left(1+\frac{\tau_R}{10}\right)^{0.846} * \left(1+\frac{\Delta T_{min}}{100}\right)^{0.897}}{(1+P_s)^{3.91} * (1+\emptyset)^{1.635} * \left(1+\frac{D}{10}\right)^{0.43}} \quad R^2 = 0.80 \tag{6.6}$$

$$\Delta_x = \frac{0.0023 * \left(1+\frac{L}{100}\right)^{3.12} * \left(1+\frac{\tau_R}{10}\right)^{1.84} * (1+1000*Z)^{1.38} * (1+100000\,\alpha_c)^{1.37}}{(1+P_s)^{9.51} * \left(1+\frac{D}{10}\right)^{0.96}} \quad R^2 = 0.78 \tag{6.7}$$

$$\Delta_{x|} = \frac{0.0063 * \left(1+\frac{L}{100}\right)^{2.614} * (1+1000*Z)^{1.7} * (1+P_s)^{1.41} * \left(1+\frac{D}{10}\right)^{0.24} * (1+100000\,\alpha_c)^{1.63} * \left(1+\frac{\Delta T_{min}}{100}\right)^{2.154}}{\left(1+\frac{\tau_R}{10}\right)^{0.397}} \quad R^2 = 0.95 \tag{6.8}$$

EVALUATION OF ALTERNATIVES AND OPTIMIZATION

Following the independent analysis of both alternatives, an evaluation of each should reveal the most useful reinforcement design. Here, the conceptual description of friction in Figure 6.3 was considered the key to the proper evaluation of alternative methods. When a frictional resistance value was used in Equation 6.1 or Equation 6.2, the same value is assumed for every longitudinal segment of the slab. However, in the JRCP-5 computer program, the frictional resistance magnitude is proportional to the magnitude of the movement of the particular longitudinal slab segment. The reason for using longitudinal segments and not transverse segments is that the JRCP geometric model is one dimensional; moreover, the longitudinal direction is always more critical than the transverse direction when friction, concrete, and steel stress are under consideration.

SIGNIFICANCE OF FINDINGS

After developing the percent-reinforcement regression equations, the research team compared the subgrade drag formula with the alternatives. As mentioned in the reinforcement section of this chapter, an old formula was revised to render it more realistic; but it was also explained that, in actuality, JRCP-5 includes more factors to predict pavement response than those included in the formula (new). Therefore, the regression equations were developed for three design criteria: steel stress, crack width, and joint opening. Only the steel stress equation, which is more compatible with the theoretical formula than the others, was used for comparison.

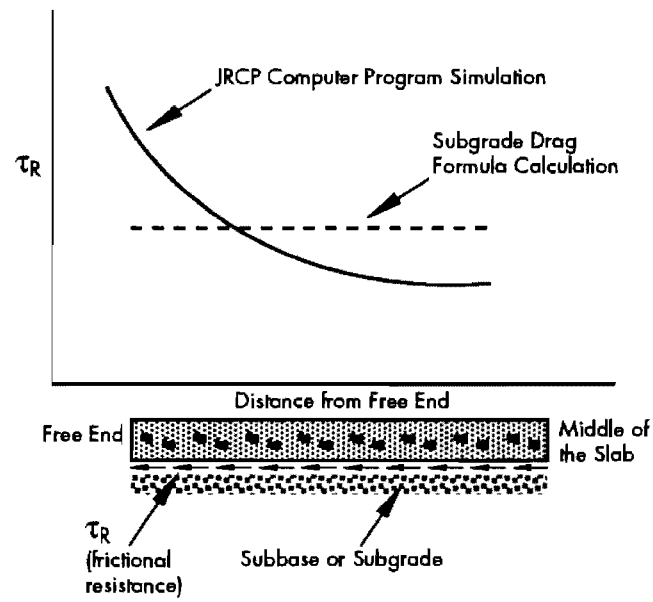

Figure 6.3 Conceptual comparison of the frictional resistance in the theoretical formula and in the simulation of the computer program JRCP

Figures 6.4–6.6 show the relationship between percent reinforcement and the parameters used in all of the equations. In the development of the figures, 60,000 psi was used for steel yield strength. The reason for using only three parameters is to show the significant effect of these parameters on Equations 6.1 and 6.2, and the minimum effect of these parameters on Equation 6.6, which is used for the figures. In Figure 6.4, both Equations 6.1 and 6.2 yielded the same result, i.e., when the thickness is 12 inches, both equations gave identical results. Because Equation 6.6 includes the effect of parameters not considered in the others, its prediction differs.

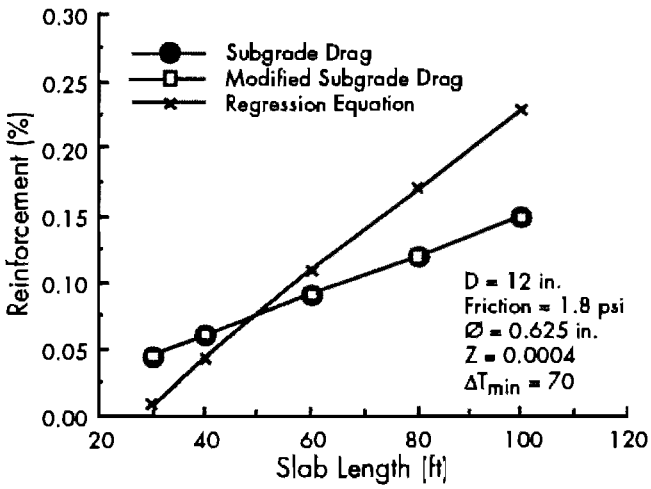

Figure 6.4 Relationship between percent reinforcement and slab length for the prediction formulas, f_y = 60,000 psi

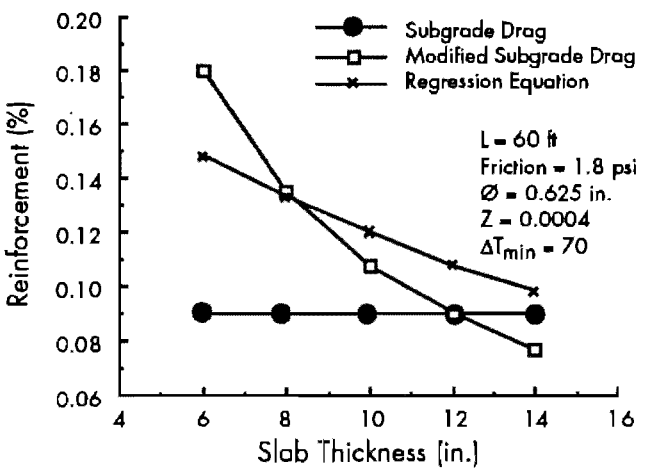

Figure 6.5 Relationship between percent reinforcement and slab thickness for the prediction formulas, f_y = 60,000 psi

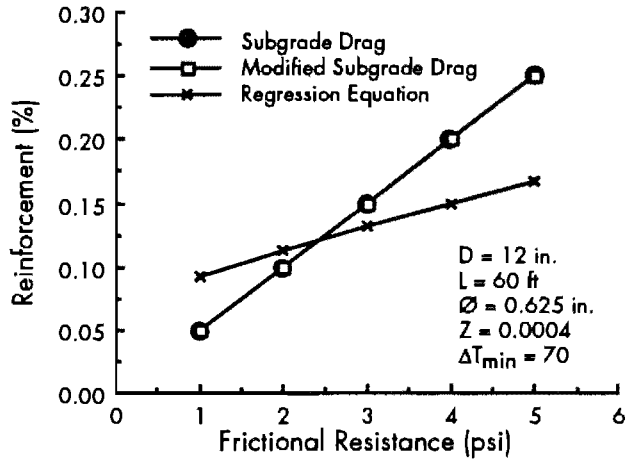

Figure 6.6 Relationship between percent reinforcement and frictional resistance for the prediction formulas, f_y = 60,000 psi

The use of the regression equation shows that, regardless of the variation in the other input parameters, the optimum percent steel lies between 0.2 and 0.3 percent. Some of the results are shown in Figures 6.4, 6.5, and 6.6.

IMPLEMENTATION OF THE BEST METHOD FOR REINFORCEMENT DESIGN

The main advantage of this program is its ability to estimate quickly the optimum steel percent for given conditions. Accuracy in this estimate is not necessarily sacrificed because of the speed of PRO1. In fact, engaging this procedure is less time-consuming than running the JRCP-5 analysis program the number of times required to arrive at an answer that meets the limiting criteria.

As explained above, PRO1 is also useful in estimating optimum percent steel for CRCP tie-bar reinforcement design. The limiting criteria built into the program will prevent the user from exceeding the limiting values for each criterion.

JOINT SPACING

For the same slab, higher frictional resistance causes higher tensile stresses than does lower frictional resistance. By keeping in mind the effects of interface condition, the designer should select the slab length accordingly. Wimsatt (Ref 3) implemented the results of push-off tests for concrete slabs on different subbase types to determine

the maximum joint spacing required to prevent crack formation. Tensile strength is used as a criterion in selecting the joint spacing.

The computer program Prestressed Concrete Pavement Version 1 (PCP1) was used for the analysis. The limiting joint spacings for each subbase type are shown in Figure 6.7, which illustrates the impact of subbase type on slab length. Here the emphasis is on staying within the tensile strength of concrete; thus, any other criteria obviously will yield joint spacings different from those based on tensile strength criteria. The slab lengths given in Figure 6.7 are estimated by using frictional resistance values higher than those used for the long-term formulation. Following several contractions and expansions, the frictional resistance decreases considerably (an action that should be kept in mind when considering Figure 6.7).

SUMMARY

In conclusion, the updated JRCP-5 computer program represents an improvement over the simpler, earlier theoretical models (i.e., the subgrade drag formula). The new program allows the user to explore the input parameter combinations not available in the theoretical formula. Most importantly, the percent steel reinforcement estimated by the new program is higher than that predicted by the theoretical formulas.

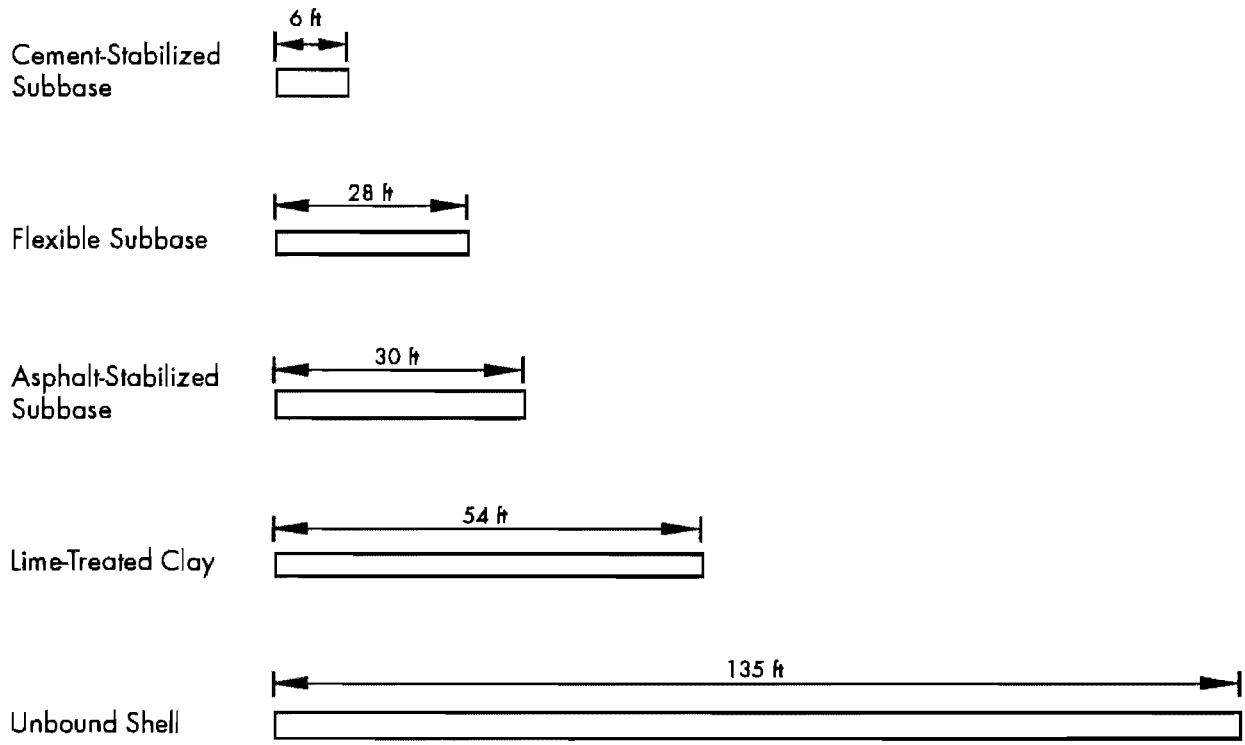

Figure 6.7 Maximum slab lengths for different subbases using tensile strength as the criterion

CHAPTER 7. IMPLEMENTATION

This chapter describes the implementation of the design subsystems developed in Chapters 4, 5, and 6. Specifically, it documents the development of graphical procedures (design charts) that assist both in the design of transverse reinforcement for concrete pavements, and in the determination of concrete pavement sawing time and depth. The research team believes that the essential findings of this study, as outlined in this chapter, will provide immediate and long-term benefits to TxDOT's pavement design procedure.

DEVELOPMENT OF GUIDELINES

The regression equations, theoretical equations, and computer programs developed in Chapters 5 and 6 are used in this section as design guidelines. The first guideline relates to sawing time, while subsequent guidelines pertain to sawing depth and reinforcement design.

Guidelines for Sawing Time

The modeling of concrete strength variability, along with its related assumptions, was developed in earlier chapters of this study. That probabilistic method addressed only the depth of sawing (other parameters were known and the model was independent of sawing time). It was noted that sawing depth is primarily a function of concrete strength and thickness variation. Sawing time, on the other hand, is a function of both those parameters and of sawing depth. The guidelines developed here sought to reflect this necessary interrelationship, and the required sawing depth was used to estimate the optimum sawing time.

In developing the guidelines for sawing time, the study group used the steel stress at the crack as a limiting criterion. This stress is calculated as follows: First, Equations 5.1 and 5.2 (Chapter 5) are used to calculate the concrete stress and steel stress. Then, concrete stress is divided by percent reinforcement, which is the ratio of steel area to concrete area for a given cross section. Finally, the result of the second step is added to Equation 5.2.

The Use of the Sawing Time Formulas

Optimum use of the regression equations relating to sawing time requires either a computer program or a spreadsheet template to calculate the steel stress. Accordingly, two graphs were created to estimate the deviation of steel stress from the standard stress shown in Figure 7.1 for concrete with the coarse aggregate types siliceous river gravel (Figure 7.2) and limestone (Figure 7.3). Thus, these graphs should be used with Figure 7.1, which contains a set of variables with constant values. When using a parameter value other than that used to develop the graph, the following steps should be followed. First, the coarse aggregate type is used to select the appropriate graph. Then, the percent deviation of the parameter, for example slab length (L), should be determined. The difference in the steel stress will

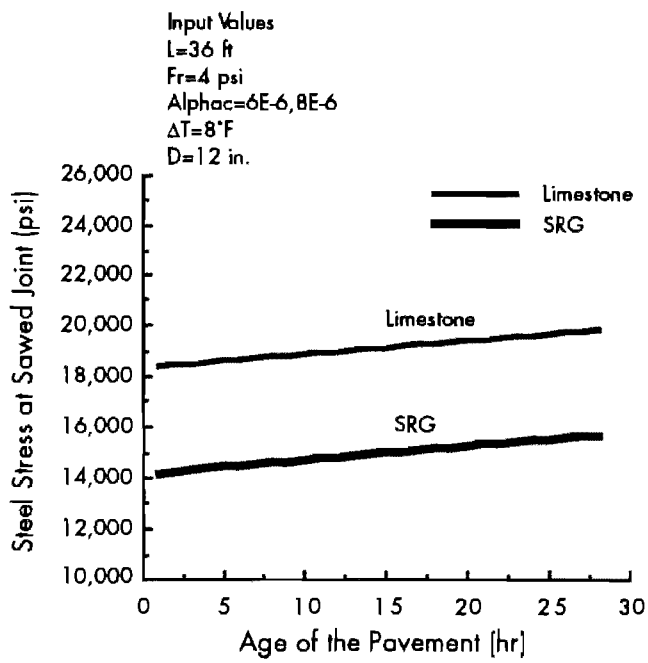

Figure 7.1 Prediction of steel stress at the crack as a function of coarse aggregate type and age of pavement

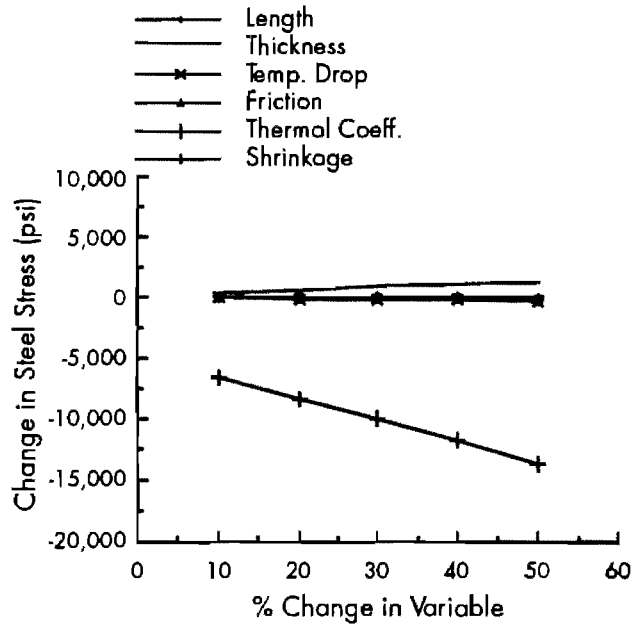

Figure 7.2 *Change in steel stress at the crack as a function of percent change in the predicting variables used in Equations 5.1 and 5.2 for the coarse aggregate type siliceous river gravel*

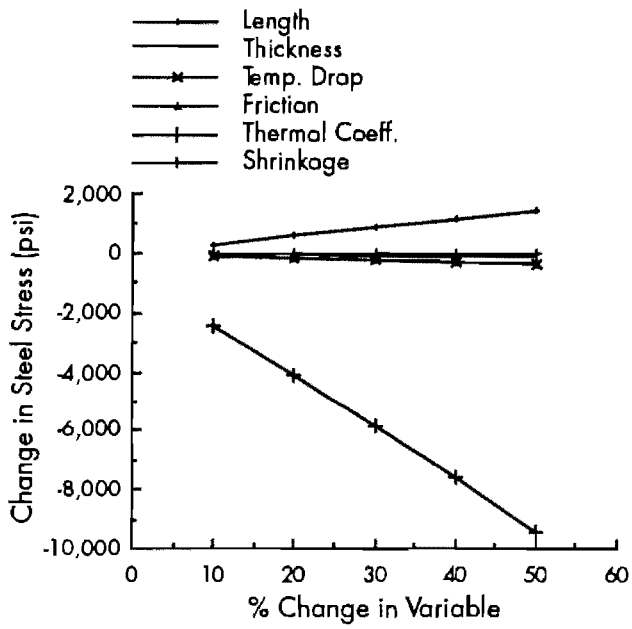

Figure 7.3 *Change in steel stress at the crack as a function of percent change in the predicting variables used in Equations 5.1 and 5.2 for the coarse aggregate type limestone*

be estimated by using the percent change of the slab length. The steel stress values in Figures 7.2 and 7.3 are calculated by the following expression:

$$\Delta\sigma_s = \sigma_{s1} - \sigma_{s2}$$

where:

$\Delta\sigma_s$ = difference in steel stress, psi;
σ_{s1} = steel stress measured from Figure 7.1; and
σ_{s2} = calculated steel stress when a parameter has a value different from that used for Figure 7.1.

Guidelines for Sawing Depth

The guidelines on sawing depth, developed from the computer simulations explained in this chapter, are presented below in six graph groups (Figures 7.4 through 7.9). Each graph group consists of four individual graphs, which represent four different tensile strength variations: 5, 10, 15, and 20 percent. Each graph group represents the existence of reinforcement at cross section y-y. The bar sizes (in inches) are: no bar, 0.375 (#3), 0.500 (#4), 0.625 (#5), 0.750 (#6), and 0.875 (#7). The graphs present the reliability level as a function of the unit tensile strength ratio for various sawing depths. For the given mean strength ratio (i.e., the ratio of mean tensile strength of concrete at sections y-y and x-x, the unit of tensile strength being psi), the required saw depth increases as the desired reliability level increases.

Assume that you want 85 percent of the cracks confined in the joint; that is, you seek a reliability level of 85 percent. The mean strength ratio and coefficient of variation of tensile strength are given as 0.9 and 15 percent, respectively, and no effect of reinforcement at section y-y is assumed. Since there is no reduction in the thickness at section y-y, Figure 7.4a should be used. Using the reliability level and mean strength ratio, the required sawing depth ratio is about 0.33 times the actual thickness of the concrete pavement.

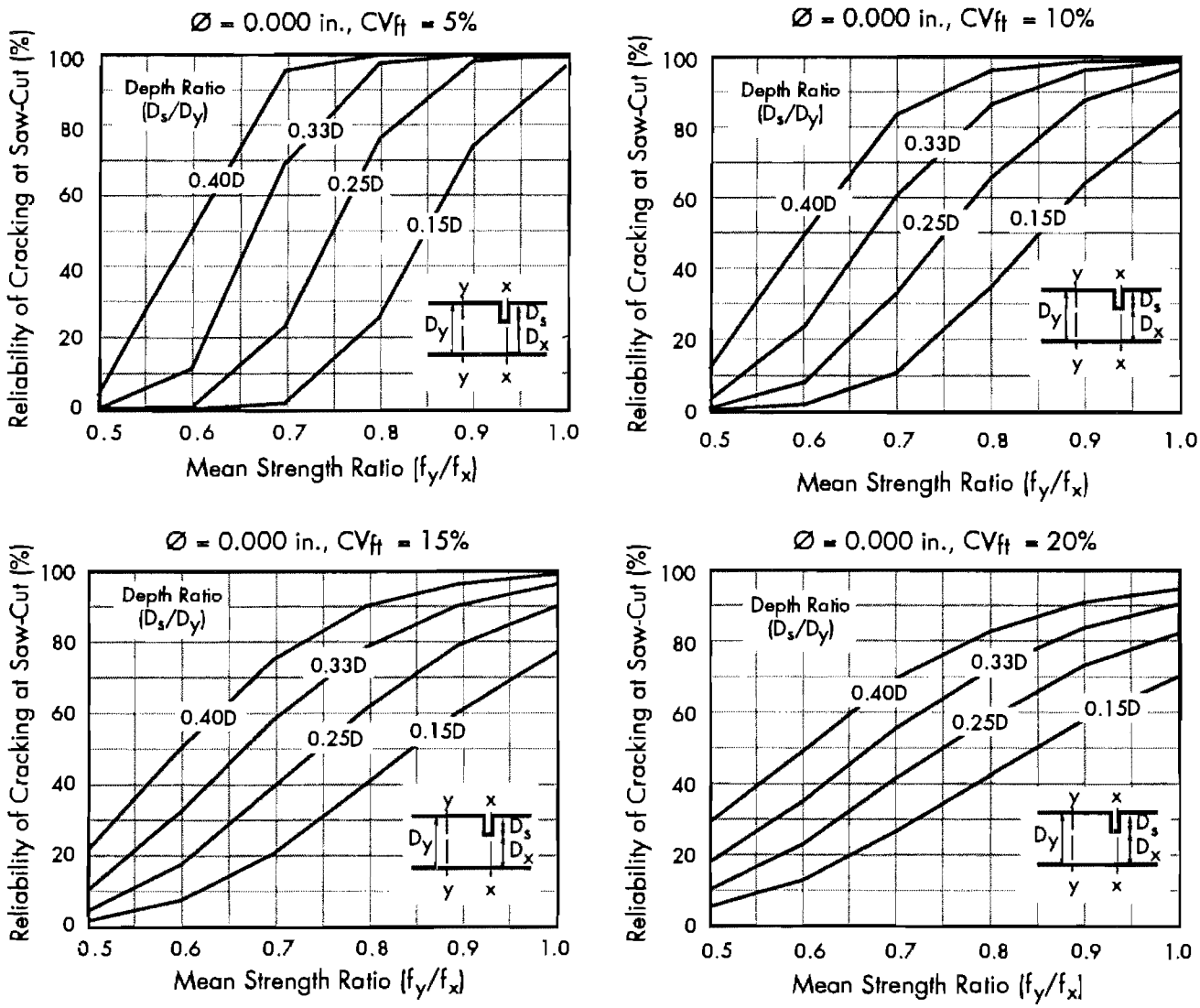

Figure 7.4 ***Effect of concrete weakness away from joint on sawing depth and reliability level with different mean strength variation (effect of bar diameter is excluded)***

GUIDELINES ON REINFORCEMENT DESIGN

In Chapter 6, two sets of regression equations were developed for use in reinforcement design. Because of the complexity of the formulas, it is not practical to develop charts for every case. Thus, the PRO1 computer program should be used for reinforcement design. Meanwhile, several plots were made to compare the subgrade drag formula with the modified subgrade formula and with the long-term steel stress formula (Equation 6.6).

The important conclusion to be drawn from these graphs is the influence of concrete slab length, thickness, and frictional resistance on the prediction of subgrade drag theory and modified drag theory. Because it represents the other parameters, the regression equation (Equation 6.6) provides more realistic predictions. As mentioned before, three parameters can be used as limiting

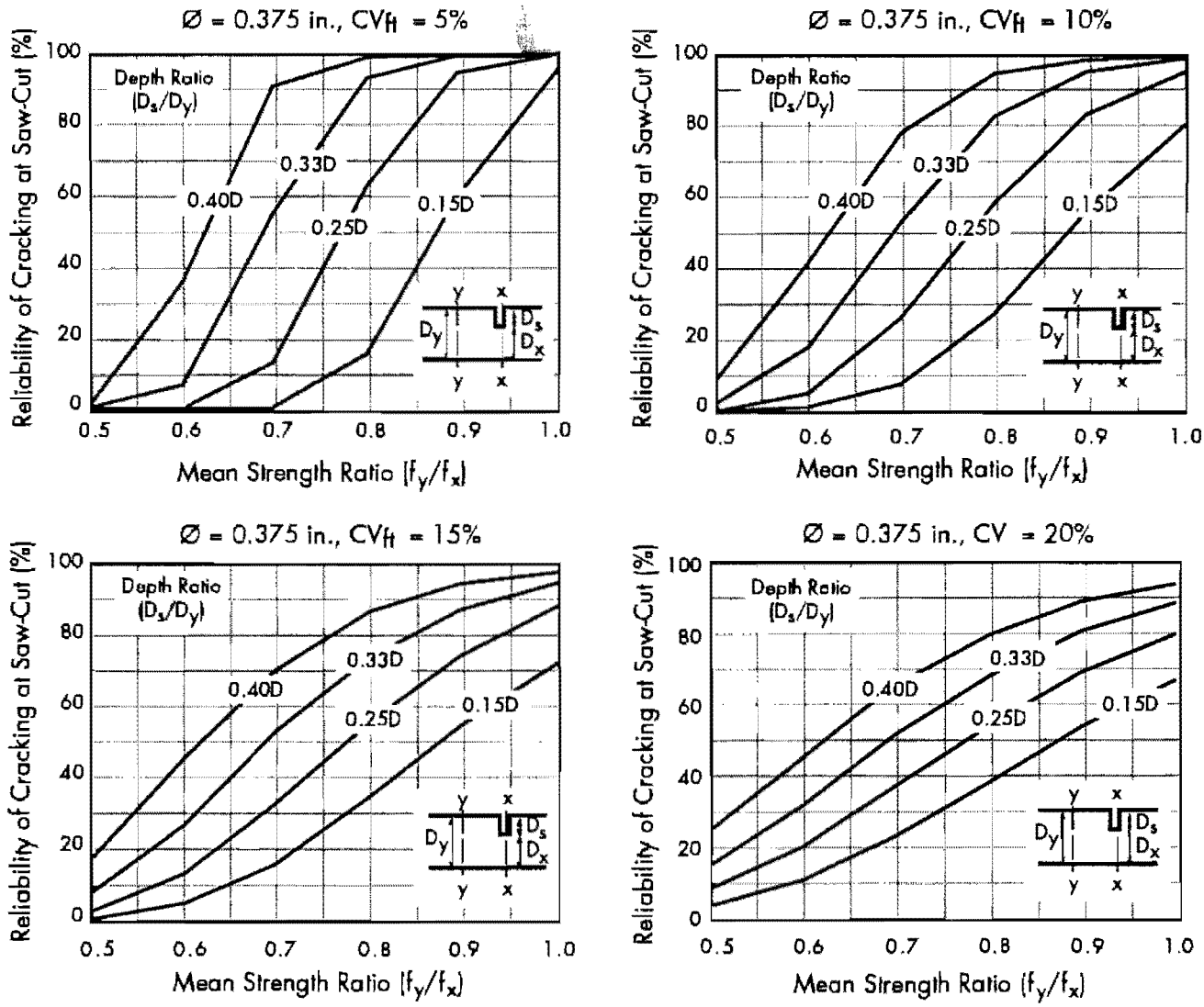

Figure 7.5 ***Effect of concrete weakness away from joint on sawing depth and reliability level with different mean strength variation (bar diameter is 0.375 inches [#3])***

criteria for reinforcement design: steel stress, crack width, and joint opening. Figure 7.10 illustrates how crack width can be used to determine the minimum amount of steel needed to satisfy crack-width criteria. Similarly, the use of steel stress as a criterion is illustrated in Figure 7.11. Although joint opening can be used in reinforcement design, its major advantage is in joint sealant design. The use of the joint opening in sealant design is described in the following section.

The subgrade drag formula and modified subgrade drag formula predictions show an increasing trend as slab length, thickness, and frictional resistance increase. In contrast, the prediction of Equation 6.6 (steel stress regression equation for predicting long-term behavior) converges in a range between 0.2 and 0.3 percent. Thus, because this formula represents almost all the factors affecting steel stress, it is recommended for determining required percent reinforcement.

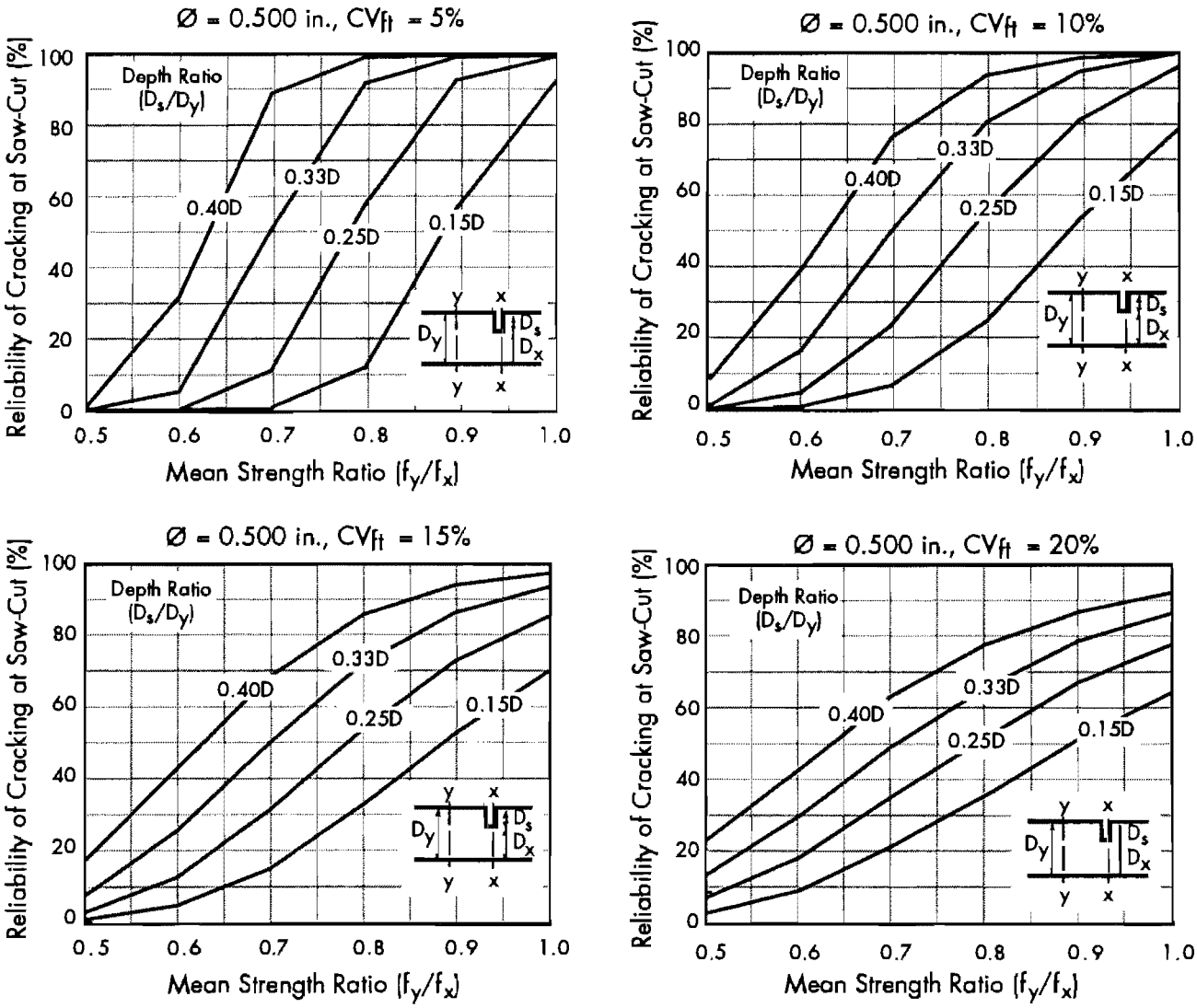

Figure 7.6 ***Effect of concrete weakness away from joint on sawing depth and reliability level with different mean strength variation (bar diameter is 0.500 inches [#4])***

The shrinkage prediction model within the JRCP-5 computer program (used for the reinforcement design factorial) did not include the effect of slab thickness. Hence, the guidelines on reinforcement design carry a hidden "safety factor." In other words, the results are conservative, more or less in proportion to the thickness of the pavement. The predicted concrete response is less conservative for long-term prediction, where the temperature variation is dominant. A more nearly precise percent reinforcement value can be obtained by using the PRO1 computer program.

RECOMMENDATIONS ON JOINT SEALANT DESIGN

Because each set of regression equations contains one equation on joint movement, these equations should be used in lieu of that recommended in Ref 15 to predict joint movement.

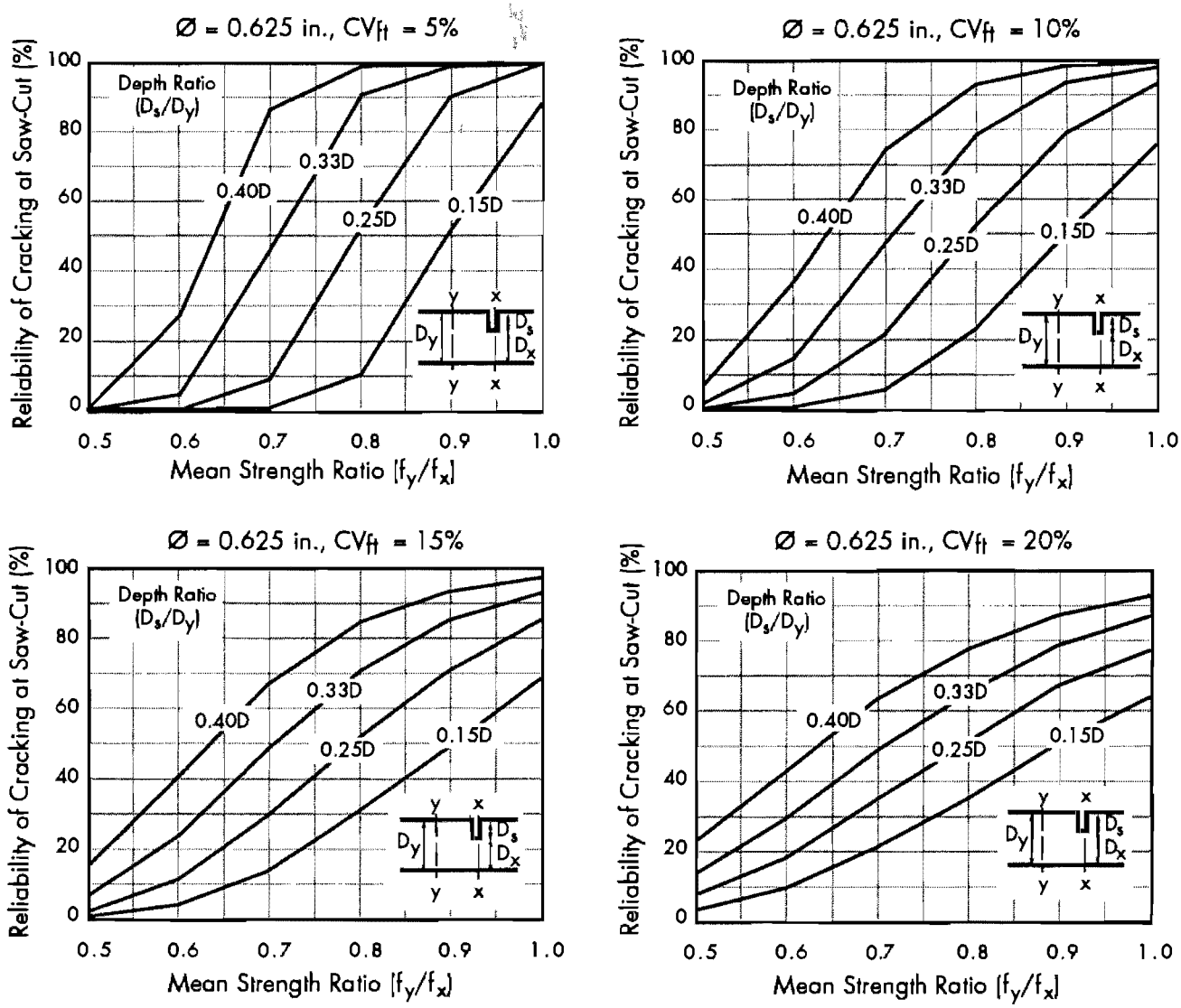

Figure 7.7 Effect of concrete weakness away from joint on sawing depth and reliability level with different mean strength variation (bar diameter is 0.675 inches [#5])

Figure 7.12 conceptually describes how the reinforcement design equations should be used for sealant design.

SUMMARY

In this chapter, a probabilistic sawing model has been developed to provide useful guidelines for sawing depth and time. Some of the significant parameters affecting sawing depth include reliability level and weakness of concrete strength away from the saw joint. Sawing time, on the other hand, is affected mostly by the magnitude of concrete stress, saw depth, and coarse aggregate type.

Regression equations were also developed for the prediction of percent reinforcement for the

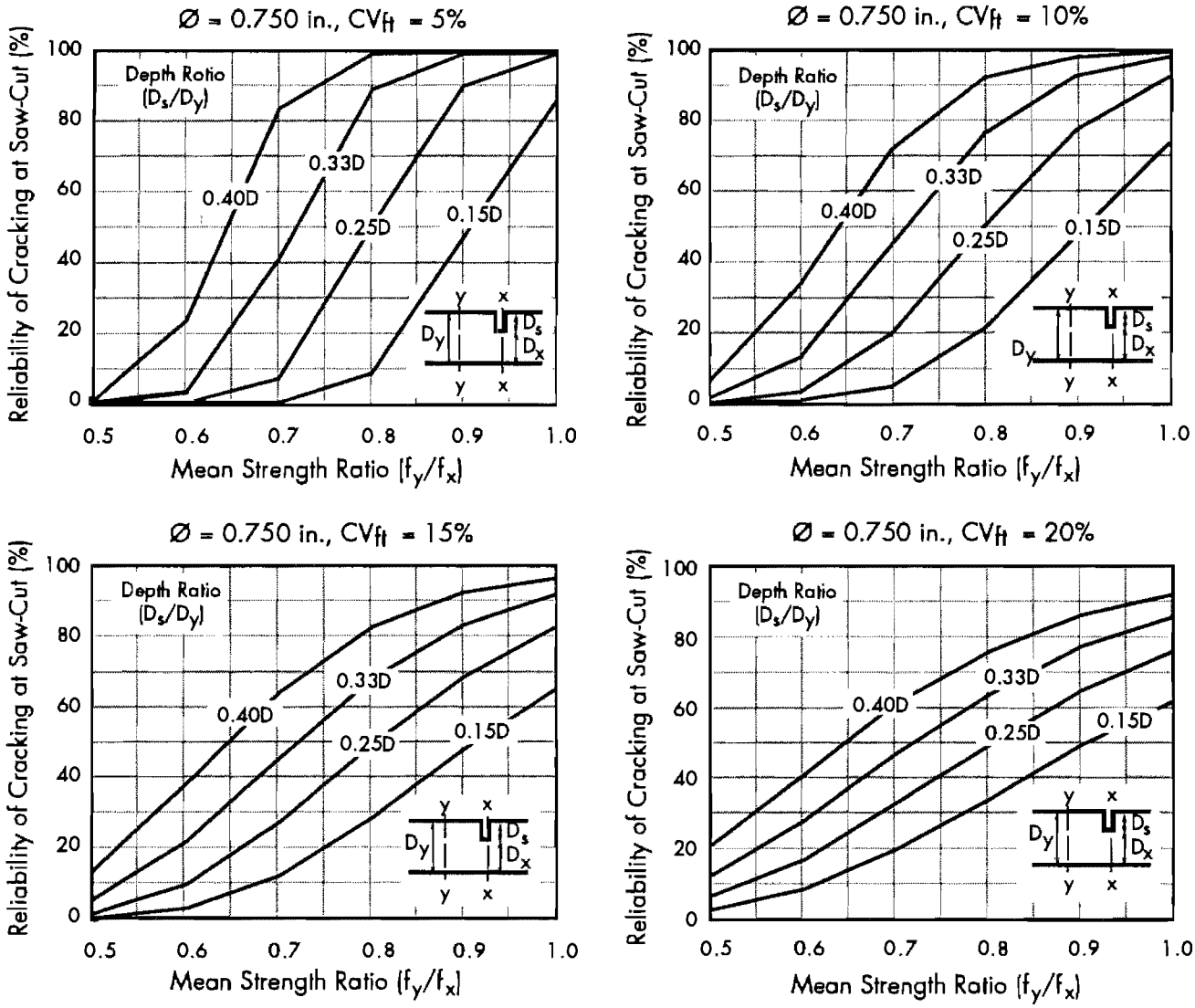

Figure 7.8 ***Effect of concrete weakness away from joint on sawing depth and reliability level with different mean strength variation (bar diameter is 0.750 inches [#6])***

design of steel reinforcement in continuously reinforced concrete pavements.

Finally, both the sawing and reinforcement procedures outlined in this study allow the designer to recommend a detailed design for the particular environmental conditions appropriate to the locality. The procedures are comprehensive, are easy to implement, and allow the designer to specify a range of values for design parameters corresponding to design uncertainty.

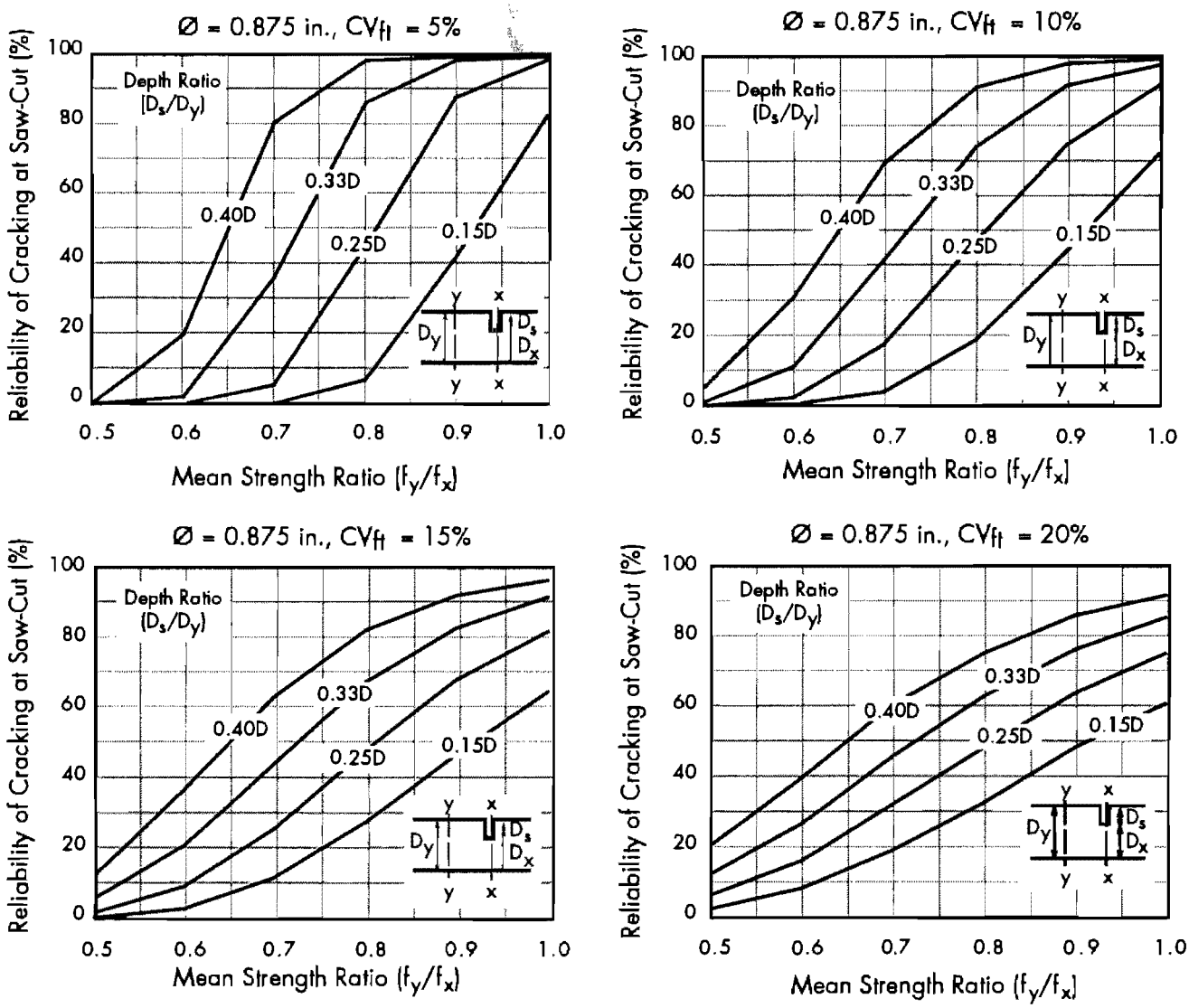

Figure 7.9 Effect of concrete weakness away from joint on sawing depth and reliability level with different mean strength variation (bar diameter is 0.875 inches [#7])

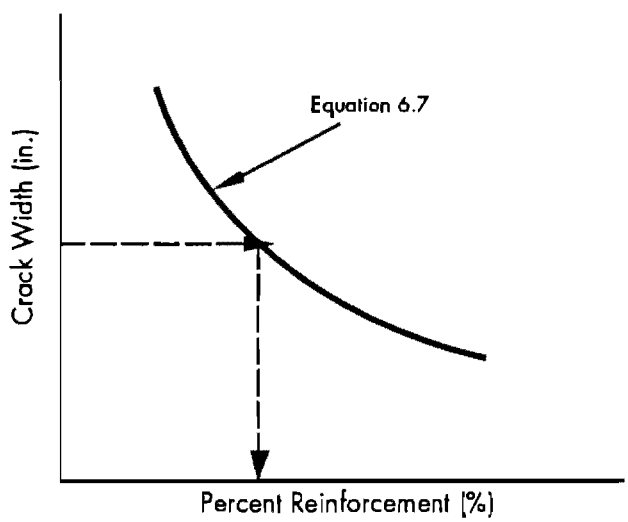

Figure 7.10 Conceptual description based on the use of crack width as a limiting criterion for reinforcement design

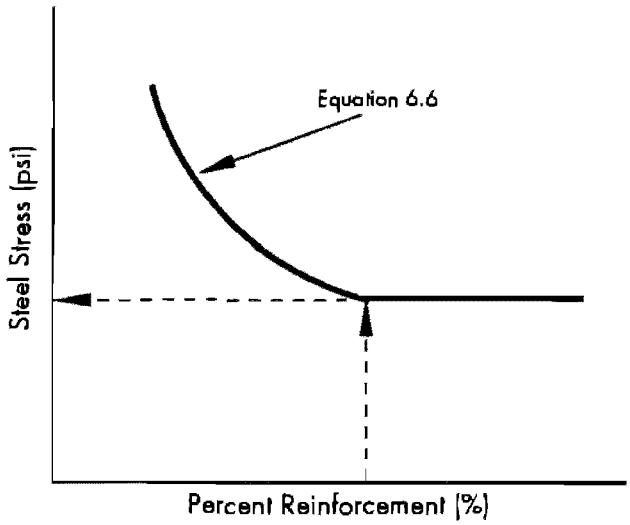

Figure 7.11 ***Conceptual description based on the use of steel stress as a limiting criterion for reinforcement design***

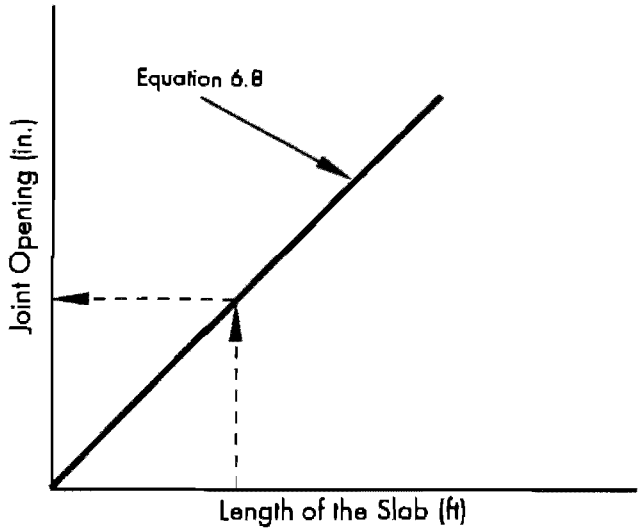

Figure 7.12 ***Conceptual description based on the use of joint opening as a limiting criterion for reinforcement design***

CHAPTER 8. EVALUATION OF THE RESEARCH FINDINGS

INTRODUCTION

Using recent concrete property findings, the research team revised the JRCP analysis program to improve its concrete pavement response prediction capability. With this revision, the major goal of this study—the improvement of design and construction procedures for concrete pavements based on mechanistic modeling techniques—has been achieved. Overall, the significant accomplishments of this project include: (1) the modification of prediction models for concrete properties, (2) the incorporation of these modifications into the JRCP-5 computer program, (3) the development of a series of transverse reinforcement prediction equations based on limiting criteria of concrete pavements, and (4) the development of probabilistic design charts for sawing depth prediction using such parameters as reliability level, bar diameter, and concrete weakness. In addition to the tensile strength model, we modified modulus of elasticity, compressive strength, and drying shrinkage models. Further modification of the drying shrinkage model incorporated the effect of slab thickness on the predicted drying shrinkage value. Recommendations concerning possible future modifications of concrete properties models are provided below.

The JRCP-5 computer program has been used to develop a relationship among percent reinforcement, concrete pavement geometry, concrete properties, and environmental variation. As a result of this reinforcement analysis, two sets of regression equations were developed, one short term and the other long term. Each set of three equations consists of formulas for steel stress, crack width, and joint movement. One important finding of this analysis was the significant difference in the required percent reinforcement, compared with the percent reinforcement calculated by using the subgrade drag formula. The steel requirement of concrete pavements varies with respect to two main groups of factors: (1) concrete pavement geometry and subbase friction, and (2) concrete properties (which are functions of CAT and temperature variation).

As a part of this study, a probabilistic method has been developed to predict sawing depth. Among the parameters used in this model, the most significant are reliability level, diameter of reinforcement parallel to the joint, and mean weakness of the tensile strength of concrete away from the sawed joint. To perform the sawing analysis, a computer program, PROSAW, was developed. The use of PROSAW in many sawing simulations led to the development of a set of design charts that can be used to determine sawing depth for a given reliability level.

Significant additions to the Texas Rigid Pavement Design Procedure (presented in Chapter 7) include:

1. a set of design charts to predict sawing depth and time for a desired reliability level and for certain field conditions, and
2. a computer program (PRO1, developed from a series of regression equations) that replaces the transverse reinforcement nomograph of the *AASHTO Design Guide.*

CONCLUSIONS

The primary conclusion of this study is that the modifications made to the concrete property prediction models have eliminated the discrepancies previously found when comparing predicted and actual properties. Other conclusions are the following:

1. Inclusion of coarse aggregate type (CAT) in the prediction models resulted in an improved prediction of the concrete properties. The new models are applicable to all coarse aggregate types currently used in Texas.
2. The effect of thickness shown in the shrinkage formulation resulted in improved estimation of the early-age concrete tensile stress. In addition to the improvement mentioned in

conclusion No. 1, the shrinkage prediction model required additional modification to handle the effect of thickness as it relates to the shrinkage rate.

3. The subgrade drag theory incorrectly predicts the required amount of reinforcement. One explanation for this is the simplicity of the formula, which excludes some of the significant factors.
4. Reinforcement equations developed in this study are more representative of actual conditions than the subgrade drag formula. Besides including all the significant factors, the relationship between amount of reinforcement and concrete pavement design criteria—crack width, joint movement, and steel stress—is well established.
5. There is a difference in predictive ability between the regression equations and the subgrade drag formula; additionally, the regression equations differ from the subgrade drag formula in that they incorporate the effect of coarse aggregate type.
6. In developing the sawing model, it was assumed that the concrete section next to a sawed joint has an effective thickness. The effective thickness is the actual thickness minus the bar diameter parallel to the section.
7. A probabilistic sawing time prediction model was developed and implemented into the computer program. This model, PROSAW, is capable of simulating up to 10,000 cases (in which the required sawing depth is calculated for each case). The summary of these simulations yields the mean and the standard deviation of the required sawing depth. Thus, the sawing depth needed at any reliability level can be calculated.

The findings presented here are based on the JRCP-5 computer program, which is designed to predict early-age concrete pavement response under prevailing environmental conditions. The developed methods and guidelines require continued field observations and measurements for possible future modifications. Compared with earlier methods, those recommended in this report are more representative of actual concrete pavement responses.

RECOMMENDATIONS

Possibilities for future research concerning the evaluation, development, and improvement of the JRCP-5 computer program are given below.

1. For future study, water/cement and aggregate/cement ratios should be considered in the factorial design of shrinkage measurement experiments. Without this information, the available prediction models can be used with only limited confidence, since during different seasons of the year it is recommended that different water/cement and aggregate/cement ratios be used. Aggregate/cement ratios, especially, depend on the availability of aggregate at the construction site.
2. Long-term effects of material variation on pavement performance should be mathematically modeled. In particular, the damage caused by the combination of indirect environmental effects and traffic load should be further researched. The JRCP-5 computer program, while capable of predicting short-term pavement responses, cannot predict long-term response. Such long-term response prediction is necessary in estimating the actual life of the pavement—not the design life estimated from deterministic methods. This capability will help to allocate funds when they are needed.
3. The simulation of heat of hydration after concrete placement should yield more reasonable results. The distribution of temperature is necessary for the prediction of sawing depth and time.
4. The sawing depth prediction should be calibrated by using field data and more than one set of seasonal temperature data.
5. The wheel load stress should be included in the program. The combined effect of environment and traffic load will help predict the behavior of the pavement after it is opened to traffic.
6. The temperature differential through the slab thickness should be considered in model development. This will require the inclusion of curling stress as an environmentally induced stress.
7. The bond stress assumption should be modified to include the variable strain at different crack depths. This modification should improve the prediction considerably.
8. To improve predictions of random crack location and time, concrete property variability should be implemented into the JRCP-5 computer program.
9. The design nomograph of the *AASHTO Pavement Design Guide* for transverse reinforcement should be replaced by a more representative nomograph that includes a set of

limiting criteria and concrete properties as input parameters. Concrete property models do not consider the effect of mix design on the predicted value. Therefore, for future modifications of the prediction models, it is highly recommended that mix-design effect be incorporated.

10. Future field measurements are necessary to calibrate the models for concrete properties.
11. The prediction of concrete properties assumes that there is no temperature-level effect on predicted value. Enhancement of prediction models with temperature effect should improve pavement response prediction considerably.
12. The stress calculation algorithm of JRCP-5 should be improved to change the comparison of temperature at any time with placement temperature. The program should compare two successive temperature values, corresponding to two successive time increments. To implement this approach, the program should be capable of storing the stress history of the pavement, at least during early age.
13. The drying shrinkage model should be updated by implementing (1) the recommended improvement for mix design, and (2) differential drying shrinkage. The implementation of differential shrinkage modeling may require a two-dimensional JRCP model (in place of the current one-dimensional model).

REFERENCES

1. Rivero-Vallejo, F., and B. F. McCullough, "Drying Shrinkage and Temperature Drop Stresses in Jointed Reinforced Concrete Pavement," Center for Highway Research, RR 177-1, The University of Texas at Austin, August 1975.

2. Wesevich, J. W., B. F. McCullough, and N. H. Burns, "Stabilized Subbase Friction Study for Concrete Pavements," Research Report 459-1, Center for Transportation Research, The University of Texas at Austin, November 1987.

3. Wimsatt, A. J., and B. F. McCullough, "Subbase Friction Effects on Concrete Pavements," *Proceedings,* Fourth International Conference on the Design and Rehabilitation of Concrete Pavements, Purdue University, Lafayette, Indiana, April 1989.

4. Richardson, J. M., and J. M. Armaghani, "Stress Caused by Temperature Gradient in Portland Cement Concrete Pavements," *Transportation Research Record 1121,* Washington, D.C., January 1987.

5. Abou-Ayyash, A., "Mechanistic Behavior of Continuously Reinforced Concrete Pavement," Doctoral Dissertation, The University of Texas at Austin, May 1974.

6. Mindess, S., and J. F. Young, *Concrete,* Prentice-Hall, Englewood Cliffs, New Jersey, 1981.

7. Neville, A. M., *Properties of Concrete,* Third Edition, Pitman, Great Britain, 1981.

8. Hansen, T. C., and A. H. Mattock, "Influence of Size and Shape of Members on the Shrinkage and Creep of Concrete," *Journal of the American Concrete Institute,* Vol 63, February 1966.

9. Castedo, H., and T. Dossey, "Proposed Drying Shrinkage (Z) Prediction Models for Pavement Concrete Made with Various Coarse Aggregate," Technical Memorandum 422-50, Center for Transportation Research, The University of Texas at Austin, February 1989.

10. Robertson, N., "A Study of the JRCP Computer Program for Cracking Analysis of Jointed Reinforced Concrete Pavement," Technical Memorandum 472-4, Center for Transportation Research, The University of Texas at Austin, December 1985.

11. Lu, J., H. Castedo, and B. F. McCullough, "Normalization of Models 1 and 2 for Tensile Strength (f_t), Modulus of Elasticity (E) and Drying Shrinkage (Z) of Pavement Concrete Made with Texas Coarse Aggregates," Technical Memorandum 422-38, Center for Transportation Research, The University of Texas at Austin, February 1988.

12. Saraf, C. L., and B. F. McCullough, "Controlling Longitudinal Cracking in Concrete Pavements," *Transportation Research Record 1043,* Washington, D.C., 1985.

13. Deen, R. C., J. H Haven, A. S. Rahal, and W. V. Azevedo, "Cracking in Concrete Pavements," *ASCE Transportation Engineering Journal,* Vol 106, No. TE2, March 1980.

14. McCullough, B. F., and C. L. Saraf, "Longitudinal Cracking of CRCP in the Houston Area," Technical Memorandum 388-2, Center for Transportation Research, The University of Texas at Austin, December 1983.

15. AASHTO, *Guide for Design of Pavement Structures*, AASHTO, Washington, D.C., 1986.

16. Kunt, M. M., and B. F. McCullough, "Evaluation of the Subbase Drag Formula by Considering Realistic Subbase Friction Values," *Transportation Research Record 1286*, Washington, D.C., 1990.

17. Heinrichs, K. W., M. J. Liu, M. I. Darter, S. H. Carpenter, and A. M. Ioannides, "Rigid Pavement Analysis and Design," FHWA-RD-88-068, June 1989.

18. Black, B., "Documentation of CRCP and JRCP Rigid Pavement Programs," Technical Memorandum 422-59, Center for Transportation Research, The University of Texas at Austin, May 1989.

19. Marshall, B. P., and T. W. Kennedy, "Tensile and Elastic Characteristics of Pavement Materials," Research Report 183-1, Center for Highway Research, The University of Texas at Austin, January 1974.

APPENDIX A

JRCP-5 COMPUTER PROGRAM SAMPLE INPUT FILE

```
 FACTORIAL ANALYSIS FOR SAWING TIME
   97      <== DATA SET NO.
       32.        100          0        100          5.
    1        .250E+00  .500E+00  .290E+08  .500E-05
  .120E+02  .600E-05
      450.000000  4000000.000000     3.000000E-04      4000.000000
        7.000000            1
    3        .00  .00 1.00 -.01 1.50 -.02
100.0   28  93.  84.  84.  84.  84.  84.  82.  82.  82.  82.  82.  82.  82.  82.
            82.  82.  82.  82.  82.  82.  82.  82.  82.  82.  82.  82.  82.  82.
             .0
```

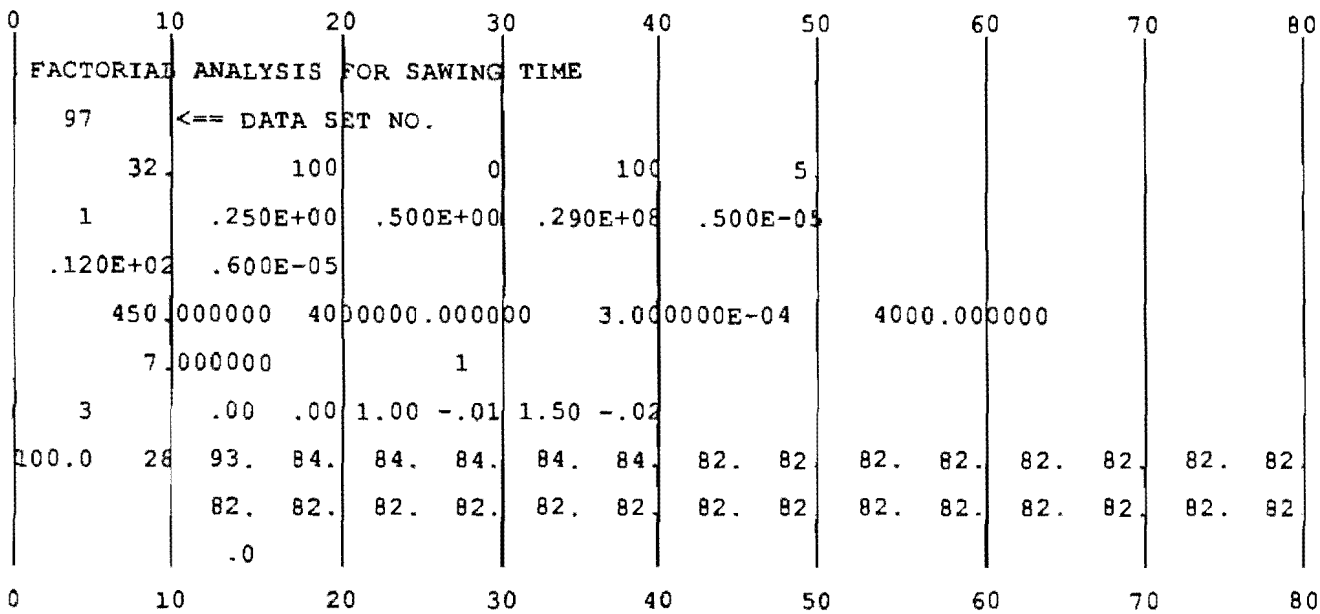

APPENDIX B

JRCP-5 COMPUTER PROGRAM SAMPLE OUTPUT FILE

```
      JJJJJJ\   RRRRRRRRR\   CCCCCCCCC\ PPPPPPPP\   555555\
        JJ\     RR\     RR\ CC\         PP\    PP\  55\
        JJ\     RR\    RR\  CC\         PP\    PP\  55\
        JJ\     RRRRRRRR\   CC\         PPPPPPPP\    55555\
        JJ\     RR\ RR\     CC\         PP               55\
        JJ\     RR\  RR\    CC\         PP\              55\
     JJJJJ\     RR\   RR\    CCCCCCCCC\ PP\         555555\
```

THIS PROGRAM HAS BEEN MODIFIED BY MEHMET M. KUNT, MAY 1991
THE MODIFICATIONS ARE EXPLAINED IN RR 1169-4

```
1              PROGRAM JRCP5   UPDATED: 20 MAY 1991

0     PROBLEM NUMBER   97
        = DATA S

0         ************************************************
          *                                              *
          *              PROBLEM DEFINITION              *
          *                                              *
          ************************************************
0               SLAB LENGTH (FT.)        =      32.0
                NUMBER OF INCREMENTS     =       100
                CRACK FORCING FLAG       =         0
                MAX. NO. OF ITERATIONS   =       100
                REL. CLOSURE TOLERANCE   =       5.0

0         ************************************************
          *                                              *
          *                STEEL PROPERTIES              *
          *                                              *
          ************************************************
0               TYPE OF LONGITUDINAL REINFORCEMENT IS
                          DEFORMED BARS
0               PERCENT REINFORCEMENT =       .25
                BAR DIAMETER          =       .50
                ELASTIC MODULUS       =  .290E+08
                THERMAL COEFFICIENT   =  .500E-05

0         ************************************************
          *                                              *
          *              CONCRETE PROPERTIES             *
          *                                              *
          ************************************************

                SLAB THICKNESS       =      12.0
                THERMAL COEFFICIENT =  .600E-05
```

ULTIMATE SHRINKAGE = .300E-03

1 PROGRAM JRCP5 UPDATED: 20 MAY 1991

0 PROBLEM NUMBER 97
= DATA S
COARSE AGGREGATE TYPE IS LIMESTONE

****
* TIME DEPENDENT VARIABLES *
****

TIME DAY	TENSILE STRENGTH	MODULUS OF ELASTICITY	DRYING SHRINKAGE
1.	.18490E+03	.28287E+07	.16756E-06
2.	.26656E+03	.33140E+07	.33497E-06
3.	.30980E+03	.35982E+07	.50221E-06
4.	.33736E+03	.37647E+07	.66929E-06
5.	.35748E+03	.38622E+07	.83622E-06
6.	.37332E+03	.39193E+07	.10030E-05
7.	.38623E+03	.39527E+07	.11696E-05
8.	.39693E+03	.39723E+07	.13360E-05
9.	.40586E+03	.39838E+07	.15023E-05
10.	.41332E+03	.39905E+07	.16685E-05
11.	.41956E+03	.39944E+07	.18344E-05
12.	.42479E+03	.39967E+07	.20003E-05
13.	.42917E+03	.39981E+07	.21659E-05
14.	.43284E+03	.39989E+07	.23314E-05
15.	.43592E+03	.39993E+07	.24968E-05
16.	.43850E+03	.39996E+07	.26620E-05
17.	.44065E+03	.39998E+07	.28270E-05
18.	.44246E+03	.39999E+07	.29919E-05
19.	.44398E+03	.39999E+07	.31566E-05
20.	.44525E+03	.40000E+07	.33211E-05
21.	.44631E+03	.40000E+07	.34856E-05
22.	.44720E+03	.40000E+07	.36498E-05
23.	.44795E+03	.40000E+07	.38139E-05
24.	.44857E+03	.40000E+07	.39779E-05
25.	.44910E+03	.40000E+07	.41416E-05
26.	.44953E+03	.40000E+07	.43053E-05
27.	.44990E+03	.40000E+07	.44688E-05
28.	.45021E+03	.40000E+07	.46321E-05

```
0          ************************************************
           *                                              *
           *      SLAB-BASE FRICTION CHARACTERISTICS      *
           *               F-Y RELATIONSHIP               *
           *                                              *
           ************************************************
0               TYPE OF FRICTION CURVE IS A MULTILINEAR CURVE
0                          F(I)      Y(I)

                           .000      .000

                          1.000    -.010

                          1.500    -.020
```

1 PROGRAM JRCP5 UPDATED: 20 MAY 1991

0 PROBLEM NUMBER 97
= DATA S

0 **********
* *
* TEMPERATURE DATA *
* *
****

0 CURING TEMPERATURE=100.0

DAY	MINIMUM TEMPERATURE	DROP IN TEMPERATURE
1	93.0	7.0
2	84.0	16.0
3	84.0	16.0
4	84.0	16.0
5	84.0	16.0
6	84.0	16.0
7	82.0	18.0
8	82.0	18.0
9	82.0	18.0
10	82.0	18.0
11	82.0	18.0
12	82.0	18.0
13	82.0	18.0
14	82.0	18.0
15	82.0	18.0
16	82.0	18.0
17	82.0	18.0
18	82.0	18.0
19	82.0	18.0
20	82.0	18.0
21	82.0	18.0
22	82.0	18.0
23	82.0	18.0
24	82.0	18.0
25	82.0	18.0
26	82.0	18.0
27	82.0	18.0
28	82.0	18.0

MINIMUM TEMPERATURE EXPECTED AFTER
CONCRETE GAINS FULL STRENGTH IS .0 DEGREES FARENHEIT.

1 PROGRAM JRCP5 UPDATED: 20 MAY 1991

0 PROBLEM NUMBER 97
= DATA S
0 ***** BEFORE FIRST CRACK **********

TIME DAY	MAXIMUM CONCRETE STRESS	TENSILE STRENGTH	JOINT OPENING
1.	6.849	184.9	-.1554E-01
2.	14.22	266.6	-.3587E-01
3.	14.28	309.8	-.3602E-01
4.	14.32	337.4	-.3613E-01
5.	14.36	357.5	-.3621E-01
6.	14.39	373.3	-.3629E-01
7.	15.70	386.2	-.4089E-01
8.	15.73	396.9	-.4095E-01
9.	15.75	405.9	-.4102E-01
10.	15.78	413.3	-.4108E-01
11.	15.81	419.6	-.4114E-01
12.	15.83	424.8	-.4121E-01
13.	15.86	429.2	-.4127E-01
14.	15.88	432.8	-.4133E-01
15.	15.91	435.9	-.4139E-01
16.	15.94	438.5	-.4145E-01
17.	15.96	440.7	-.4152E-01
18.	15.99	442.5	-.4158E-01
19.	16.01	444.0	-.4164E-01
20.	16.04	445.2	-.4170E-01
21.	16.06	446.3	-.4176E-01
22.	16.09	447.2	-.4182E-01
23.	16.11	447.9	-.4188E-01
24.	16.14	448.6	-.4195E-01
25.	16.16	449.1	-.4201E-01
26.	16.19	449.5	-.4207E-01
27.	16.21	449.9	-.4213E-01
28.	16.24	450.2	-.4219E-01

NO CRACK OCCURS AT END OF 28 DAYS.

FOR MINIMUM EXPECTED TEMPERATURE (.0 DEGREES) THE STRESSES ARE:
29.55 450.2 -.2303

APPENDIX C

FEATURES OF JRCP VERSIONS 1-5

FEATURES OF JRCP VERSIONS 1-5

In focusing on the JRCP program, this appendix hopefully will provide the user with a better understanding of the contents of the program (e.g., variables and their order of input).

Previous versions of the JRCP computer program are specifically discussed. Some of the features explained were implemented in JRCP-5, with the remaining features to be implemented in future versions of the program.

C.1 JRCP PROGRAM DESCRIPTIONS

C.1.1 JRCP-1

JRCP-1, written in 1975 by B.F. McCullough, Felipe Rivero-Vallejo, and Thomas Hainze, is a computer system used for designing and analyzing jointed reinforced concrete pavement slabs subjected to drying shrinkage and temperature changes. Crack width, longitudinal steel stress, and concrete stress are predicted as functions of time, temperature, and drying shrinkage. JRCP-1 functions included:

(1) analyzing a given slab design by checking the width of the cracks, the steel and concrete stresses, and the joint widths;
(2) designing the percentage of reinforcement for a concrete slab based on the maximum allowable crack width and maximum allowable steel stresses for the given slab geometry and environmental conditions; and
(3) designing the required dimensions of a non-reinforced slab that will perform without cracking.

The reader is referred to CTR Research Report 177-1 for more information.

C.1.2 JRCP-2

This second version represented an improvement over the previous JRCP version in that it permitted the determination of stresses from a minimum temperature after the concrete had reached its full strength.

C.1.3 JRCP-3

JRCP-3 was the result of several modifications of JRCP-2 undertaken by Prentiss Riddle in 1981. These modifications included:

(1) removal of the steel design and non-reinforcement design options; and
(2) inclusion of an option to control the formation of the first crack in the slab.

C.1.4 JRCP-4

JRCP-4 was the result of several modifications of JRCP-3 undertaken by Neil Robertson in 1985. The modifications included:

(1) revision of the Model 1 algorithm to eliminate approximating assumptions;
(2) incorporation of data and looping structures similar to those used in the Model 2 solution; and
(3) calculation of joint widths as output before and after the development of the first crack.

For more information refer to CTR Technical Memorandum 472-4.

C.1.5 JRCP-5

The JRCP-5 model supersedes JRCP-4 by including the normalized material property relationships generated in phase two of CTR Project 422.

C.2 JRCP-5 INPUT GUIDE

THIS PROGRAM WAS CREATED AND USED ON THE CDC DUAL CYBER 170/750. IT WAS COMPILED USING THE FTN5 COMPILER.

CURRENTLY THE PROGRAM RUNS ON IBM PS/2 AND COMPATIBLES. THE COMPILER IS MICROSOFT FORTRAN (VERSION 5). THE FOLLOWING SEQUENCE OF COMMANDS IS NECESSARY TO COMPILE AND EXECUTE THE FORTRAN PROGRAM:

FL JRCP5.FOR
JRCP5

THE INPUT FILENAME IS J5IN.DAT AND THE OUTPUT FILENAME IS JR5.OUT.

CARDS 3 THROUGH 10 FORM A SET, WHICH MAY BE REPEATED FOR AS MANY PROBLEMS AS DESIRED.

SIGN CONVENTIONS:

— TENSION IS POSITIVE.
— FRICTION FORCES IN THE POSITIVE X-DIRECTION ARE POSITIVE.
— MOVEMENTS IN THE POSITIVE X-DIRECTION ARE POSITIVE.

— TEMPERATURE DROP AT A GIVEN TIME IS DEFINED AS THE DIFFERENCE BETWEEN THE TEMPERATURE AT WHICH THE CONCRETE SET AND THE TEMPERATURE AT THAT TIME.

ALL VALUES ARE FREE FORMAT UNLESS COLUMN LOCATIONS ARE SPECIFIED.

C.3 VARIABLES USED IN JRCP-5

AAA	COUNTER FOR THE NUMBER OF ITERATIONS FOR FRICTION CLOSURE
AGE	AGE OF CONCRETE GENERATED BY PROGRAM
AGEU()	AGE OF CONCRETE INPUT BY USER FOR AGE-STRENGTH RELATIONSHIP
AGGTYP	AGGREGATE TYPE
ALPHAC	THERMAL COEFFICIENT OF CONCRETE
ALPHAS	THERMAL COEFFICIENT OF STEEL
ANTEMP	LAST DAY ON TIME TEMPERATURE CURVE
AN1()	PROGRAM IDENTIFICATION CARDS
AN2()	PROBLEM IDENTIFICATION CARD
COMP28	28-DAY COMPRESSIVE STRENGTH
COMSTR	COMPRESSIVE STRENGTH
CONSTR()	CONCRETE STRESS
CURTEMP	CURING TEMPERATURE
DELTAT	DROP IN TEMPERATURE AT ANY TIME
DELTATM	MAXIMUM DROP IN TEMPERATURE
DELTAX	INCREMENT LENGTH
DIA	DIAMETER OF INDIVIDUAL BAR
DT()	DAILY TEMPERATURES
EC	MODULUS OF ELASTICITY OF CONCRETE
EP	PRECISION ERROR
ES	MODULUS OF ELASTICITY OF STEEL
ELAS 28	28-DAY MODULUS OF ELASTICITY
F(9)	FRICTION FORCE
FEXP()	FLEXURAL STRENGTH
FPC	COMPRESSIVE STRENGTH
FU	MAXIMUM FRICTION FORCE
H	INCREMENT WIDTH (L/NT)
IFORCE	FIST CRACK FORCING INPUT FLAG
IFY	NUMBER OF POINTS DEFINING THE FRICTION MOVEMENT CURVE
INDEX	CLOSURE CONTROL
ISAW	INDEX FOR SIMULATION AGE (HOURLY OR DAILY)
ITEB	COUNTER FOR THE NUMBER OF ITERATIONS ON BOND LENGTH
ITYPER	OPTION FOR THE TYPE OF REINFORCEMENT
L	LENGTH OF JRCP3 MODEL
MAXITE	MAXIMUM ALLOWABLE NUMBER OF ITERATIONS
N	INDEX FOR READING DATA
NPROB	PROBLEM NUMBER (PROGRAM STOPS IF BLANK)
NSTRN	INPUT FLAG DESIGNATING WHETHER AGE-STRENGTH RELATIONSHIP IS GIVEN BY THE USER
NT	TOTAL NUMBER OF INCREMENTS IN JRCP3 MODEL
NTEMP	NUMBER OF DAILY TEMPERATURES
NTP1	NT + 1
P	PERCENT LONGITUDINAL REINFORCEMENT
PERCENT	PERCENTAGE OF 28-DAY FLEXURAL STRENGTH
REFF	UPPER BOUND ON FU (maximum friction force)
SHRN28	28-DAY SHRINKAGE
SS()	STEEL STRAIN
STRAIN()	CONCRETE STRAIN
STRESSS()	STEEL STRESS
STRNMUL	TRANSFORMATION FACTOR BETWEEN TENSILE AND FLEXURAL STRENGTH
STRSC1()	CONCRETE STRESS FOR MODEL-1
STRSC2()	CONCRETE STRESS FOR MODEL-2
STRSS2()	STEEL STRESS
TENS28	28-DAY TENSILE STRENGTH
TENSION()	CONCRETE TENSILE STRENGTH INPUT BY USER FOR AGE-STRENGTH RELATIONSHIP
THICK	SLAB THICKNESS
TIME	TIME IN DAYS
TOL	TOLERANCE FOR CLOSURE CRITERIA
VDS	VOLUME TO SURFACE AREA RATIO
XBAR	SLAB LENGTH
Y()	CONCRETE MOVEMENT
YEXP()	MOVEMENT OF THE FRICTIONAL-RESISTANCE CURVE
YP()	MOVEMENT FOR TESTING CRITERIA
YPITE()	MOVEMENT FROM THE PREVIOUS ITERATION
Y1()	JOINT WIDTH
Z	DRYING SHRINKAGE AT ANY TIME

APPENDIX D

PROSAW COMPUTER PROGRAM SAMPLE INPUT FILES

Filename:

```
  12.0   6.0E-006   288.0
  1.0E-001   7.50000E-001   500.0
  370.0   3.0E-004   4967.0
```

Filename:

```
 LIMESTONE
  1.          12.44          12.77          -.2462E-01
  2.          12.45          25.05          -.2466E-01
  3.          12.46          36.86          -.2469E-01
  4.          12.46          48.23          -.2471E-01
  5.          12.47          59.16          -.2474E-01
  6.          12.48          69.69          -.2476E-01
  7.          12.48          79.82          -.2478E-01
  8.          12.49          89.57          -.2480E-01
  9.          12.50          98.96          -.2482E-01
 10.          12.50          108.0          -.2484E-01
 11.          12.51          116.7          -.2486E-01
 12.          12.51          125.1          -.2487E-01
 13.          12.52          133.2          -.2489E-01
 14.          12.52          141.0          -.2490E-01
 15.          12.53          148.5          -.2492E-01
 16.          12.53          155.8          -.2493E-01
 17.          12.54          162.8          -.2495E-01
 18.          12.54          169.5          -.2496E-01
 19.          12.55          176.1          -.2497E-01
 20.          12.55          182.4          -.2498E-01
 21.          12.55          188.4          -.2500E-01
 22.          12.56          194.3          -.2501E-01
 23.          12.56          200.0          -.2502E-01
 24.          12.57          205.5          -.2503E-01
 25.          12.57          210.8          -.2504E-01
 26.          12.57          215.9          -.2505E-01
 27.          12.58          220.8          -.2506E-01
 28.          12.58          225.6          -.2507E-01
```

APPENDIX E

PROSAW COMPUTER PROGRAM SAMPLE OUTPUT FILES

Filename:

****SEED NUMBER IS 2.356896797000000E+010
AT THE END OF THE SIMULATION THE MEAN STANDARD DEVIATION
AND 95PERCENTILE ARE:

Time	ft	Mean	Standard Deviation	95 Percentile
1.0	12.77	.510	2.643	4.859
2.0	25.05	-.054	2.369	3.844
3.0	36.86	.422	2.583	4.670
4.0	48.23	.080	2.717	4.550
5.0	59.16	.513	2.634	4.846
6.0	69.69	.633	2.333	4.471
7.0	79.82	.638	2.389	4.567
8.0	89.57	.508	2.662	4.887
9.0	98.96	.589	2.262	4.309
10.0	108.00	.673	2.402	4.624
11.0	116.70	.196	2.540	4.374
12.0	125.10	.326	2.738	4.830
13.0	133.20	-.097	2.910	4.690
14.0	141.00	.100	2.773	4.662
15.0	148.50	.236	2.977	5.133
16.0	155.80	.702	3.610	6.640
17.0	162.80	.344	2.406	4.301
18.0	169.50	.465	2.933	5.290
19.0	176.10	.389	2.640	4.732
20.0	182.40	.522	2.556	4.727
21.0	188.40	.017	2.614	4.317
22.0	194.30	.672	2.282	4.426
23.0	200.00	.933	2.631	5.262
24.0	205.50	.521	2.843	5.198
25.0	210.80	.387	2.369	4.285
26.0	215.90	.587	2.711	5.048
27.0	220.80	.738	2.596	5.008
28.0	225.60	.350	2.522	4.498

APPENDIX F

PRO1 COMPUTER PROGRAM SAMPLE INPUT FILES

```
.191   .750   112.0    14.0     4.0    .000006    .0003    100.
```

APPENDIX G

PRO1 COMPUTER PROGRAM SAMPLE OUTPUT FILE

1

```
*************************************************
* THIS PROGRAM PREDICTS PERCENT REINFORCEMENT *
* FOR BOTH JRCP(LONGITUDINAL) AND             *
* CRCP(TRANSVERSE) REINFORCEMENT.             *
* DEVELOPED BY MEHMET M. KUNT, APRIL 1990     *
* THE CENTER FOR TRANSPORTATION RESEARCH      *
* THE UNIVERSITY OF TEXAS AT AUSTIN           *
*************************************************
```

THE CURRENT INPUT VALUES ARE

```
****************************
```

<PER>	<DIA>	<SLEN>	<THICK>	<FRIC>	<ALPHAC>	<Z28>	<CT>
.300	.500	112.0	14.0	1.5	.000006	.0003	100.

1 ****THE PREDICTED VALUES ARE****

	SHORT TERM			LONG TERM		
Ps	STEEL STRESS	CRACK WIDTH	JOINT* OPENING	STEEL STRESS	CRACK WIDTH	JOINT* OPENIN
.300	46162.7	.0018	.5745	66352.5	.0030	1.1454

* Joint opening is for jointed reinforced concrete pavement and it is equal to twice the end movement of continuously reinforced pavement

1

```
**************************************
**************************************
**   THANKS FOR USING THE PROGRAM    **
**   HAVE A NICE DAY.                **
**************************************
**************************************
```

APPENDIX H

LABORATORY DATA USED FOR MODEL DEVELOPMENT

FERGUSON STRUCTURAL ENGINEERING LABORATORY
MEASUREMENTS OF CONCRETE MIX PROPERTIES

Table H.1 SRG modulus of elasticity (10^4 psi)

SILICEOUS RIVER GRAVEL							
MOISTURE CONDITION (% HUMIDITY)		40% REL. HUMIDITY			100% REL. HUMIDITY		
CURING TEMPERATURE (°F)		50°F	75°F	100°F	50°F	75°F	100°F
CURING TIME	TEST SAMPLE						
1 DAY	1	298.8	421.2	335.3	333.3	374.6	395.3
	2	248.4	199.3	322.4	234.2	230.0	766.3
	3	257.8	469.4	440.1	357.6	304.2	293.4
	AVG.	268.3	363.3	365.9	308.4	302.9	485.0
3 DAYS	1	336.3	233.2	412.6	495.1	255.0	460.8
	2	528.9	195.6	516.8	478.6	522.7	358.6
	3	526.4	325.2	443.5	420.3	664.7	480.7
	AVG.	463.9	251.3	457.6	464.7	388.9	433.4
7 DAYS	1	415.7	219.5	287.4	652.1	387.2	479.4
	2	612.2	328.4	355.4	583.7	602.1	853.4
	3	411.5	442.5	287.4	1309.9	1064.8	533.6
	AVG.	479.8	330.1	310.1	848.6	684.7	622.1
28 DAYS	1	362.5	452.8	378.3	457.1	539.0	769.0
	2	515.0	501.4	427.5	524.5	580.7	605.4
	3	410.9	575.0	354.6	375.8	662.7	599.0
	AVG.	429.5	509.7	368.8	452.5	534.1	657.8
90 DAYS	1	611.7	314.2	592.8	1440.7	238.7	1084.9
	2	506.6	602.1	215.0	467.5	668.6	1580.8
	3	602.1	524.5	650.4	787.7	452.8	1026.8
	AVG.	573.5	480.3	486.1	898.6	453.4	1230.8

Table H.2 LS modulus of elasticity (10^4 psi)

SILICEOUS RIVER GRAVEL							
MOISTURE CONDITION (% HUMIDITY)		40% REL. HUMIDITY			100% REL. HUMIDITY		
CURING TEMPERATURE (°F)		50°F	75°F	100°F	50°F	75°F	100°F
CURING TIME	TEST SAMPLE						
1 DAY	1	348.8	403.5	430.0	301.9	314.4	324.6
	2	120.9	628.4	333.3	320.0	1320.6	541.6
	3	366.9	465.6	549.5	298.0	960.4	415.7
	AVG.	278.9	499.2	437.6	306.6	865.1	427.3
3 DAYS	1	385.8	417.2	670.6	569.0	320.9	449.2
	2	479.4	392.5	489.4	560.5	563.3	461.8
	3	563.3	448.8	520.4	599.2	485.6	531.8
	AVG.	476.2	419.5	560.1	576.2	456.6	480.9
7 DAYS	1	516.8	291.2	387.2	701.4	500.7	549.3
	2	539.0	405.2	574.8	710.3	682.7	356.5
	3	428.3	414.2	373.0	663.8	426.7	450.6
	AVG.	494.7	370.2	445.0	691.8	536.7	452.1
28 DAYS	1	692.8	399.3	560.7	220.7	539.9	299.5
	2	577.7	487.3	547.6	129.2	351.7	583.8
	3	539.9	635.4	416.9	283.8	527.5	457.9
	AVG.	603.5	507.3	508.4	211.2	473.0	447.1
90 DAYS	1	638.9	1007.2	1185.6	694.0	849.4	526.9
	2	527.5	300.3	281.9	539.9	566.2	701.2
	3	577.7	—	184.9	631.9	293.3	1063.7
	AVG.	581.4	653.8	550.8	621.9	569.6	763.9

Table H.3 SRG split cylinder tensile strength (psi)

SILICEOUS RIVER GRAVEL							
MOISTURE CONDITION (% HUMIDITY)		40% REL. HUMIDITY			100% REL. HUMIDITY		
CURING TEMPERATURE (°F)		50°F	75°F	100°F	50°F	75°F	100°F
CURING TIME	TEST SAMPLE						
1 DAY	1	191.8	266.9	271.3	232.6	350.7	273.0
	2	183.2	254.3	303.3	203.6	313.9	274.3
	3	158.2	255.2	287.9	192.7	308.4	291.7
	AVG.	177.7	258.8	287.5	209.6	324.3	279.7
3 DAYS	1	249.6	345.5	318.3	334.6	380.6	377.4
	2	269.4	288.9	363.3	289.3	411.9	322.1
	3	254.1	329.8	308.1	370.3	373.0	305.9
	AVG.	257.7	321.4	329.9	331.4	388.5	335.1
7 DAYS	1	309.6	370.8	412.5	313.5	441.1	343.1
	2	325.3	397.3	383.9	333.8	457.1	344.6
	3	334.0	377.8	417.6	360.8	440.1	320.3
	AVG.	322.9	381.9	404.7	336.0	446.1	336.0
28 DAYS	1	329.0	429.2	355.3	346.8	528.2	435.3
	2	326.6	372.6	403.2	420.1	543.9	380.5
	3	340.6	374.6	337.8	399.2	492.8	390.7
	AVG.	332.1	392.2	365.5	388.7	521.6	402.2
90 DAYS	1	361.4	400.7	376.6	384.9	—	464.5
	2	399.5	422.3	428.5	387.6	—	409.9
	3	260.1	425.3	333.7	404.1	—	471.3
	AVG.	340.3	416.1	379.6	392.2	—	448.6

Table H.4 LS split cylinder tensile strength (psi)

SILICEOUS RIVER GRAVEL							
MOISTURE CONDITION (% HUMIDITY)		40% REL. HUMIDITY			100% REL. HUMIDITY		
CURING TEMPERATURE (°F)		50°F	75°F	100°F	50°F	75°F	100°F
CURING TI ME	TEST SAMPLE						
1 DAY	1	203.2	242.0	291.0	239.6	249.6	302.0
	2	194.2	316.3	276.0	248.7	249.4	313.3
	3	269.4	269.2	288.9	228.7	237.9	350.6
	AVG.	222.3	275.9	285.3	239.0	245.6	322.0
3 DAYS	1	348.1	357.3	433.2	294.9	284.4	413.5
	2	315.8	395.5	353.0	329.1	340.2	316.4
	3	337.6	351.2	391.8	383.6	322.6	339.8
	AVG.	333.8	368.0	392.7	335.8	315.7	356.6
7 DAYS	1	352.3	400.8	323.6	426.8	284.4	449.2
	2	337.9	427.9	413.9	370.4	379.3	451.2
	3	335.7	407.8	428.8	367.5	371.1	404.8
	AVG.	342.0	412.2	388.8	388.2	344.9	435.1
28 DAYS	1	456.8	515.3	465.2	398.3	423.7	463.1
	2	404.8	494.1	320.5	363.9	432.3	357.1
	3	463.0	355.1	445.9	376.4	407.9	456.3
	AVG.	441.5	454.9	410.5	379.5	421.3	425.5
90 DAYS	1	411.2	476.8	277.0	372.5	437.0	443.2
	2	456.5	370.6	339.1	362.2	419.9	408.8
	3	—	393.6	384.8	488.2	451.6	391.8
	AVG.	433.9	413.7	333.6	409.6	436.2	414.6

Table H.5 SRG flexural strength (psi)

SILICEOUS RIVER GRAVEL							
MOISTURE CONDITION (% HUMIDITY)		40% REL. HUMIDITY			100% REL. HUMIDITY		
CURING TEMPERATURE (°F)		50°F	75°F	100°F	50°F	75°F	100°F
CURING TIME	TEST SAMPLE						
1 DAY	1	255.9	316.7	418.3	225.6	365.0	409.9
	2	237.1	414.4	384.7	195.4	325.0	465.3
	3	234.9	390.9	367.6	225.6	300.0	409.9
	AVG.	242.6	374.0	390.2	215.5	330.0	428.4
3 DAYS	1	343.2	446.2	347.8	352.1	435.5	437.8
	2	414.6	485.0	357.2	432.7	425.0	482.9
	3	413.6	470.2	361.9	393.7	410.7	487.1
	AVG.	390.5	467.1	355.6	392.8	430.2	469.3
7 DAYS	1	409.4	420.0	313.2	493.2	475.1	553.7
	2	488.8	382.3	345.2	488.5	596.4	535.8
	3	375.4	446.8	366.6	501.5	529.0	533.4
	AVG.	424.5	416.3	341.7	494.4	533.5	541.0
28 DAYS	1	460.5	470.1	398.4	599.7	600.2	652.5
	2	465.3	417.9	406.5	605.9	493.2	700.4
	3	436.9	524.1	427.0	588.9	528.9	546.1
	AVG.	454.2	470.7	410.6	598.1	544.1	633.0
90 DAYS	1	514.3	540.6	489.9	741.6	648.3	732.1
	2	519.6	597.6	480.0	651.4	653.2	707.6
	3	519.2	533.2	528.3	677.9	643.3	781.9
	AVG.	517.7	557.1	499.4	690.3	648.3	740.5

Table H.6 LS flexural strength (psi)

SILICEOUS RIVER GRAVEL							
MOISTURE CONDITION (% HUMIDITY)		40% REL. HUMIDITY			100% REL. HUMIDITY		
CURING TEMPERATURE (°F)		50°F	75°F	100°F	50°F	75°F	100°F
CURING TIME	TEST SAMPLE						
1 DAY	1	352.5	401.6	465.2	308.7	437.2	400.7
	2	319.6	415.7	370.3	294.8	388.0	404.8
	3	386.2	426.7	446.7	323.8	411.7	418.7
	AVG.	352.8	414.7	427.4	309.1	412.3	408.1
3 DAYS	1	424.1	488.2	441.8	478.7	506.2	513.6
	2	521.1	483.9	456.0	460.6	523.8	523.2
	3	538.1	474.3	451.2	456.0	483.6	484.4
	AVG.	494.5	482.1	449.7	465.1	504.6	507.1
7 DAYS	1	551.8	383.1	479.2	544.3	550.9	442.3
	2	585.0	456.1	474.4	546.1	543.5	497.1
	3	542.7	416.0	370.3	563.1	519.9	469.7
	AVG.	559.8	418.4	441.3	551.2	538.1	469.7
28 DAYS	1	524.1	422.2	437.2	656.3	673.9	568.2
	2	583.0	475.2	484.8	676.5	612.2	547.2
	3	575.1	480.0	465.5	669.6	630.3	492.9
	AVG.	560.7	459.1	462.5	667.5	638.8	536.1
90 DAYS	1	602.5	620.6	612.3	721.9	618.9	593.7
	2	603.7	673.9	562.4	761.2	693.4	597.6
	3	585.3	—	566.4	773.9	700.5	617.4
	AVG.	597.2	647.3	580.4	752.3	670.9	602.9

Table H.7 SRG thermal coefficient (10^{-6} in./in./°F)

SILICEOUS RIVER GRAVEL							
MOISTURE CONDITION (% HUMIDITY)		40% REL. HUMIDITY			100% REL. HUMIDITY		
CURING TEMPERATURE (°F)		50°F	75°F	100°F	50°F	75°F	100°F
CURING TIME	TEST SAMPLE						
1 DAY	1	6.95	7.27	7.93	7.46	6.65	4.50
	2	7.88	7.96	7.55	7.75	5.70	7.27
	3	7.83	7.83	8.26	7.71	7.36	6.92
	AVG.	7.55	7.69	7.91	7.64	6.57	6.23
3 DAYS	1	8.88	8.02	6.49	6.84	8.16	7.04
	2	9.51	8.86	7.10	7.16	8.33	7.51
	3	8.45	8.42	7.32	6.89	—	7.27
	AVG.	8.95	8.43	6.97	6.96	8.24	7.27
7 DAYS	1	10.07	7.41	7.51	8.13	6.78	6.61
	2	8.96	7.21	7.92	8.06	10.50	6.87
	3	7.92	7.56	7.20	8.18	7.27	6.83
	AVG.	8.98	7.39	7.54	8.12	8.18	6.77
28 DAYS	1	8.48	8.17	8.82	8.58	7.72	8.50
	2	9.21	8.18	9.36	8.35	7.77	8.27
	3	8.91	8.21	9.36	9.48	7.58	7.90
	AVG.	8.87	8.18	9.18	8.80	7.69	8.22

Table H.8 LS thermal coefficient (10^{-6} in./in./°F)

SILICEOUS RIVER GRAVEL							
MOISTURE CONDITION (% HUMIDITY)		40% REL. HUMIDITY			100% REL. HUMIDITY		
CURING TEMPERATURE (°F)		50°F	75°F	100°F	50°F	75°F	100°F
CURING TIME	TEST SAMPLE						
1 DAY	1	5.40	5.10	6.06	7.13	5.41	5.75
	2	4.38	4.89	6.66	7.42	5.53	5.83
	3	5.04	6.09	5.21	6.23	5.07	—
	AVG.	4.94	5.36	5.98	6.93	5.34	5.84
3 DAYS	1	5.32	5.66	5.70	4.62	4.58	5.33
	2	3.72	5.65	—	4.64	4.87	4.45
	3	5.59	6.77	—	2.82	5.19	5.59
	AVG.	4.88	6.02	5.70	4.03	4.88	5.12
7 DAYS	1	5.64	6.03	5.13	5.31	5.11	4.44
	2	6.03	6.12	5.20	5.49	5.16	4.78
	3	5.77	6.31	4.68	5.57	4.69	4.21
	AVG.	5.81	6.15	5.00	5.45	4.99	4.48
28 DAYS	1	6.38	5.86	6.30	5.26	5.68	7.85
	2	6.23	6.42	6.69	6.00	6.11	8.81
	3	6.47	6.60	6.71	6.15	6.12	7.67
	AVG.	6.36	6.29	6.57	5.80	5.97	8.11

Table H.9 Modulus of rupture at 7 days (psi)

SILICEOUS RIVER GRAVEL							
MOISTURE CONDITION (% HUMIDITY)		40% REL. HUMIDITY			100% REL. HUMIDITY		
CURING TEMPERATURE (°F)		50°F	75°F	100°F	50°F	75°F	100°F
CURING TIME	TEST SAMPLE						
7 DAYS	1	498.2	534.3	400.7	552.7	717.5	649.9
	2	554.6	530.4	381.5	554.6	846.2	704.7
	3	496.5	483.9	413.6	646.7	591.5	693.2
	AVG.	516.4	516.2	398.6	584.7	718.4	682.6
7 DAYS	1	589.6	531.1	507.4	618.4	628.1	575.3
	2	635.6	487.5	473.7	633.9	618.7	488.0
	3	580.5	588.3	548.1	601.8	635.6	576.9
	AVG.	601.9	535.6	509.8	618.0	627.5	546.7

Table H.10 SRG drying shrinkage (10^{-4} in./in.)

Curing Time (Days)	Curing Temp. (°F)	Specimen 1				Specimen 2			
		1	2	3	Avg.	1	2	3	Avg.
.91	69	17.05	13.81	54.31	28.39	59.17	2.47	30.01	30.55
3.74	71	22.80	35.76	71.40	43.32	57.53	35.76	62.49	51.96
6.27	70	40.58	61.64	97.28	66.50	83.51	53.54	85.94	74.33
11.86	69	108.58	105.34	143.41	119.11	115.87	94.81	135.31	115.33
19.84	69	157.18	154.75	176.62	162.85	165.28	132.88	173.38	157.18
25.93	69	179.86	177.43	199.30	185.53	182.29	152.32	196.06	176.89
39.04	69	209.83	204.16	236.56	216.85	217.12	184.72	230.89	210.91
61.24	69	238.99	241.41	273.82	251.41	251.95	209.02	262.48	241.15
89.14	79	315.53	320.39	350.36	328.76	328.49	284.75	328.49	313.91
131.04	73	265.88	300.71	363.08	309.89	295.04	268.31	282.08	281.81
261.12	75	358.30	366.40	390.70	371.80	373.59	320.23	371.26	355.06

Table H.11 LS drying shrinkage (10^{-4} in./in.)

Curing Time (Days)	Curing Temp. (°F)	Specimen 1				Specimen 2			
		1	2	3	Avg.	1	2	3	Avg.
1.04	70	20.64	28.74	10.92	20.10	18.21	42.51	19.02	26.58
2.52	69	16.20	16.20	5.67	12.69	21.06	40.50	27.54	29.70
5.86	69	48.60	54.27	51.84	51.57	46.17	81.00	59.94	61.37
12.59	69	124.74	121.50	132.84	126.36	100.44	140.94	119.88	120.42
20.69	69	179.82	166.05	171.72	172.53	139.32	184.68	155.52	159.84
34.03	69	222.75	220.32	223.56	222.21	196.02	233.28	204.12	211.14
56.23	69	284.31	268.11	287.55	279.99	243.81	273.78	249.48	255.69
84.12	78	355.86	331.56	356.67	348.03	307.26	334.80	313.74	318.60
126.04	73	348.24	340.14	351.48	348.62	281.01	329.61	306.12	305.58
256.10	75	448.65	432.45	465.66	448.92	375.75	416.25	403.29	398.43

SPLITTING TENSILE STRENGTH

SPLITTING TENSILE STRENGTH (PSI)					
SPECIMEN	NO.	1-DAY	3-DAY	7-DAY	28-DAY
GRANITE	1	-------	336	398	486
	2	221	319	482	551
	3	199	402	437	551
	AVG.	210	353	439	529

SPLITTING TENSILE STRENGTH (PSI)					
SPECIMEN	NO.	1-DAY	3-DAY	7-DAY	28-DAY
DOLOMITE	1	197	317	470	533
	2	238	363	444	506
	3	227	436	448	442
	AVG.	221	372	454	494

SPLITTING TENSILE STRENGTH (PSI)					
SPECIMEN	NO.	1-DAY	3-DAY	7-DAY	28-DAY
VEGA	1	107	334	464	442
	2	79	255	349	463
	3	93	310	405	419
	AVG.	93	300	406	441

SPLITTING TENSILE STRENGTH (PSI)					
SPECIMEN	NO.	1-DAY	3-DAY	7-DAY	28-DAY
BRIDGEPORT TIN TOP	1	190	352	365	462
	2	176	306	461	452
	3	177	332	454	408
	AVG.	181	330	427	441

SPLITTING TENSILE STRENGTH (PSI)					
SPECIMEN	NO.	1-DAY	3-DAY	7-DAY	28-DAY
WESTERN TASCOSA	1	225	301	378	458
	2	245	313	361	388
	3	241	345	375	450
	AVG.	237	320	371	432

SPLITTING TENSILE STRENGTH (PSI)					
SPECIMEN	NO.	1-DAY	3-DAY	7-DAY	28-DAY
FERRIS	1	259	394	313	466
	2	258	322	383	501
	3	238	361	402	460
	AVG.	252	359	366	476

COMPRESSIVE STRENGTH

COMPRESSIVE STRENGTH (PSI)					
SPECIMEN	NO.	1-DAY	3-DAY	7-DAY	28-DAY
GRANITE	1	1506	2792	4040	4996
	2	1474	2861	3796	5077
	3	1291	2809	3549	4828
	AVG.	1424	2821	3795	4967

COMPRESSIVE STRENGTH (PSI)					
SPECIMEN	NO.	1-DAY	3-DAY	7-DAY	28-DAY
DOLOMITE	1	1343	2678	3356	4408
	2	1837	3507	4626	3942
	3	1167	2535	4028	5045
	AVG.	1449	2907	4004	4465

COMPRESSIVE STRENGTH (PSI)					
SPECIMEN	NO.	1-DAY	3-DAY	7-DAY	28-DAY
VEGA	1	915	2822	4008	4674
	2	1077	2875	2622	3343
	3	953	2941	4239	---
	AVG.	982	2879	3623	4008

COMPRESSIVE STRENGTH (PSI)					
SPECIMEN	NO.	1-DAY	3-DAY	7-DAY	28-DAY
BRIDGEPORT TIN TOP	1	1163	2877	3260	4104
	2	1123	2493	3285	3796
	3	1255	3074	3993	4380
	AVG.	1180	2815	3513	4093

COMPRESSIVE STRENGTH (PSI)					
SPECIMEN	NO.	1-DAY	3-DAY	7-DAY	28-DAY
WESTERN TASCOSA	1	1396	2949	3869	4222
	2	1344	2609	3534	3950
	3	1304	2848	3461	4246
	AVG.	1348	2802	3621	4139

COMPRESSIVE STRENGTH (PSI)					
SPECIMEN	NO.	1-DAY	3-DAY	7-DAY	28-DAY
FERRIS	1	1592	2676	3475	4010
	2	1405	2642	3630	4012
	3	1487	2805	3532	3945
	AVG.	1495	2708	3546	3989

MODULUS OF ELASTICITY

		MODULUS OF ELASTICITY (x 10E06 PSI)			
SPECIMEN	NO.	1-DAY	3-DAY	7-DAY	28-DAY
GRANITE	1	2.572	3.203	3.409	3.537
	2	2.738	3.203	3.075	3.42
	3	2.497	3.144	3.215	3.458
	AVG.	2.602	3.183	3.233	3.472

		MODULUS OF ELASTICITY (x 10E06 PSI)			
SPECIMEN	NO.	1-DAY	3-DAY	7-DAY	28-DAY
DOLOMITE	1	2.978	4.577	4.39	4.491
	2	2.695	3.612	3.979	4.964
	3	3.773	4.446	4.391	5.144
	AVG.	3.149	4.212	4.253	4.866

		MODULUS OF ELASTICITY (x 10E06 PSI)			
SPECIMEN	NO.	1-DAY	3-DAY	7-DAY	28-DAY
VEGA	1	1.121	2.497	2.663	4.042
	2	2.497	3.753	3.426	3.856
	3	2.234	3.395	3.593	3.745
	AVG.	1.9505	3.215	3.228	3.882

		MODULUS OF ELASTICITY (x 10E06 PSI)			
SPECIMEN	NO.	1-DAY	3-DAY	7-DAY	28-DAY
BRIDGEPORT TIN TOP	1	2.695	3.858	3.773	3.773
	2	2.4604	3.691	3.903	4.287
	3	2.978	3.691	3.836	4.223
	AVG.	2.711	3.746	3.837	4.094

		MODULUS OF ELASTICITY (x 10E06 PSI)			
SPECIMEN	NO.	1-DAY	3-DAY	7-DAY	28-DAY
WESTERN TASCOSA	1	2.4604	2.874	3.482	3.628
	2	2.695	3.203	3.4296	3.84
	3	2.358	2.966	3.482	3.409
	AVG.	2.504	3.014	3.465	3.625

		MODULUS OF ELASTICITY (x 10E06 PSI)			
SPECIMEN	NO.	1-DAY	3-DAY	7-DAY	28-DAY
FERRIS	1	3.075	3.537	3.837	4.135
	2	2.978	3.537	3.903	4.073
	3	3.368	3.612	3.836	4.135
	AVG.	3.141	3.562	3.859	4.114

GEORGETOWN CRUSHED LIMESTONE — PHASE II

MODULUS OF ELASTICITY (x 10E06 PSI)					
SPECIMEN	NO.	1-DAY	3-DAY	7-DAY	28-DAY
CRUSHED STONE	1	2.498	2.829	3.537	3.691
	2	2.832	3.115	3.493	3.731
	3	2.927	3.265	3.389	3.691
	AVG.	2.752	3.069	3.473	3.704

SPLIT CYLINDER (PSI)					
SPECIMEN	NO.	1-DAY	3-DAY	7-DAY	28-DAY
CRUSHED STONE	1	183	268	431	389
	2	195	269	367	398
	3	183	283	376	510
	AVG.	187	274	391	432

COMPRESSIVE STRENGTH (PSI)					
SPECIMEN	NO.	1-DAY	3-DAY	7-DAY	28-DAY
CRUSHED STONE	1	1277	2729	3951	4922
	2	1176	2706	3695	4817
	3	1193	2830	3917	5259
	AVG.	1215	2755	3854	4999

MODULUS OF RUPTURE (PSI)					
SPECIMEN	NO.			7-DAY M.C.	
CRUSHED STONE	1			632	
	2			648	
	3			661	
	AVG.			647	

SPLIT CYLINDER (PSI) 28-DAY MOIST CURED					
SPECIMEN	NO.				28-DAY M.C.
CRUSHED STONE	1				539
	2				525
	3				404
	AVG.				482

COLORADO RIVER GRAVEL — PHASE II

MODULUS OF ELASTICITY (x 10E06 PSI)					
SPECIMEN	NO.	1-DAY	3-DAY	7-DAY	28-DAY
RIVER GRAVEL	1	3.395	4.206	4.716	4.397
	2	3.858	4.323	4.556	4.172
	3	3.858	3.939	4.301	4.119
	AVG.	3.704	4.156	4.524	4.229

SPLIT CYLINDER (PSI)					
SPECIMEN	NO.	1-DAY	3-DAY	7-DAY	28-DAY
RIVER GRAVEL	1	208	286	431	463
	2	156	232	465	445
	3	175	258	435	458
	AVG.	180	259	443	455

COMPRESSIVE STRENGTH (PSI)					
SPECIMEN	NO.	1-DAY	3-DAY	7-DAY	28-DAY
RIVER GRAVEL	1	1510	2822	4128	4779
	2	1270	2902	4298	4937
	3	1374	2750	4015	4896
	AVG.	1385	2825	4147	4871

MODULUS OF RUPTURE (PSI)					
SPECIMEN	NO.			7-DAY M.C.	
RIVER GRAVEL	1			588	
	2			707	
	3			588	
	AVG.			628	

SPLIT CYLINDER (PSI) 28-DAY MOIST CURED					
SPECIMEN	NO.				28-DAY M.C.
RIVER GRAVEL	1				536
	2				505
	3				495
	AVG.				512

COEFFICIENT OF THERMAL EXPANSION

Coefficient of Thermal Expansion (x10E-6 in/in/°F)					
SPECIMEN	NO.				28-DAY
GRANITE	1				5.94
	2				5.49
	3				5.79
	AVG.				5.74

Coefficient of Thermal Expansion (x10E-6 in/in/°F)					
SPECIMEN	NO.				28-DAY
DOLOMITE	1				5.74
	2				5.82
	3				6.14
	AVG.				5.9

Coefficient of Thermal Expansion (x10E-6 in/in/°F)					
SPECIMEN	NO.				28-DAY
VEGA	1				6.87
	2				6.83
	3				5.8
	AVG.				6.5

Coefficient of Thermal Expansion (x10E-6 in/in/°F)					
SPECIMEN	NO.				28-DAY
BRIDGEPORT TIN TOP	1				4.56
	2				4.96
	3				4.5
	AVG.				4.84

Coefficient of Thermal Expansion (x10E-6 in/in/°F)					
SPECIMEN	NO.				28-DAY
WESTERN TASCOSA	1				6.05
	2				5.95
	3				6.44
	AVG.				6.15

Coefficient of Thermal Expansion (x10E-6 in/in/°F)					
SPECIMEN	NO.				28-DAY
FERRIS	1				5.4
	2				5.1
	3				5.82
	AVG.				5.44

TABLE-4. COEFFICIENT OF THERMAL EXPANSION (10E-6)

CURING TIME (DAYS)	40 % R H			100 % R H		
	CURING TEMPERATURE					
	50	75	100	50	75	100
SILICEOUS RIVER GRAVEL						
1	7.55	7.69	7.91	7.64	6.57	6.23
3	8.95	8.43	6.97	6.96	8.24	7.27
7	8.98	7.39	7.54	8.12	8.18	6.77
28	8.87	8.18	9.18	8.80	7.69	8.22
90	7.50	7.50	8.02	7.93	6.31	7.21
LIMESTONE						
1	4.94	5.36	5.98	6.93	5.34	5.84
3	4.88	6.02	5.70	4.03	4.88	5.12
7	5.81	6.15	5.00	5.45	4.99	4.48
28	6.36	6.29	6.57	5.80	5.97	8.11
90	5.94	6.03	6.31	5.75	5.13	5.61

: B : : D : : F : : H : : J : : L : : N : : P : : R : : T : : V : : X :

0 -100 600 300 DRYING SHRINKAGE TEST

Test code[SHR-40-75-5] CTE[5.25] FILE[5407557]
Curing Condition[40% R.H., 75°F Initial Date[7/03/86]

DATE	DAY	TEMPERATURE °F	ZERO BAR	SPECIMEN 1			AVE. 1	SPECIMEN 2			AVE. 2
				SHRINK. 1	SHRINK. 2	SHRINK. 3	AVERAGE	SHRINK. 1	SHRINK. 2	SHRINK. 3	AVERAGE
7/03/86	.00	69	849.7								
7/03/86	.00	69	849.7	0	0	0	0	0	0	0	0
7/04/86	1.04	70	850	20.64	28.74	10.92	20.1	18.21	42.51	19.02	26.58
7/06/86	2.52	69	851.7	16.2	16.2	5.67	12.69	21.06	40.5	27.54	29.7
7/09/86	5.86	69	842.1	48.6	54.27	51.84	51.57	46.17	81	59.94	62.37
7/16/86	12.59	69	849.1	124.74	121.5	132.84	126.36	100.44	140.94	119.88	120.42
7/24/86	20.69	69	842.9	179.82	166.05	171.72	172.53	139.32	184.68	155.52	159.84
8/06/86	34.03	69	842.9	222.75	220.32	223.56	222.21	196.02	239.28	204.12	211.14
8/20/86	56.23	69	843.5	284.31	268.11	287.55	279.99	243.81	273.78	249.48	255.69
9/25/86	84.12	78	843.2	355.86	331.56	356.67	348.03	307.26	394.8	319.74	318.6
11/6/86	126.04	79	840.5	348.24	340.14	351.48	346.62	281.01	329.61	306.12	305.58
5/16/87	256.10	75	841.9	440.65	432.45	465.66	448.92	375.75	416.25	403.29	398.43
				-848.82	-900.69	-265.05	-278.01	-389.79	-276.39	-281.25	-315.81

: B : : D : : F : : H : : J : : L : : N : : P : : R : : T : : V : : X :

0 -100 600 300 DRYING SHRINKAGE TEST

Test code[SHR-40-100-5] CTE[5.25] FILE[54010050]
Curing Condition[40% R.H., 100°F Initial Date[6/27/86]

DATE	DAY	TEMPERATURE °F	ZERO BAR	SPECIMEN 1			AVE. 1	SPECIMEN 2			AVE. 2
				SHRINK. 1	SHRINK. 2	SHRINK. 3	AVERAGE	SHRINK. 1	SHRINK. 2	SHRINK. 3	AVERAGE
6/27/86	.00	90	847								
6/27/86	.00	90	847	0	0	0	0	0	0	0	0
6/28/86	1.08	96	1050.7								
6/30/86	2.94	95	852								
7/01/86	4.10	96	1061.3	66.33	101.16	80.2	85.23	133.56	95.49	216.99	148.68
7/03/86	5.90	96	847.3	71.19	74.43	93.93	59.85	74.43	80.69	111.69	72.27
7/10/86	12.78	101	849.7	136.32	73.95	103.92	104.73	157.88	120.12	197.88	158.46
7/16/86	19.01	99	850	138.78	79.65	90.18	102.87	141.21	116.91	181.71	146.61
7/23/86	26.74	102	851	195.03	138.33	144	159.12	173.16	130.23	208.8	170.73
7/29/86	32.99	102	851	257.4	195.03	192.6	215.01	241.2	195.03	7080.03	218.115
8/06/86	39.83	101	851	252.15	189.78	184.92	208.95	230.28	230.28	7074.78	230.28
8/29/86	62.98	98	850	280.23	213	215.43	236.22	264.03	255.93	345.03	259.98
9/25/86	89.93	100	851	357.06	376.5	284.97	339.51	330.33	352.2	405.66	341.265
11/6/86	132.07	104	1098	378.06	408.03	302.73	362.94	351.33	381.3	434.76	366.315
5/27/87	244.89	94	840.9	403.32	509.95	306.12	431.13	349.05	389.55	430.05	369.3
				-421.47	-518.67	-440.1	-460.08	-380.97	-437.67	-348.57	-409.32

B D F H J L N P R T V X

0 -100 600 300 DRYING SHRINKAGE TEST

Test Code[SHR-40-75-G] CTEC 0.143 FILEC540750G7]
Curing Condition[40% R.H., 75°F] Initial Date[6/28/86]

DATE	DAY	TEMPERATURE °F	ZERO BAR	SPECIMEN 1			AVE. 1	SPECIMEN 2			AVE. 2
				SHRINK. 1	SHRINK. 2	SHRINK. 3	AVERAGE	SHRINK. 1	SHRINK. 2	SHRINK. 3	AVERAGE
6/28/86	.00	68	845.7								
6/29/86	.00	68	845.7	0	0	0	0	0	0	0	0
7/02/86	.91	69	921.4	17.05	13.81	54.31	28.39	59.17	2.47	30.01	30.55
7/03/86	3.74	71	921.8	22.9	85.76	71.4	43.32	57.63	35.76	62.49	51.96
7/04/86	4.27	70	850	40.58	61.64	97.28	66.5	83.51	53.54	85.94	74.33
7/07/86	11.06	69	842.4	100.38	105.34	143.41	119.11	113.87	94.81	135.31	115.33
7/10/86	19.04	69	843.1	157.18	154.75	176.62	162.85	165.28	132.88	173.38	157.18
7/14/86	25.93	69	842.9	179.86	177.43	199.3	185.53	188.29	152.32	196.06	176.89
8/04/86	39.04	69	842.9	209.03	204.16	236.56	216.85	217.12	184.72	230.69	210.91
8/29/86	61.24	69	843.5	238.99	241.42	273.82	251.41	251.95	209.02	262.48	241.15
9/25/86	89.14	79	843.2								
11/6/86	131.04	73	841.5	265.08	300.71	363.08	309.89	295.04	240.31	282.08	201.81
2/16/87	241.12	75	841.2	358.3	366.4	890.7	371.8	379.69	320.23	371.26	355.06
				~~-69.72~~	-470.09	-496.82	~~-512.21~~	~~-427.16~~	-459.56	-435.26	-440.66

B D F H J L N P R T V X

0 -100 600 300

SHRINKAGE TEST

Test Code[SHR-40-100-G] CTEC 0.143 FILEC540100G0]
Curing Condition[40% R.H., 100°F] Initial Date[6/28/86]

DATE	DAY	TEMPERATURE °F	ZERO BAR	SPECIMEN 1			AVE. 1	SPECIMEN 2			AVE. 2
				SHRINK. 1	SHRINK. 2	SHRINK. 3	AVERAGE	SHRINK. 1	SHRINK. 2	SHRINK. 3	AVERAGE
6/28/86	.00	83	847								
6/29/86	.00	83	847	0	0	0	0	0	0	0	0
6/30/86	1.88	95	863								
7/02/86	3.86	96	847.3	49.12	29.68	83.95	54.25				
7/03/86	5.68	94	850	81.44	62	100.07	81.17	65.24	70.2	133.28	92.24
7/10/86	11.65	101	850	136.42	122.22	160.39	143.01	111.69	132.75	203.22	149.22
7/18/86	19.60	100	852								
7/25/86	26.73	102	852	170.86	165.19	211.36	182.47	154.66	167.62	241.33	187.87
8/04/86	38.64	102	851	209.26	183.82	238.09	208.39	176.58	189.49	251.06	205.96
8/29/86	61.80	92	850	194.76	186.66	227.16	202.86	157.5	180.99	240.93	193.14
9/25/86	87.92	100	851	238.01	232.34	294.71	255.02	227.48	256.64	308.48	264.2
11/6/86	130.12	104	1110.3	262.47	291.63	341.04	298.38	268.14	288.53	343.47	298.38
2/27/87	242.07	94	840.5	304.19	271.79	330.92	302.3	239.89	274.22	317.96	277.19
				~~-613.92~~	-608.89	-602.72	610.01	~~2796.85~~	-616.49	-637.65	-514.27

DRYING SHRINKAGE (MICROSTRAINS)

	7540DL		10040DL	
DAY	AVERAGE 1	AVERAGE 2	AVERAGE 1	AVERAGE 2
1	0	0	0	0
2	33	52	74	117
3	55	50	53	91
6	58	50	52	89
7	55	57	78	133
10	92	60	107	147
15	88	96	75	167
17	126	93	88	167
22	151	154	91	187
29	167	146	140	195
60	234	210		
63			245	276

	7540GT		10040GT	
DAY	AVERAGE 1	AVERAGE 2	AVERAGE 1	AVERAGE 2
1	0	0	0	0
3	83	56	110	118
6	129	135	143	145
7	138	162	162	178
11	186	199	208	211
14	223	264		
17	264	297	235	246
25	277	320	280	299
30	323	377	310	377

	7540FR		10040FR	
DAY	AVERAGE 1	AVERAGE 2	AVERAGE 1	AVERAGE 2
1	0	0	0	0
2	33	49	67	64
3	96	83	120	112
7	127	103	177	202
10	174	152	208	237
15	220	231	259	291
18	262	265		
21	282	288	307	343
29	311	322	364	393

DRYING SHRINKAGE (MICROSTRAINS)

	7540BTT		10040BTT	
DAY	AVERAGE 1	AVERAGE 2	AVERAGE 1	AVERAGE 2
1	0	0	0	0
2	25	36	16	27
4	23	21	62	54
6	20	69	59	62
11	89	130	111	124
18	100	138	114	127
20	141	176	135	130
25	127	164	167	159
28	154	186	167	159
62	299	293	281	287

	7540VG		10040VG	
DAY	AVERAGE 1	AVERAGE 2	AVERAGE 1	AVERAGE 2
1	0	0	0	0
3	13	51	86	89
7	50	82	134	128
12	122	97	178	167
14	143	122	196	199
19	188	196	245	231
26	216	219	251	284
28	228	226	256	259
68	371	382	355	407

	7540WT		10040WT	
DAY	AVERAGE 1	AVERAGE 2	AVERAGE 1	AVERAGE 2
1	0	0	0	0
3	60	30	25	63
8	57	71	37	69
10	104	125	66	85
15	116	124	101	107
18	143	184	98	96
24	189	224	169	169
28	198	235	221	231
52	276	303	314	325